

Aus der Klinik für Kinder- und Jugendmedizin  
Direktorin: Frau Prof. Dr. med. Stefanie Weber

des Fachbereichs Medizin der Philipps-Universität Marburg

---

MAGED2 is essential for  $G\alpha_s$  and cAMP/PKA signaling  
under hypoxia, which promotes induction of HIF-1 $\alpha$  and  
inhibits stress-induced autophagy

---

Inaugural-Dissertation

zur Erlangung des Doktorgrades der Naturwissenschaften  
dem Fachbereich Medizin der Philipps-Universität Marburg

vorgelegt von

Sadiq Nasrah from Latakia

Marburg, 2024

Angenommen vom Fachbereich Medizin der Philipps-Universität Marburg am:

15.02.2024

Gedruckt mit Genehmigung des Fachbereichs Medizin

Dekan/in: Prof. Dr. Denise Hilfiker-Kleiner

Referent: Prof. Dr. Martin Kömhoff

1. Korreferent: Prof. Dr. Johannes Graumann

To my cherished family,

my parents: Jamal Nasrah and Amal Mohammed, my siblings: Amjad and Ayman Nasrah, as well as my sister-in-law Suzan Motwj and my nephew Ali Nasrah.

With profound gratitude, I dedicate this thesis to you. Your unwavering support, boundless inspiration, and endless encouragement have been the driving forces behind my pursuit of knowledge. This achievement stands as a testament to the love and strength you have instilled in me.

# Table of Contents

<b>1. Abstract.....</b>	<b>1</b>
<b>2. Zusammenfassung.....</b>	<b>2</b>
<b>3. Introduction .....</b>	<b>3</b>
3.1. Transient antenatal Bartter's syndrome .....	3
3.2. Structure and biological functions of MAGED2 .....	4
3.3. G-alpha-S .....	7
3.4. Hypoxic induction of HIF-1 $\alpha$ .....	8
3.5. Stress-induced autophagy.....	9
<b>4. Results.....</b>	<b>11</b>
4.1. MAGED2 is required for G $\alpha$ s localization at the plasma membrane under hypoxic conditions.....	11
4.2. MAGED2 depletion promotes endocytosis of G $\alpha$ s mediated by MDM2-dependent ubiquitination .....	11
4.3. Consequences of G $\alpha$ s internalization on cAMP/ PKA pathway and downstream substrates.....	12
4.4. cAMP/ PKA pathway activation downstream of G $\alpha$ s reverses the impact of MAGED2 depletion on hypoxic HIF-1 $\alpha$ induction .....	13
4.5. HIF-1 $\alpha$ enhances MAGED2 expression under hypoxic condition .....	14
4.6. MAGED2 depletion promotes stress-induced autophagy .....	15
4.7. ER stress, genotoxic stress and nutritional stress induce autophagy upon MAGED depletion .....	16
4.8. Depletion of G $\alpha$ s promotes autophagy while forskolin activation of the cAMP/ PKA pathway inhibits it ...	16
<b>5. Discussion .....</b>	<b>18</b>
<b>6. References.....</b>	<b>25</b>
<b>7. Appendix .....</b>	<b>I</b>
7.1. List of abbreviations .....	I
7.2. Curriculum Vitae.....	V
7.3. Academic teachers .....	VIII
7.4. Acknowledgment.....	IX
7.5. Full lists of publications .....	X
7.6. Contribution to the published papers.....	XI
7.7. Reprints of original publications .....	XIII



## 1. Abstract

*MAGED2* mutations cause a severe but transient form of antenatal Bartter syndrome, known as transient Bartter syndrome (tBS or Bartter type 5). This condition is characterized by significant renal salt wasting in affected fetuses and newborns, resulting in pronounced fetal urine production and excessive amounts of amniotic fluid leading to preterm birth, as well as increased perinatal mortality. Remarkably, all these symptoms resolve spontaneously starting at 30 weeks of gestational age. Given the physical interaction between Gas and *MAGED2*, as well as the role of Gas in activating the membrane-bound adenylyl cyclase, which subsequently generates cAMP and promotes renal salt reabsorption via protein kinase A (PKA), the impact of *MAGED2* for the function of Gas was investigated. These investigations were conducted under both normoxic and hypoxic conditions, considering that spontaneous recovery occurs alongside the developmental increase of renal oxygenation. In contrast to normoxia, physical and chemical hypoxia induced internalization of Gas upon *MAGED2* depletion in renal and cancer cell lines. This internalization was accompanied by a significant reduction in cAMP generation and PKA activity. Importantly, hypoxic internalization of Gas was shown to require dynamin and was completely reversible upon re-oxygenation. The process was shown to be mediated by the ubiquitin E3 ligase MDM2, which ubiquitinates Gas, resulting in its endocytosis. The latter was abrogated by mutating critical lysine-residues (ubiquitin receptor sites) of Gas, by MDM2 inhibitors or knockdown of MDM2, respectively. Hence, *MAGED2* is crucial under hypoxia to regulate Gas endocytosis by blocking its MDM2-dependent ubiquitination, thereby maintaining proper induction of the cAMP/ PKA pathway. Reduced cAMP/ PKA activation upon *MAGED2* depletion impaired HIF-1 $\alpha$  induction. Notably, forskolin, a cAMP/ PKA activator acting downstream of Gas rescued HIF-1 $\alpha$  expression, highlighting the essential role of *MAGED2* in Gas functioning under hypoxic condition. Additionally, forskolin treatment increased the abundance of *MAGED2* at both mRNA and protein levels. Interestingly, PKA type II specifically regulates the expression of HIF-1 $\alpha$  and the latter reciprocally increases PKA activity under hypoxia and promotes *MAGED2* expression. Finally, *MAGED-2* was identified as inhibitor of autophagy under various stress conditions. Induction of autophagy by depleting Gas and its reversal by forskolin demonstrate the inhibitory role of the cAMP/ PKA pathway governed by *MAGED2*. In contrast to other MAGE family members, such as *MAGEA3/A6* whose absence initiates autophagy, *MAGED-2* specifically blocks autophagy under stress conditions. Given that autophagy (at least under hypoxia) is induced upon Gas depletion and inhibited by the cAMP/ PKA activator forskolin, the context-dependent regulation of Gas by *MAGED2* could be the underlying molecular switch of autophagy induction.

## 2. Zusammenfassung

Das transiente Bartter-Syndrom (tBS) ist die schwerste Form des renalen Salzverlustes, der sich bei den betroffenen Föten durch massives Polyhydramnion, Frühgeburtlichkeit und eine erhöhte perinatale Sterblichkeit bemerkbar macht. Bemerkenswert ist, dass sich alle Symptome spontan zurückbilden. tBS wird durch Mutationen in *MAGED2* verursacht, das für das Melanom-assoziierte Antigen D2 kodiert. Angesichts der Interaktion zwischen Gas und *MAGED2* und der Rolle von Gas bei der Aktivierung der membrangebundenen Adenylatzyklase, die anschließend cAMP erzeugt und die renale Salzrückresorption über Proteinkinase A (PKA)-abhängige Phosphorylierung von Salztransportern fördert, wurde die Rolle von *MAGED2* für die Funktion von Gas untersucht. Da die spontane Erholung mit dem entwicklungsbedingten Anstieg der Sauerstoffversorgung der Nieren einhergeht, wurden diese Studien unter normoxischen und hypoxischen Bedingungen durchgeführt. Im Gegensatz zu Normoxie verursachte physikalische und chemische Hypoxie bei Knockdown von *MAGED2* in Nieren- und Krebszelllinien eine Internalisierung von Gas, die mit einer signifikanten Verringerung der cAMP-Bildung und der PKA-Aktivität einherging. Die Internalisierung von Gas erforderte Dynamin und war durch erneute Sauerstoffzufuhr vollständig reversibel. Die Endozytose von Gas erforderte die Ubiquitinierung durch die Ubiquitin-E3-Ligase MDM2, wie durch die Aufhebung der Wirkung der *MAGED2*-Depletion auf die Endozytose von Gas 1) durch Mutation kritischer Lysinreste (Ubiquitin-Rezeptorstellen) von Gas, 2) MDM2-Inhibitoren und 3) MDM2-Depletion gezeigt wurde. Daher ist *MAGED2* unter Hypoxie entscheidend für die Regulierung der Gas-Endozytose, indem es seine MDM2-abhängige Ubiquitinierung blockiert. Die gestörte HIF-1 $\alpha$ -Induktion bei Abwesenheit von *MAGED2* konnte durch Forskolin, das downstream von Gas wirkt, wiederhergestellt werden, was die wesentliche Rolle von *MAGED2* für die Funktion von Gas unter hypoxischen Bedingungen unterstreicht. Ferner erhöhte Forskolin die Expression von *MAGED2* auf mRNA- und Protein-Ebene. Interessanterweise reguliert PKA Typ II spezifisch die Expression von HIF-1 $\alpha$ , und letzteres erhöht unter Hypoxie wechselseitig die PKA-Aktivität und fördert die *MAGED2*-Expression. Schließlich wurde gezeigt, dass *MAGED2* auch unter einer Reihe von Stressbedingungen erforderlich ist, um Autophagie zu hemmen. Die Induktion der Autophagie durch Gas-Knockdown und ihre Umkehrung durch Forskolin zeigen die hemmende Rolle des von *MAGED2* gesteuerten cAMP/ PKA-Signalwegs. Analog zur kontextabhängigen Funktion von *MAGED2* in Bezug auf die Endozytose von Gas nur unter Hypoxie zeigt sich auch in Bezug auf die Autophagie, dass *MAGED2* nur unter Stressbedingungen benötigt wird, im Gegensatz zu den bisher bekannten Mitgliedern der MAGE-Familie MAGEA3/A6, deren Verlust bereits in ungestressten Zellen Autophagie induziert. Da die Induktion der Autophagie auch durch Hypoxie und Depletion von Gas induziert und durch den cAMP/ PKA-Aktivator Forskolin gehemmt wird, könnte die kontextabhängige Regulation von Gas durch *MAGED2* der zugrunde liegender molekularer Schalter sein, der nur unter Stressbedingungen aktiviert wird.

### 3. Introduction

#### 3.1. Transient antenatal Bartter's syndrome

The kidneys, located along the posterior abdominal wall of the retroperitoneum, are vital organs that play essential roles in excretion of water-soluble waste products, maintenance of body fluids and electrolyte composition, acid-base balance, blood pressure regulation and production of hormones. The nephrons, approximately 1 million per kidney, constitute the functional units, each consisting of the renal corpuscle (including the glomerulus and Bowman's capsule) generating the ultrafiltrate and the renal tubule, which processes the ultrafiltrate. The renal tubule is divided into distinct sections with specific roles in reabsorption and secretion. These sections include the proximal tubule, the loop of Henle (comprising a thin descending limb, a hairpin turn, which ascends through the thin ascending limb into the thick ascending limb (TAL)), the distal convoluted tubule (DCT), and the collecting duct. Kidney diseases encompass a broad spectrum of conditions that can impair the normal functioning of these vital organs. One notable tubular condition is Bartter's syndrome (BS), a rare genetic disorder, characterized by severe hypokalemia and metabolic alkalosis. Of note, patients have low to normal arterial blood pressure despite their hyperreninemic hyperaldosteronism [1, 2]. This syndrome is caused by mutations in genes coding for ion transporters and/ or regulatory subunits in TAL and/ or DCT, which impair renal electrolyte reabsorption. Mutations in *SLC12A1* encoding for the luminal, furosemide-sensitive  $\text{Na}^+$ - $\text{K}^+$ - $2\text{Cl}^-$  co-transporter NKCC2 cause BS1 (type 1) [3], while mutations in *KCNJ1* encoding for the luminal  $\text{K}^+$  channel ROMK cause BS2 [4]. BS3 is caused by mutations in *CLCNKB* encoding for the basolateral  $\text{Cl}^-$  channel [5, 6]. BS4a combined with sensorineural deafness, results from loss of function mutations in *BSND*, the regulatory  $\beta$  subunit of chloride channels, Barttin [7, 8] while simultaneous mutations in both *CLCNKA* and *CLCNKB* encoding for the basolateral  $\text{Cl}^-$  channels lead to BS4b [9, 10]. Apart from BS3, the three other types of BS have a prenatal onset. A recently identified X-linked recessive form ("tBS5") caused by mutations in *MAGED2* (Melanoma-Associated Antigen D2) [11] leads to intracellular retention of both the furosemide-sensitive  $\text{Na}^+$ - $\text{K}^+$ - $2\text{Cl}^-$  co-transporter NKCC2 and its close homologue the thiazide-sensitive  $\text{Na}^+$ - $\text{Cl}^-$  co-transporter NCC. Impairment of both salt-transport proteins explains the severe polyuria as it

corresponds to simultaneous inhibition of salt-transport with the diuretics furosemide and thiazide (so called “sequential nephron blockade”).

*MAGED2* mutations primarily affect males as the gene is located in Xp11.2, a region characterized as a hot spot for mental retardation. Intriguingly, tBS5 was also detected in 2 girls from the French cohort due to skewed X-inactivation. To date, 26 different *MAGED2* mutations have been described [12], all of which cause polyhydramnios or Bartter syndrome. Of these, 19 functional knockouts comprising 2 entire gene deletion and 17 splice site, frameshift and nonsense mutations which result in premature termination codons (PTC) and potentially trigger a process known as nonsense-mediated decay (NMD). NMD serves as an important RNA quality control mechanism that removes PTC-containing mRNA transcripts, ensuring integrity and quality of the entire transcriptome [13]. The other seven mutations consist of three in frame deletions and four missense mutations, which ultimately reduce the stability of the protein.

Compared to BS1-4, tBS completely resolves over time despite its marked polyuria and fetal macrosomia [2]. Because *MAGED2* is constitutively expressed in the distal tubule from early fetal development into adulthood [14], it does not explain the spontaneous recovery from transient Bartter’s syndrome. Resolution of symptoms implies the involvement of external factors causing the termination of polyuria. In this research project, I studied the potential effects of hypoxia, a condition to which the fetal kidneys are subjected until the 30th week of gestation and which is essential for normal kidney nephrogenesis. This investigation is the result of the hypothesis that changes in the cellular microenvironment may be influenced by hypoxia, especially in cases of tBS, where the onset of spontaneous recovery coincides temporally with the cessation of hypoxia.

### 3.2. Structure and biological functions of *MAGED2*

*MAGED2* is a member of the Melanoma associated antigen (MAGE) gene family, which is conserved across eukaryotes (~ 40 genes). This family is subdivided into two groups according to their tissue distribution [15]. Type I MAGEs (MAGEs A-C), also defined as cancer-testis antigens, are primarily expressed in the testis. Type II MAGEs (MAGEs D-G) are ubiquitously expressed [16]. *MAGED2* encodes 11 exons in contrast to the majority of other family members containing one exon. This indicates *MAGED2* to be the ancestral gene [17-19], from which the other members

were derived as “retrogenes”. At the structural level, all members of the MAGE-family share a common feature known as MAGE homology domain (MHD) which spans a stretch of ~200 amino acids [20]. The dynamic flexibility of the MHD provides unique binding preferences and enables MAGE proteins to exert their functions through binding to specific E3 ligases (both RING and HECT type ligases). These E3 ligases form a diverse group of over 700 proteins acting as scaffolds to facilitate ubiquitin transfer to client proteins, thereby modulating ubiquitination and deciding their fate [21, 22]. Ubiquitination is a posttranslational modification that involves the transfer of a highly conserved ubiquitously expressed protein hence called Ubiquitin (75 amino acids) in a multistep ATP-dependent manner to specific lysine-residues on target proteins in single or multi ubiquitin chains. This process requires three enzymes: an ubiquitin-activating enzyme (E1), an ubiquitin conjugating enzyme (E2) and an ubiquitin ligase (E3). Ubiquitination regulates, among other functions, endocytic removal of plasma membrane protein, trafficking, sorting or ubiquitin-dependent degradation. Ubiquitin itself contains seven lysine residues (K6, K11, K27, K29, K33, K48, K63), each capable of forming isopeptide bonds with the COOH terminus of other ubiquitin molecules [23]. As a result, various chains with different combinations of ubiquitin linkages can be formed, leading to diverse functional outcomes. For instance, K48-linked chains result in the proteasomal degradation of target proteins, while substrates conjugated with K63 chains are subjected to nonproteasomal processes.

The MAGE family is engaged in diverse cellular functions and contribute to maintain normal physiology. Besides its role in ubiquitination regulation, numerous MAGE proteins have been implicated in transcriptional regulation, either through direct binding to the transcription factors or indirectly through regulating their cognate E3 ligases [24]. For example, MAGE-A3/6 and MAGE-C2 serve as specific regulators of the functional activity of TRIM28 in the context of transcriptional regulation, autophagy, apoptosis, and cell metabolism, thereby promoting cell growth and tumor survival [25-28]. Under genotoxic and nutritional stress, MAGE-A proteins are indispensable to maintain spermatogenesis [29]. Analogously, MAGE-B2/-b4 impede the formation of stress granule and enhance cellular stress tolerance, providing a growth advantage to cancer cells and heat tolerance to male germ cells [30]. Furthermore, MAGE-G1 is essential to preserve genome stability, insofar as missense mutations in MAGE-G1 are associated with lung disease immunodeficiency and chromosome breakage syndrome [31]. MAGE-L2 regulates endosomal protein trafficking and its variations contribute to the neurodevelopmental disorder

[32]. MAGE-D1 is required for orchestrating apoptosis during embryonic development and neurogenesis [33]. Lastly, MAGE-F1 emerges as a key player in regulating the cytosolic iron-sulfur (Fe-S) assembly (CIA) pathway [34].

MAGED2 localizes to the cytoplasm, nucleoplasm, and nucleoli, which changes throughout the cell cycle and in response to cellular stress [35]. Under conditions of genotoxic or nucleolar stress, MAGED2 is translocated from nucleoli to the nucleoplasm as a result of destabilization of the nucleoli. This exclusion process is dependent on the phosphorylation activity of mitogen-activated protein kinases (MAPKs) and indicates a potential role of MAGED2 in the regulation of cell cycle [35], similar to MAGED1, which was earlier reported to regulate cell cycle and proliferation [20, 36]. Additionally, DNA lesions following camptothecin treatment in MAGED2 depleted U2OS cells revealed its role in the DNA damage response (DDR). ATM (Ataxia-telangiectasia mutated) and ATR (ATM-and Rad3-Related) kinases are the key upstream transducers of the DDR cascade. These kinases transmit signals to mediators and effectors that govern various cellular processes including cell cycle arrest, DNA repair, regulation of transcription factors, and initiation of apoptosis. MAGED2 modulates phosphorylation of specific downstream targets of these kinases, and plays a crucial role in regulating the levels of two major cyclin-dependent kinase inhibitors p21 and p27, which are essential for facilitating cell cycle arrest [37]. These roles provide valuable insights into the significance of MAGED2 in maintaining genome stability.

Moreover, MAGED2 protein is upregulated in colorectal cancer and correlates positively with the occurrence of metastasis in the liver [38]. It was suggested to be a potential biomarker for assessing the malignant characteristics of gastric cancer (GC), both in gastric tissues and serum samples [39]. MAGED2 was further reported to be upregulated following a mineral dust-induced gene (mdig)-knockout in triple-negative breast cancer TNBC MDA-MB-231 cells. The acquisition of the metastatic potential and the epithelial-mesenchymal transition (EMT) characteristics of the cancer cells is suggested to occur due to increased enrichment of histone H3 lysine 36 trimethylation (H3K36me3) on the genome and specific genes, including MAGED2. Importantly, depletion of MAGED2 through siRNA silencing resulted in a reduction of the invasive potential of the mdig-KO cells, indicating that MAGED2 might be a positive regulator for the invasive migration, motility, or metastatic capabilities of the mdig-KO cells [40].

MAGED2 was found to interact physically with p53, the known regulator of apoptosis or cell cycle arrest, and impair its transcriptional activity in human cancer cells [41]. The p53 protein is classified as a tumor suppressor, characterized by its possession of domains responsible for transcriptional activation, DNA binding, and oligomerization. Its role in suppressing tumorigenesis is realized through the initiation of a diverse array of effector pathways [42]. In response to diverse cellular stressors, including DNA damage, oxidative stress, and aberrant oncogenic signaling, p53 undergoes activation. This activation transforms p53 into a transcription factor, instigating a series of events that encompass DNA repair, cell cycle arrest, programmed cell death, and cellular senescence [43]. MAGED2 interaction with p53 is cell-specific and dependent on the cellular microenvironment [41]. Additionally, MAGED2 negatively regulates the expression of tumor necrosis factor-related apoptosis-inducing ligand (TRAIL), thereby protecting melanoma cells from TRAIL-induced apoptosis [44].

### 3.3. G-alpha-S

Heterotrimeric guanine-nucleotide-binding regulatory proteins (G-proteins) are essential mediators of communication between external stimuli and intracellular responses. They primarily convey the signals from G-protein-coupled receptors (GPCRs) activated by diverse ligands, thereby acting as versatile molecular switches to regulate a variety of cellular activities, including neurotransmission, hormone signaling, cell proliferation and immunological responses [46-48]. G-proteins comprise 3 subunits:  $\alpha$ ,  $\beta$  and  $\gamma$ .  $G\alpha$  subunit consists of two domains: a Ras-like GTPase domain (RasD) and an  $\alpha$ -helical domain (AHD). In between lies a deep cleft where GDP or GTP tightly binds, representing inactive / active states, respectively, based on the ligand binding to the receptor (antagonists, inverse agonists, or agonists) [49]. There are 4 types of  $G\alpha$  subunits:  $G\alpha_s$  (stimulating adenylate kinase),  $G\alpha_i$  (inhibiting adenylate kinase),  $G\alpha_q$ , and  $G\alpha_{12}$  according to the sequence and functional similarities. The  $G\alpha_s$  family has 2 members;  $G\alpha_s$ , which is expressed in most cells and  $G\alpha_{olf}$ , which is specific for the olfactory sensory neurons. Both  $\beta$  and  $\gamma$  are closely associated as one functional dimer  $G\beta\gamma$  [50]. The crystal structure of  $G\beta\gamma$  demonstrates that  $G\beta$  folds into 7 blades of  $\beta$ -propeller, where each blade consists of four-stranded  $\beta$ -sheets. The  $\alpha$ -helical segment in the N-terminal of  $G\beta$  establish a tight coiled-coil interaction with the  $\alpha$ -helical

segment in the N-terminal of  $G\gamma$  subunit while the C-terminal  $G\gamma$   $\alpha$  helix interacts with the face of  $G\beta$  subunit propeller. Upon agonist binding, GPCRs acts as (GEF) guanine nucleotide exchange factors accelerating the release of the bound guanosine diphosphate (GDP) from  $G\alpha$  and its replacement by guanosine triphosphate (GTP) in a process defined as switch [51, 52]. This conformational change leads to  $G\alpha$  dissociation from  $G\beta\gamma$ , and initiates the downstream signals. Both the  $\alpha$  subunit and the  $\beta\gamma$  dimer can independently interact with various effector molecules, such as adenylyl cyclases, ion channels, or phospholipases, thereby initiating downstream signaling pathways. The signaling of  $G\alpha$  is terminated by the intrinsic  $G\alpha$ -GTPase activity which hydrolyzes the bound GTP to GDP. Interestingly, GDP re-association also ends the signaling of  $G\beta\gamma$ . The well-established function of  $G_{\alpha s}$ , our main focus, is to stimulate the membrane-bound adenylyl cyclases to convert ATP into cAMP, which results in activation of protein kinase A (PKA), EPAC (a GEF for Rap small GTP-binding proteins), and cyclic nucleotide-gated channels [53]. In contrast,  $G_{\alpha i}$  inhibits specific isotypes of adenylyl cyclases, while the  $G_{\alpha q}$  family on the other hand activates the  $\beta$ -isoforms of phospholipase C ( $\beta 1-4$ ) [54].

Previous studies have revealed the importance of  $G_{\alpha s}$  in promoting salt reabsorption. Specifically, heterozygous loss of  $G_{\alpha s}$  reduced the expression of NKCC2 total protein by 50 % [55]. Conversely, activation of the cAMP/ PKA pathway was observed to promote the cell-surface expression of NKCC2 [56] and enhance the activity of NCC [57]. The severity of symptoms associated with tBS and its spontaneous resolution paralleled by a developmental increase of renal oxygenation could point to impaired  $G_{\alpha s}$  signaling under hypoxic stress as a consequence of *MAGED2* mutations. In support of a potentially protective role of *MAGED2* against hypoxic stress, recent studies demonstrated that the *MAGE* family protects against diverse forms of stress (radiation, genotoxic, and nutritional stress) [15]. Concurring with this notion, the expression of *MAGED2* is upregulated in murine kidneys in response to AKI caused by an overdose of folic acid [58].

### 3.4. Hypoxic induction of HIF-1 $\alpha$

Hypoxia-inducible factor 1 (HIF-1) is a transcription factor which has critical roles in the cellular responses to hypoxia, as well as in a variety of physiological and pathological circumstances



(myocardial and cerebral ischemia, and tumor angiogenesis) [59]. It consists of a constitutively expressed HIF-1 $\beta$  and an oxygen-regulated HIF-1 $\alpha$  subunit [60]. Under normoxic conditions, HIF-1 $\alpha$  is hydroxylated by prolyl hydroxylases (PHDs), resulting in its recognition by the von Hippel-Lindau tumor suppressor protein (pVHL), an E3 ubiquitin-ligase subunit, which targets HIF-1 $\alpha$  for proteasomal degradation [61]. Under hypoxic conditions, PHDs are inactivated [62] leading to HIF-1 $\alpha$  stabilization and translocation along with HIF-1 $\beta$  into the nucleus. The dimer binds to specific DNA sequences, defined as hypoxia response elements (HREs), located in the promoters of genes responsible for orchestrating adaptive responses to oxygen deprivation; the vascular endothelial growth factor (*VEGF*) which promotes vasculogenesis [63] and erythropoietin (*EPO*) which stimulates red-cell production. Moreover, under hypoxic condition, HIF-1 $\alpha$  modulates metabolism by targeting glucose transporters (*GLUT1*, *GLUT3*) and glycolytic enzymes, which elicits a switch from oxidative to glycolytic metabolism. Additionally, HIF-1 $\alpha$  upregulates the expression of pyruvate dehydrogenase kinase 1 (*PDK1*) to suppress the mitochondrial oxidative metabolism [64]. During gestation, HIF-1 $\alpha$  is of great importance considering the potential exacerbation of fetal hypoxia caused by a variety of internal (maternal anemia, placental insufficiency, umbilical cord pre-eclampsia, cardiac and pulmonary disease) and external factors (smoking, environmental pollutants, and living at high altitude ~140 million people worldwide). In this study, the potential role of MAGED2 on HIF-1 $\alpha$  induction was investigated based on the finding of PKA-dependent phosphorylation which stabilizes HIF-1 $\alpha$  [65].

### 3.5. Stress-induced autophagy

Autophagy is a lysosome-based highly conserved catabolic process to ensure cellular homeostasis by efficient recycling of cellular components. The term "autophagy" originates from the Greek words αὐτό (self) and φαγος (devouring). It is a fundamental process to eliminate damaged organelles, protein aggregates, and pathogens, thus serving as the major stress-induced quality control machinery [66]. This role is in tandem with the ubiquitin–proteasome system (UPS), which is in charge of small, short-lived proteins [67]. Autophagy enables cells to adapt to metabolic stresses, and facilitates renovation during development and cellular differentiation [68]. Dysregulation of autophagy is linked to various diseases including neurodegeneration and cardiovascular disorders, infectious diseases, immune response malfunction and aging [69-73].

The molecular mechanisms of autophagy have been comprehensively studied and involve a series of tightly controlled steps. The core machinery is driven by ATGs (autophagy related genes) and the induction is initiated by Atg1 complex (mammalian complex ULK) [74, 75]. The mechanistic target of rapamycin complex 1 (mTORC1), which senses nutrients and cellular stress, is an upstream negative regulator of this complex [76]. Upon numerous cellular stresses, ULK1 is activated, resulting in the phosphorylation of multiple downstream factors, thereby triggering the autophagy cascade. Proteins and lipids are then recruited to the phagophore formation site (PAS) through the activation of a phosphatidylinositol 3-kinase (PtdIns3K) complex which consists of the lipid kinase Vps34 together with the regulator proteins Beclin-1, Vps15, and Atg14 [77]. Membranes emerging at PAS expand by receiving a supply from the ER or circulating vesicles. Most of the intracellular organelles, including the ER, Golgi, endosomes, mitochondria and the plasma membrane have been reported to contribute to the formation of autophagosomes [78-82]. Two ubiquitin-like (Ubl) conjugation systems, Atg8 and Atg12, play essential roles in vesicle expansion and completion. Atg8 becomes conjugated to the lipid phosphatidylethanolamine (PE), while Atg12 forms a complex with Atg5. When the autophagosome is completed and sealed, it fuses with the lysosome to form an autolysosome, where the sequestered cytosolic cargos are degraded. In this work, we addressed the potential effects of MAGED2 depletion on stress-induced autophagy, considering the general role of the MAGE-protein family in protection against numerous stress conditions [15]. For instance, impaired spermatogenesis in response to nutritional or genotoxic stress was reported in MAGE-A2/A6/A8 knockout (KO) mice [29]. Furthermore, 2 members of the family, namely MAGEA3 and MAGEA6, inhibit autophagy. Their expression is confined to germline cells but they are reactivated in tumor cells following demethylation of the promoter. They are essential for the viability of cancer cells by triggering proteasomal degradation of AMPK via the E3 ubiquitin ligases TRIM28. The latter blocks AMPK-dependent autophagy, enhancing proliferation downstream of mTORC1, and promoting tumorigenicity [83]. The effects of MAGED2 depletion on the induction of autophagy were analyzed in vitro using 3 different cell lines exposed to a number of stress conditions; physical hypoxia, oxidative stress, ER stress (brefeldin A and tunicamycin), genotoxic stress and nutritional stress.

## 4. Results

### 4.1. MAGED2 is required for G $\alpha$ s localization at the plasma membrane under hypoxic conditions

Immunocytochemistry was used to monitor the distribution of endogenous and transiently expressed G $\alpha$ s (the stimulatory subunit of G-protein), in control and MAGED2 depleted HeLa and HEK293 cells. Under normoxia, MAGED2 depletion had no effect on the localization of G $\alpha$ s at the cell surface. However, when the cells were exposed to physical hypoxia or treated with CoCl<sub>2</sub> (Cobalt chloride, a hypoxia mimetic which inhibits prolyl hydroxylase activity [84]), the depletion of MAGED2 resulted in a striking change in the subcellular localization of G $\alpha$ s. Upon reoxygenation for 2 h and treatment with cycloheximide, a protein synthesis inhibitor which is used to eliminate the potential involvement of newly synthesized proteins, the colocalization of G $\alpha$ s at the plasma membrane was restored. The specificity of MAGED2's effect on G $\alpha$ s trafficking was further analyzed by examining the distribution of a prototypical member of GPCRs, the  $\beta$ 2-adrenergic receptor ( $\beta$ 2AR), which is well-known to interact physically and functionally with G $\alpha$ s. Immunocytochemistry and biotinylation assays were used to evaluate the cell surface expression of endogenous and transiently expressed  $\beta$ 2AR. Indeed, MAGED2 depletion did not affect the distribution of  $\beta$ 2AR under both normoxic and hypoxic conditions as evident by colocalization with biotinylated plasma membrane proteins and by immunoblotting against the endogenous  $\beta$ 2AR which revealed no difference in localization between control and MAGED2 depleted cells under the same condition. Of note, the degree of internalized  $\beta$ 2AR was significantly higher for both control and MAGED2 depleted cells under hypoxia. This observation has already been made and explained by the activation of the  $\beta$ 2-adrenergic receptor in response to hypoxia [85, 86].

### 4.2. MAGED2 depletion promotes endocytosis of G $\alpha$ s mediated by MDM2-dependent ubiquitination

The internalization of G $\alpha$ s under hypoxia may be attributed to endocytosis following MAGED2 depletion. To investigate this possibility, HeLa cells were treated with dynasore, a small molecule acting as GTPase inhibitor of dynamin-mediated endocytosis, which fully blocked the

internalization of G $\alpha$ s. Hence, we hypothesized that the inhibitory effect of MAGED2 on G $\alpha$ s endocytosis could result from inhibition of MDM2 (ubiquitin E3 ligase from the RING family) in response to the hypoxic stress [87, 88] given that MAGED2 interacts with both of G $\alpha$ s [14, 45, 89] and the ubiquitin E3 ligase MDM2 [90, 91], with the latter known to regulate G $\alpha$ s [89].

Co-immunoprecipitation (Co-IP) experiments were initially conducted to confirm the aforementioned interactions and MAGED2 pulled down both G $\alpha$ s and MDM2. Next, we addressed the question regarding the potential increase of MDM2-dependent ubiquitination of G $\alpha$ s following MAGED2 depletion. Indeed, immunoprecipitation (IP) revealed enhanced ubiquitination of G $\alpha$ s in MAGED2 depleted HEK293 cells compared to control cells. In further support of the hypothesis, immunocytochemistry demonstrated that MDM2 silencing by siRNA or chemical inhibition (using either HLI-373 or Sp-141 [92]), blocked endocytosis of G $\alpha$ s in MAGED2 depleted HeLa cells and G $\alpha$ s colocalized at the biotinylated plasma membrane. Finally, we mutated the 5 (out of 13) most exposed lysine residues of G $\alpha$ s, which are thought to be the acceptor sites for ubiquitin based on their accessibility, and substituted them with arginine. Compared to the internalization of overexpressed wildtype (WT) G $\alpha$ s, endocytosis of mutated G $\alpha$ s, triggered by hypoxia upon MAGED2 depletion, was blocked in HeLa cells as judged by immunocytochemistry. Notably, cholera toxin, which activates G $\alpha$ s by directly catalyzing ADP ribosylation of arginine 201 residue, causing its internalization [95], was used to verify the internalization of our mutated G $\alpha$ s construct to exclude the possibility that mutating the lysine residues locks mutated G $\alpha$ s irreversibly in the membrane.

#### 4.3. Consequences of G $\alpha$ s internalization on cAMP/ PKA pathway and downstream substrates

Upon agonist binding to GPCRs, a conformational change allows the receptor to interact with the heterotrimeric G protein, triggering its activation. The G $\alpha$  subunit dissociates then from the G $\beta\gamma$  dimer and, in the case of G $\alpha$ s, it stimulates the membranous adenylyl cyclase, which catalyzes the conversion of ATP to cAMP. G $\alpha$ s internalization and subcellular localization upon MAGED2 depletion is predicted to impair the cAMP generation. Therefore, cAMP levels and PKA activity (downstream of G $\alpha$ s) were assayed using ELISA and PepTag nonradioactive protein kinase assay,

respectively. Under hypoxia, reduced basal levels of cAMP in both HeLa and HEK293 cell lines following *MAGED2* depletion were observed combined with lower PKA activity. IBMX, a phosphodiesterase inhibitor, failed to abrogate the reduction while FSK reversed it implying that the observed reduction originates from impaired *G $\alpha$ s* signaling and not due to defects in the enzymes adenylyl cyclase or phosphodiesterase.

Considering that the cAMP/ PKA pathway phosphorylates and as a result stabilizes HIF-1 $\alpha$ , thereby enhancing its transcriptional activity [65, 96], we hypothesized that reduced PKA activity following *MAGED2* depletion might impair the induction of HIF-1 $\alpha$  in response to hypoxia. Immunoblots of *MAGED2* depleted HeLa and HEK293 cells demonstrated a significant reduction of HIF-1 $\alpha$  protein abundance compared to control. Since PKA phosphorylation was reported to stabilize HIF-1 $\alpha$  by suppressing its proteasomal degradation [65], cells were treated with the proteasome inhibitor MG132 in order to validate the link between impaired hypoxic induction of HIF-1 $\alpha$  and decreased PKA activity. Indeed, MG132 neutralized the reduction of HIF-1 $\alpha$  protein to control levels. Impaired induction of HIF-1 $\alpha$  in *MAGED2* depleted cells was independently verified for its functional importance by quantifying the mRNA level of HIF-1 $\alpha$  transcriptional target *GLUT1*, which showed a lower quantity compared to control cells [97]. In further support of our hypothesis, *G $\alpha$ s* depletion also reduced the hypoxic induction of HIF-1 $\alpha$ .

#### 4.4. cAMP/ PKA pathway activation downstream of *G $\alpha$ s* reverses the impact of *MAGED2* depletion on hypoxic HIF-1 $\alpha$ induction

To independently determine whether the effect of *MAGED2* knockdown on HIF-1 $\alpha$  expression is mediated by *G $\alpha$ s*, hypoxic *MAGED2* depleted HeLa and HEK293 cells were treated with two activators of cAMP/ PKA pathway. Isoproterenol, a  $\beta$ 2AR agonist which operates upstream of *G $\alpha$ s*, and forskolin acting downstream of *G $\alpha$ s* as direct activator of adenylyl cyclase. While forskolin significantly reversed the impaired induction of HIF-1 $\alpha$ , isoproterenol failed to induce HIF-1 $\alpha$  expression, thereby confirming that the essential regulation of *MAGED2* on HIF-1 $\alpha$  induction in response to hypoxia is mediated by *G $\alpha$ s*.

Interestingly, forskolin treatment promoted not only the expression of HIF-1 $\alpha$  but also that of *MAGED2*. Since the promoter of *MAGED2* contains four CREB1 (cAMP responsive element

binding protein 1) binding sites [98], FSK treatment and subsequent cAMP/ PKA activation was thought to trigger binding of the transcription factor CREB to the corresponding CREB1 sites. *MAGED2* mRNA levels were quantified by qPCR and confirmed higher gene transcription upon FSK treatment.

The primary cellular mediator of cAMP is protein kinase A (PKA), which is assembled as an inactive tetrameric holoenzyme composed of two regulatory (R) and two catalytic (C) subunits. The activation of PKA occurs upon cAMP binding to two sites on each of the R subunits, leading to holoenzyme dissociation and subsequent activation of the phosphorylation activity of the catalytic subunits [99]. There are two distinct types of R subunits, namely RI and RII, and each type has two isoforms: RI $\alpha$ , RI $\beta$ , RII $\alpha$ , and RII $\beta$ . Holoenzymes containing either RI or RII subunits are referred to as PKA type I or type II, respectively. The key difference between RI and RII lies in the inhibitory sequence (IS) which affect the holoenzyme assembly and the activity inhibition. RII subunits can be autophosphorylated, whereas RI subunits function as pseudosubstrates [100].

We next investigated which PKA isoform was responsible for activating HIF-1 $\alpha$  expression using two PKA inhibitors. We used (Rp-8-Br-cAMPs), a selective inhibitor for type I which activates PKA type II [101] and the non-selective Rp-cAMPs, which inhibits both type I and II. Treatment with Rp-8-Br-cAMPs significantly induced HIF-1 $\alpha$  expression as evidenced by immunoblotting while the unselective Rp-cAMPs slightly lowered it. To further validate our findings, immunoblotting against the regulatory subunits RII $\alpha$  and RII $\beta$  was performed. Both RII $\alpha$  and RII $\beta$  were downregulated under hypoxic Rp-8-Br-cAMPs treatment reflecting higher PKA II activation. In line with this notion, *MAGED2* silencing in hypoxic HEK293 increased RII $\alpha$  and RII $\beta$  levels confirming the reduction of PKA type II activity.

#### 4.5. HIF-1 $\alpha$ enhances *MAGED2* expression under hypoxic condition

PKA type II promotes HIF-1 $\alpha$  expression and conversely, HIF-1 $\alpha$  increases the activity of PKA under hypoxic conditions [102]. Moreover, under hypoxia, PKA activation induced by FSK treatment augmented both mRNA and protein levels of *MAGED2*. We evaluated the effect of HIF-1 $\alpha$  depletion under hypoxia on *MAGED2* transcriptional and protein levels and observed a significant decrease in *MAGED2* levels following HIF-1 $\alpha$  silencing in HEK293 cells.

#### 4.6. MAGED2 depletion promotes stress-induced autophagy

Based on the established functional roles of MAGE family genes and their reported protective effects against stress, together with our recent finding concerning the fundamental role of MAGED2 in activating the cAMP/ PKA pathway and its corresponding protection from hypoxic stress, we sought to investigate the effect of MAGED2 depletion on autophagy, the major quality control stress-induced pathway, responsible for cell homeostasis.

The autophagic response was primarily investigated in the renal cell line HEK293 by immunoblotting against p62/SQSTM1 (a classical selective autophagy receptor), ATGs (autophagy related genes) and LC3B (a standard marker for autophagosome). Additionally, immunocytochemistry was used to monitor the LC3B puncta, not only in HEK293 but also in HeLa and U2OS cells. Unlike HeLa and HEK293, U2OS harbors functional p53.

Under normoxic condition, MAGED2 depletion had no effect neither on ATG5-ATG12 complex levels, which alongside ATG16 are crucial for autophagosome formation, nor on the conversion to the lipidated form LC3II. In contrast, physical hypoxia or oxidative stress induced by CoCl<sub>2</sub> in MAGED2 depleted cells led to a statistically significant increase in ATG5-ATG12 complex, and LC3II levels. The autophagy flux was further assayed using p62 and the leupeptin based assay. As a protease inhibitor, leupeptin blocks the deterioration of autophagy substrates and allows monitoring of LC3B turnover. MAGED2 depletion associated with reduced p62 levels in addition to the highest accumulation of LC3II when treated with leupeptin, which confirmed a higher induction of the autophagy machinery.

The quantities of *ATG5* and *ATG12* mRNA levels were confirmed to be upregulated in MAGED2-depleted hypoxic HeLa and HEK293 cells by qPCR. Concurring, immunocytochemistry in all three cell lines exposed to hypoxia, revealed a markedly higher accumulation of LC3B puncta in MAGED2 depleted cells.

#### 4.7. ER stress, genotoxic stress and nutritional stress induce autophagy upon MAGED depletion

Both the physical hypoxia and the CoCl<sub>2</sub>-induced oxidative stress display a common characteristic of provoking endoplasmic reticulum stress. This observation may indicate that other ER promoting stressors could potentially trigger autophagy significantly upon MAGED2 depletion. We investigated numerous stressors, namely;

- Tunicamycin (Tun), which disturbs the secretory pathway by inhibiting N-linked glycosylation of membrane- and secreted proteins
- Brefeldin A (BFA), which blocks the exit of secretory proteins from the ER by disintegrating the Golgi-apparatus [104].
- Camptothecin (CPT), which stabilizes the topoisomerase I cleavage complex [105] and induces cellular stress beyond DNA damage. It is known to elevate ER stress in various cancer cell lines [106, 107] and promote G<sub>2</sub>/M phase cell cycle arrest mediated by reactive oxygen species (ROS) [108].
- 2-Deoxy-D-glucose (2-DG), a glucose analog that triggers nutritional stress by inhibiting glycolysis [109, 110], thus reducing cellular ATP levels. As a consequence of its structural similarity with mannose, it also interferes with oligosaccharide synthesis causing abnormal N-linked glycosylation and hence ER stress [111].

All three cell lines treated with the aforementioned stressors exhibited increased autophagy as shown by reduced p62 levels, upregulated ATG5-ATG12 conjugate and higher LC3II abundance in MAGED2 depleted cells.

#### 4.8. Depletion of Gas promotes autophagy while forskolin activation of the cAMP/ PKA pathway inhibits it

Given that MAGED2 regulates Gas and, consequently, the cAMP/ PKA pathway, we investigated whether Gas depletion would induce autophagy under hypoxic stress. As expected, reduced levels of p62 in conjugation with elevated expression of ATG5-ATG12 complex and LC3II turnover were detected upon Gas depletion similar to MAGED2 knockdown. Interestingly, the induction was



abrogated by forskolin which was accompanied by a reduction in LC3B expression and a diminished autophagic turnover as evident by immunoblotting and immunocytochemistry.

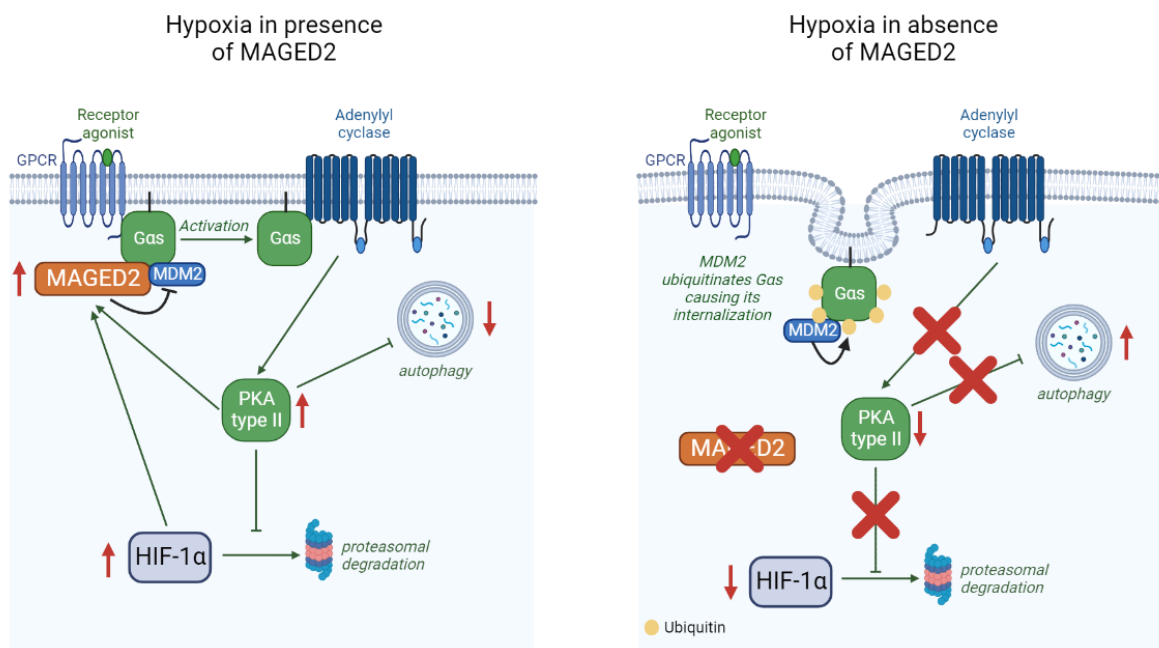


**Figure.1 A model illustrates MAGED2 roles under hypoxic stress (generated using BioRender.com.)**

MAGED2 is essential under hypoxia to inhibit endocytosis of Gαs mediated by MDM2. This inhibition secures cAMP generation and subsequent PKA activation. PKA II stabilizes HIF-1α by inhibiting its proteasomal degradation, the latter reciprocally augments the transcription of MAGED2. Endocytosis of Gαs upon MAGED2 depletion reduces cAMP/ PKA pathway activation, impairs HIF-1α induction, and promotes stress induced autophagy in response to hypoxia. Reduced expression of the salt transporters NKCC2 and NCC and hence salt-reabsorption in transient Bartter's syndrome may result from impaired cAMP generation and/ or from enhanced autophagy of the transporters under hypoxia, which may explain the transient nature of the disease.

## 5. Discussion

*MAGED2* mutations cause massive polyuria and acute early-onset polyhydramnios, a condition observed in fetuses and newborns. It is a rare X-linked recessive renal tubular disorder characterized by excessive urine production and significant renal salt wasting, due to impaired salt reabsorption specifically in the TAL and DCT [14]. Notably, extreme prematurity and elevated perinatal mortality rates are associated with the syndrome [14]. It is known as transient Bartter syndrome (tBS), because the marked renal salt wasting gradually resolves around the 30th week of gestation despite the continuous expression of *MAGED2* in the distal tubule, persisting from early fetal development through to adulthood. This resolution suggests involvement of external factors that determines the phenotype of transient Bartter syndrome, ultimately terminating the polyuria. In this thesis, the significance of hypoxia, a crucial determinant during kidney development, was addressed given that the onset of recovery from polyuria coincides with increased renal oxygenation.

The key observation of our study was endocytosis of Gas under hypoxia upon *MAGED2* depletion. The exact mechanisms governing Gas dissociation from the plasma membrane was previously unknown. One of the proposed mechanisms include its depalmitoylation, followed by simple diffusion through the cytosol [117]. Accordingly, a diffuse cytosolic pattern of Gas upon stimulation with agonists has been reported [118, 119]. However, association with intracellular vesicles has also been observed [120-122]. Here, we report the MDM2-dependent ubiquitination of Gas and its subsequent endocytosis, demonstrating for the first-time ubiquitination of Gas as a signal for endocytosis. This mechanism relies most likely on the MHD domain, which allows MAGEs to exert their functions through interactions with E3 ligases, thereby modulating the ubiquitination of target proteins and guiding their fate [21]. In particular, *MAGED2* was reported to interact with both Gas [14, 45, 89] and MDM2 [90, 91], the latter of which has already been shown to promote proteasomal degradation of Gas [89]. Our finding of increased non-degradative ubiquitination and concurrent endocytosis of Gas upon *MAGED2* silencing, suggest a regulatory role of *MAGED2* similar to other members of the MAGE family, such as *MAGEA2* and *MAGEC2*, which inhibit the ligase activity of MDM2 [27, 123]. Alternatively, physical shielding of Gas by sequestering MDM2 might be a mechanism by which *MAGED2* controls the localization of membrane proteins.

Of interest, a recent study showed that the MHD-domain of MAGED2 promotes closing of the alpha helical domain of G $\alpha$ s upon binding of GTP, which occurs subsequently to activation of GPCR. However, it was not shown in this study whether the closed state of the alpha helical domain of G $\alpha$ s promotes downstream-signaling of G $\alpha$ s [116].

Our finding corroborates the previously described activity of MDM2 in regulating the distribution of GPCRs, where MDM2-dependent ubiquitination of  $\beta$ -Arrestins (ARRB2) -proteins, which turn off G-protein signaling- mediates the endocytosis of the  $\beta$ 2 adrenergic receptor under normoxia [124]. We also reveal the specificity of MAGED2's activity, considering that the intracellular trafficking of G $\alpha$ s did not correlate with internalization of the  $\beta$ 2 adrenergic receptor. Of note, compared to normoxia, hypoxia decreased  $\beta$ 2AR protein abundance at the cell surface regardless of MAGED2 depletion, consistent with previous reports of  $\beta$ 2AR activation in response to hypoxia [85, 125]. Remarkably, the activity of MDM2 is not only substrate specific but also responsive to changes in the cellular microenvironment: MAGED2 depletion under hypoxia leads to internalization of G $\alpha$ s, while during reoxygenation, G $\alpha$ s rapidly colocalizes at the plasma membrane. These observations suggest the presence of a molecular switch potentially mediated by posttranslational modifications of MDM2 and/or its interacting partners.

Internalization of G $\alpha$ s in MAGED2-depleted cells under hypoxia, reduced cAMP generation and PKA activity and impaired the induction of the downstream target HIF-1 $\alpha$ . HIF-1 $\alpha$  induction in response to hypoxic environment is critical to activate the transcription of many essential genes involved in adaption of oxygen deprivation. During gestation, the reabsorption of salt and water from the renal medulla, which has lower oxygen tension in comparison to the renal cortex [103, 126-128], is very crucial. This is evident by loss of function mutations in NKCC2, a protein expressed in the medulla and accounts for 30% of filtered sodium reabsorption, leading to profound renal salt wasting [129].

Similar to MAGED2 depletion, G $\alpha$ s silencing impaired the full induction of HIF-1 $\alpha$  under hypoxia emphasizing our findings with regard to MAGED2's essential role for G $\alpha$ s localization and cAMP generation. The impairment was fully reversed by forskolin, the adenylyl cyclase activator, acting downstream of G $\alpha$ s in contrast to the lack of effect of isoproterenol, which acts upstream of  $\beta$ 2AR. Next, using specific inhibitors, PKA type II was identified, to be the isoform engaged in this regulation, consistent with its broad expression in the majority of organs [130, 131], in contrast to

PKA type I which is primarily expressed in the brain [132].Concurreingly, MAGED2 depletion caused upregulation of the regulatory subunits RII $\alpha$  and RII $\beta$  indicating a lower induction of PKA type II in agreement with others [102].

Of note, HIF-1 $\alpha$  promotes expression of MAGED2 and vice versa. This conclusion is deduced from the decrease in both MAGED2 mRNA and protein levels following HIF-1 $\alpha$  silencing. Given that MAGED2 promoter does not have HRE elements, the possibility of direct transcriptional activation by HIF-1 $\alpha$  is excluded. Alternatively, the cAMP/ PKA pathway mediated regulation provides a plausible explanation, knowing that the promoter of *MAGED2* has four CREB1 binding sites [98]. A reduction in cAMP generation and PKA activity subsequent to HIF-1 $\alpha$  depletion may explain the observed downregulation of MAGED2 expression.

Interestingly, more than 40 years ago,  $\beta$ -blockers, which reduce generation of cAMP, were found to reduce the expression of erythropoietin, a transcriptional target of HIF-1 $\alpha$ . Additional studies characterized the links between HIF-1 $\alpha$  and the cAMP/PKA pathway: A hypoxia-specific phosphorylation of the  $\beta$ 2 receptor is critical for HIF-1 $\alpha$  activation [86], PKA phosphorylation stabilizes HIF-1 $\alpha$  [65, 96], HIF-1 $\alpha$  induces the transcription of adenylyl cyclase VI and VII taking into consideration the essential contribution of adenylyl cyclase VI in NKCC2 and NCC expression and phosphorylation [133, 134], and hypoxia increases PKA activity [102, 135]. In this study, we reported interdependent regulation of MAGED2 and HIF-1 $\alpha$  via PKA type II under hypoxic conditions and introduced an amplification loop governed by MAGED2 as a master regulator, thereby extending the unidirectional links between cAMP/PKA and HIF-1 $\alpha$  and vice versa.

Although our work was conducted in cell culture, the reciprocal regulation is likely to occur in native tissues, especially the kidney. While MAGED2 protein is constitutively expressed in the distal tubule [14, 58], HIF-1 $\alpha$  protein is absent in adult kidneys. However, both proteins are induced in the distal tubule of the kidney in rodent models of AKI [58, 136]. Additionally, HIF-1 $\alpha$  protein has been observed in humans post-engraftment biopsies following renal transplantation [137], and the exogenous activation of HIFs by small molecules or genetic techniques has been reported to confer protective effects in animal models of AKI [138]. Targeting MAGED2 as a master regulator could serve as a potential intervention to promote HIF-1 $\alpha$  induction, which might be beneficial in acute renal failure.

The links between the key players MAGED2, cAMP/PKA and HIF-1 $\alpha$  yield further insights into the transient nature of Bartter syndrome and the severe renal salt wasting attributed to the impairment of salt-transporters NKCC2 and NCC. These findings align with a prior report emphasizing the importance of Gas in promoting salt reabsorption and its significance for NKCC2 total protein expression [55]. Furthermore, the generation of cAMP induced by hormones like vasopressin, triggers renal tubular salt and water reabsorption [139] and the activation of the cAMP/ PKA pathway serves as a key regulator of cell surface expression of NKCC2 [56] and enhances NCC activity [57]. However, this may not explain entirely the profound salt wasting related to post-Golgi regulation of NKCC2 and NCC and shuttling both to the cell surface. Other cellular mechanisms engaged in homeostasis may come into play under hypoxic stress, such as ER retention and associated degradation of the cotransporters (ERAD). In this regard, we previously demonstrated that the export of proteins from the ER is essential for NKCC2 maturation and distribution to the cell surface. This process is subjected to alterations particularly under ER stress conditions [140-144]. Of note, ER stress may also result from the transient overexpression of proteins [145] especially transmembrane proteins [146]. The severity of ER stress in MAGED2 depleted cells could potentially explain the impairment in NKCC2 and NCC maturation arguing for a protective role of MAGED2 [14].

Based on the notion of stress protection conferred by the MAGE family and the reported involvement of 2 members, namely MAGEA3 and MAGEA6, in autophagy inhibition, the effect of MAGED2 silencing on autophagy was investigated. Inhibition of the ligase activity of MDM2 by MAGED2 shown in our study, and by MAGEA2 and MAGEC2 in other studies, may increase p53 levels, which could affect important experimental readouts, namely adaption to hypoxia and regulation of autophagy. p53 is the cellular “gatekeeper” which regulates autophagy either positively through transcription-dependent or -independent fashion [148] or negatively, depending on its subcellular localization [149]. Hence, the experiments were carried out in permanent cell lines with either inactive p53 (HEK293 and HeLa) or functional wildtype p53 (U2OS). Our data disclosed inhibition of stress-induced autophagy mediated by MAGED2 in various cell lines independent of p53. By validating MAGED2’s crucial role for Gas localization particularly under hypoxia while being dispensable under normoxia, we expanded the range of stressors (nutritional, genotoxic, oxidative and ER stress) and demonstrated that all induced autophagy in MAGED2 depleted cells. This induction aligns with the protective role of MAGED2 in response to stress but

differs from other studies which have reported induction of autophagy in unstressed, (HeLa, U2OS) and (A549, H1299), cells upon MAGEA3/A6 deletion [83] and/or MAGED1-depletion [150] respectively. It is conceivable that the ER-stressors are triggering endocytosis of Gas, similar to hypoxic stress, and presumably the MDM2-dependent ubiquitination of Gas upon MAGED2 depletion is the switch activated by all stressors in this study. Forskolin, the cAMP/ PKA cascade activator, reversed the observed induction of autophagy in MAGED2 depleted cells exposed to physical hypoxic or treated with tunicamycin. Its activation rescued LC3II accumulation and diminished the abundance of LC3 puncta. This may explain why the induction of autophagy is stress related, unlike unstressed conditions seen in MAGEA3/A6 knockout or MAGED1 depleted cells.

In further support of cAMP/ PKA implication, depletion of Gas induced the autophagy machinery under hypoxic conditions, in agreement with a previous study showing GPCRs regulation of autophagy through ubiquitination and proteasomal degradation of Atg14L (mammalian ortholog of yeast Atg14) controlled by ZBTB16-Cullin3-Roc1 E3 ubiquitin ligase complex. Knocking down Gas increased the levels of ATG14L and autophagic flux [151]. Furthermore, the effects of cAMP on autophagy are cell-type specific. While in yeast, high glucose levels which promote cAMP production, inhibit autophagy by the phosphorylation of Atg1 and Atg9, two key activators of macroautophagy [152], in mammalian cells, cAMP can either inhibit [153, 154] or promote autophagy [155, 156] depending on the cell type. One study stated that the differential effects of cAMP on the regulation of autophagy are based on cell-type specific compartmentalization of PKA activity [157]. Intriguingly, it was reported that only displacement of PKA type II (but not of PKA type I) reversed the effect of cAMP on autophagy, which aligns with our previous finding that MAGED2 regulates PKA type II. Because the effects of MAGED2 depletion on autophagy did not differ in cells with (U2OS) or without wildtype p53 (HEK293, HeLa), it was concluded that p53 is probably not playing a major role downstream of MAGED2 in our experimental setting.

While autophagy is currently considered insignificant for kidney development [158, 159], it plays an important role in maintaining the integrity and normal physiology of various adult kidney cells, including glomerular mesangial and endothelial cells, podocytes, and proximal tubule epithelial cells [160]. AQP2 has already been shown to be regulated by autophagy and its autophagic degradation was observed in hypokalemia-induced diabetes in rats [162], as proven by the

detection of AQP2 in autophagosomes in the inner medullary collecting duct (IMCD) cells of potassium-deprived rats using immunogold electron microscopy. Given that AQP2 is positively regulated by cAMP fits with our observation that induced autophagy and thus potentially autophagic degradation of AQP2, could be halted by activators of the cAMP/PKA pathway. A direct link between enhanced autophagy and the aberrant expression of the salt transporters NKCC2 and NCC in transient Bartter's syndrome is absent. However, lysosomal degradation of NCC is compatible with a role of autophagy in the regulation of this transporter [163]. It is worth noting that, induction of autophagy by rapamycin, which inhibits mTOR [69], has been reported to alleviate hypertension in Dahl salt sensitive rats [164] and the deletion of PKA phosphorylation substrate Raptor, which functions downstream of mTOR and inhibits autophagy, causes a Bartter's syndrome/ furosemide-like renal phenotype including the massive polyuria and hypercalciuria [165].

A very recent study revealed MAGED2 inhibition of SARS-CoV-2 genome replication in an RNA-dependent manner. The inhibition occurs through its interaction with SARS-CoV-2 nucleocapsid protein, which is essential for coronavirus genome replication and subgenomic RNA transcription. MAGED2 disrupts the association of the nucleocapsid protein (N protein) with the viral genome, thereby inhibiting viral replication [146]. Previous studies on MAGED2 were performed addressing cell proliferation and tumor biology [39, 44]. MAGED2 is expressed in many human cancers and has been linked to a poor prognosis [103, 166-169]. The hypoxic microenvironment within cancer cells is a crucial factor that influences the cellular expression program, ultimately leading to chemotherapy resistance [170]. Considering the well-known roles of Gas and HIF-1 $\alpha$  as oncoproteins in malignant processes [171-173], it is reasonable to propose that MAGED2 contributes to tumorigenesis by enhancing the cAMP/PKA-HIF-1 $\alpha$  pathway.

Because MAGED2's roles in cell-biology and tumorigenesis are complex, additional research under various experimental conditions (normoxia, hypoxia, oxidative stress, etc.) to unravel the context-dependent functions of MAGED2 is fundamental: Multiple insights have been gained from MAGED2 depletion in cells subjected to normoxic condition; the significant upregulation of AQP2 expression upon MAGED depletion in (mpkCCD) cells [161] or the reduction of the invasive potential of the mdig-KO triple negative breast cancer TNBC MDA-MB-231 cells after MAGED2 depletion [40]), which might be different under hypoxia.

In terms of therapeutic approaches, targeting the cAMP/PKA cascade downstream of G $\alpha$ s emerges as a potential treatment strategy for patients with transient Bartter syndrome. Enhancing salt reabsorption will prevent perinatal death and the complications originated from excess amniotic fluid production such as intracerebral hemorrhage which leads to preterm delivery. Although maternal hyperoxia may potentially stimulate the cAMP/PKA pathway [174], generation of reactive oxygen species precludes its use. Hence, we introduce forskolin as a direct cAMP/ PKA activator for further studies in models of transient Bartter syndrome. It can be orally administrated and has already been involved in former human clinical studies [175-179].

In conclusion, MAGED2 plays a crucial role in controlling the cAMP/PKA pathway under hypoxic conditions by regulating G $\alpha$ s membrane localization, which may explain both the altered expression of salt transporters as well as the transient nature of the syndrome. Hence, forskolin, a cAMP/PKA cascade activator acting downstream of G $\alpha$ s, is a promising potential intervention in transient Bartter's syndrome. MAGED2 is also involved in the interdependent regulation of HIF-1 $\alpha$ , influencing its induction and stabilization in renal and cancer cells. This suggests potential therapeutic applications in hypoxic tumors. Furthermore, MAGED2 inhibits autophagy, with its depletion promoting autophagy in response to various stressors. The inhibitory effect of MAGED2 on autophagy is dependent on the activation of the cAMP/PKA pathway, highlighting its significance in cancer development and kidney function. Understanding the multifaceted roles of MAGED2 in different cellular pathways under various stress conditions provides valuable insights into related diseases and offers potential avenues for therapeutic strategies.



## 6. References

1. Bartter, F.C., et al., *Hyperplasia of the juxtaglomerular complex with hyperaldosteronism and hypokalemic alkalosis. A new syndrome*. Am J Med, 1962. **33**: p. 811-28.
2. Legrand, A., et al., *Prevalence of Novel MAGED2 Mutations in Antenatal Bartter Syndrome*. Clin J Am Soc Nephrol, 2018. **13**(2): p. 242-250.
3. Simon, D.B., et al., *Bartter's syndrome, hypokalaemic alkalosis with hypercalciuria, is caused by mutations in the Na-K-2Cl cotransporter NKCC2*. Nat Genet, 1996. **13**(2): p. 183-8.
4. Simon, D.B., et al., *Genetic heterogeneity of Bartter's syndrome revealed by mutations in the K<sup>+</sup> channel, ROMK*. Nat Genet, 1996. **14**(2): p. 152-6.
5. Simon, D.B., et al., *Mutations in the chloride channel gene, CLCNKB, cause Bartter's syndrome type III*. Nat Genet, 1997. **17**(2): p. 171-8.
6. Konrad, M., et al., *Mutations in the chloride channel gene CLCNKB as a cause of classic Bartter syndrome*. J Am Soc Nephrol, 2000. **11**(8): p. 1449-1459.
7. Birkenhäger, R., et al., *Mutation of BSND causes Bartter syndrome with sensorineural deafness and kidney failure*. Nat Genet, 2001. **29**(3): p. 310-4.
8. Estévez, R., et al., *Barttin is a Cl<sup>-</sup> channel beta-subunit crucial for renal Cl<sup>-</sup> reabsorption and inner ear K<sup>+</sup> secretion*. Nature, 2001. **414**(6863): p. 558-61.
9. Kieferle, S., et al., *Two highly homologous members of the CIC chloride channel family in both rat and human kidney*. Proc Natl Acad Sci U S A, 1994. **91**(15): p. 6943-7.
10. Schlingmann, K.P., et al., *Salt wasting and deafness resulting from mutations in two chloride channels*. N Engl J Med, 2004. **350**(13): p. 1314-9.
11. Laghmani, K., et al., *Polyhydramnios, Transient Antenatal Bartter's Syndrome, and MAGED2 Mutations*. N Engl J Med, 2016. **374**(19): p. 1853-63.
12. Wu, X., et al., *A Case Report and Literature Review of a Novel Mutation in the MAGED2 Gene of a Patient With Severe Transient Polyhydramnios*. Front Pediatr, 2021. **9**: p. 778814.
13. Karousis, E.D. and O. Mühlemann, *The broader sense of nonsense*. Trends Biochem Sci, 2022. **47**(11): p. 921-935.
14. Laghmani, K., et al., *Polyhydramnios, Transient Antenatal Bartter's Syndrome, and MAGED2 Mutations*. 2016. **374**(19): p. 1853-1863.
15. Florke Gee, R.R., et al., *Emerging roles of the MAGE protein family in stress response pathways*. J Biol Chem, 2020. **295**(47): p. 16121-16155.
16. Lee, A.K. and P.R. Potts, *A Comprehensive Guide to the MAGE Family of Ubiquitin Ligases*. J Mol Biol, 2017. **429**(8): p. 1114-1142.
17. Chomez, P., et al., *An overview of the MAGE gene family with the identification of all human members of the family*. Cancer Res, 2001. **61**(14): p. 5544-51.
18. De Donato, M., et al., *Molecular evolution of type II MAGE genes from ancestral MAGED2 gene and their phylogenetic resolution of basal mammalian clades*. Mammalian Genome, 2017. **28**(9): p. 443-454.
19. Zhao, Q., et al., *Differential evolution of MAGE genes based on expression pattern and selection pressure*. PLoS One, 2012. **7**(10): p. e48240.
20. Barker, P.A. and A. Salehi, *The MAGE proteins: emerging roles in cell cycle progression, apoptosis, and neurogenetic disease*. J Neurosci Res, 2002. **67**(6): p. 705-12.
21. Doyle, J.M., et al., *MAGE-RING protein complexes comprise a family of E3 ubiquitin ligases*. Mol Cell, 2010. **39**(6): p. 963-74.
22. Hershko, A. and A. Ciechanover, *The ubiquitin system*. Annu Rev Biochem, 1998. **67**: p. 425-79.
23. Swatek, K.N. and D. Komander, *Ubiquitin modifications*. Cell Research, 2016. **26**(4): p. 399-422.

24. Foot, N., T. Henshall, and S. Kumar, *Ubiquitination and the Regulation of Membrane Proteins*. *Physiol Rev*, 2017. **97**(1): p. 253-281.
25. Xiao, T.Z., et al., *MAGE I transcription factors regulate KAP1 and KRAB domain zinc finger transcription factor mediated gene repression*. *PLoS One*, 2011. **6**(8): p. e23747.
26. Xiao, T.Z., Y. Suh, and B.J. Longley, *MAGE proteins regulate KRAB zinc finger transcription factors and KAP1 E3 ligase activity*. *Archives of Biochemistry and Biophysics*, 2014. **563**: p. 136-144.
27. Hao, J., et al., *Cancer-testis antigen MAGE-C2 binds Rbx1 and inhibits ubiquitin ligase-mediated turnover of cyclin E*. *Oncotarget*, 2015. **6**(39): p. 42028-39.
28. Pineda, Carlos T., et al., *Degradation of AMPK by a Cancer-Specific Ubiquitin Ligase*. *Cell*, 2015. **160**(4): p. 715-728.
29. Fon Tacer, K., et al. *MAGE cancer-testis antigens protect the mammalian germline under environmental stress*. *Science advances*, 2019. **5**, eaav4832 DOI: 10.1126/sciadv.aav4832.
30. Lee, A.K., et al., *Translational Repression of G3BP in Cancer and Germ Cells Suppresses Stress Granules and Enhances Stress Tolerance*. *Molecular Cell*, 2020. **79**(4): p. 645-659.e9.
31. van der Crabben, S.N., et al., *Destabilized SMC5/6 complex leads to chromosome breakage syndrome with severe lung disease*. *The Journal of Clinical Investigation*, 2016. **126**(8): p. 2881-2892.
32. Tacer, K.F. and P.R. Potts, *Cellular and disease functions of the Prader-Willi Syndrome gene MAGEL2*. *Biochem J*, 2017. **474**(13): p. 2177-2190.
33. Salehi, A.H., S. Xanthoudakis, and P.A. Barker, *NRAGE, a p75 Neurotrophin Receptor-interacting Protein, Induces Caspase Activation and Cell Death through a JNK-dependent Mitochondrial Pathway \**. *Journal of Biological Chemistry*, 2002. **277**(50): p. 48043-48050.
34. Weon, J.L., S.W. Yang, and P.R. Potts, *Cytosolic Iron-Sulfur Assembly Is Evolutionarily Tuned by a Cancer-Amplified Ubiquitin Ligase*. *Molecular Cell*, 2018. **69**(1): p. 113-125.e6.
35. Pirlot, C., et al., *Melanoma antigen-D2: A nucleolar protein undergoing delocalization during cell cycle and after cellular stress*. *Biochim Biophys Acta*, 2016. **1863**(4): p. 581-95.
36. Yang, Q., et al., *NRAGE promotes cell proliferation by stabilizing PCNA in a ubiquitin–proteasome pathway in esophageal carcinomas*. *Carcinogenesis*, 2014. **35**(7): p. 1643-1651.
37. Trussart, C., et al., *Melanoma antigen-D2 controls cell cycle progression and modulates the DNA damage response*. *Biochem Pharmacol*, 2018. **153**: p. 217-229.
38. Li, M., et al., *Genes associated with liver metastasis of colon cancer, identified by genome-wide cDNA microarray*. *Int J Oncol*, 2004. **24**(2): p. 305-12.
39. Kanda, M., et al., *The Expression of Melanoma-Associated Antigen D2 Both in Surgically Resected and Serum Samples Serves as Clinically Relevant Biomarker of Gastric Cancer Progression*. *Ann Surg Oncol*, 2016. **23 Suppl 2**: p. S214-21.
40. Thakur, C., et al., *Deletion of mdig enhances H3K36me3 and metastatic potential of the triple negative breast cancer cells*. *iScience*, 2022. **25**(10): p. 105057.
41. Papageorgio, C., et al., *MAGED2: a novel p53-dissociator*. *Int J Oncol*, 2007. **31**(5): p. 1205-11.
42. Stiewe, T., *The p53 family in differentiation and tumorigenesis*. *Nat Rev Cancer*, 2007. **7**(3): p. 165-8.
43. Pavlakakis, E. and T. Stiewe, *p53's Extended Reach: The Mutant p53 Secretome*. 2020. **10**(2): p. 307.
44. Tseng, H.Y., et al., *The melanoma-associated antigen MAGE-D2 suppresses TRAIL receptor 2 and protects against TRAIL-induced apoptosis in human melanoma cells*. *Carcinogenesis*, 2012. **33**(10): p. 1871-81.
45. Huttlin, E.L., et al., *Dual proteome-scale networks reveal cell-specific remodeling of the human interactome*. *Cell*, 2021. **184**(11): p. 3022-3040.e28.
46. Rosenbaum, D.M., S.G.F. Rasmussen, and B.K. Kobilka, *The structure and function of G-protein-coupled receptors*. *Nature*, 2009. **459**(7245): p. 356-363.

47. Gilman, A.G., *G PROTEINS: TRANSDUCERS OF RECEPTOR-GENERATED SIGNALS*. Annual Review of Biochemistry, 1987. **56**(1): p. 615-649.
48. Bourne, H.R., D.A. Sanders, and F. McCormick, *The GTPase superfamily: a conserved switch for diverse cell functions*. Nature, 1990. **348**(6297): p. 125-132.
49. Sprang, S.R., Z. Chen, and X. Du, *Structural basis of effector regulation and signal termination in heterotrimeric Galpha proteins*. Adv Protein Chem, 2007. **74**: p. 1-65.
50. Simon, M.I., M.P. Strathmann, and N. Gautam, *Diversity of G proteins in signal transduction*. Science, 1991. **252**(5007): p. 802-8.
51. Oldham, W.M. and H.E. Hamm, *Heterotrimeric G protein activation by G-protein-coupled receptors*. Nat Rev Mol Cell Biol, 2008. **9**(1): p. 60-71.
52. Vetter, I.R. and A. Wittinghofer, *The guanine nucleotide-binding switch in three dimensions*. Science, 2001. **294**(5545): p. 1299-304.
53. Wettschureck, N. and S. Offermanns, *Mammalian G proteins and their cell type specific functions*. Physiol Rev, 2005. **85**(4): p. 1159-204.
54. Rhee, S.G. and Y.S. Bae, *Regulation of phosphoinositide-specific phospholipase C isozymes*. J Biol Chem, 1997. **272**(24): p. 15045-8.
55. Ecelbarger, C.A., et al., *Decreased renal Na-K-2Cl cotransporter abundance in mice with heterozygous disruption of the G(s)alpha gene*. Am J Physiol, 1999. **277**(2): p. F235-44.
56. Ares, G.R., P.S. Caceres, and P.A. Ortiz, *Molecular regulation of NKCC2 in the thick ascending limb*. Am J Physiol Renal Physiol, 2011. **301**(6): p. F1143-59.
57. de Jong, J.C., et al., *Functional expression of the human thiazide-sensitive NaCl cotransporter in Madin-Darby canine kidney cells*. J Am Soc Nephrol, 2003. **14**(10): p. 2428-35.
58. Valiño-Rivas, L., et al., *MAGE genes in the kidney: identification of MAGED2 as upregulated during kidney injury and in stressed tubular cells*. Nephrol Dial Transplant, 2019. **34**(9): p. 1498-1507.
59. Semenza, G.L., *Oxygen homeostasis*. Wiley Interdiscip Rev Syst Biol Med, 2010. **2**(3): p. 336-361.
60. Wang, G.L., et al., *Hypoxia-inducible factor 1 is a basic-helix-loop-helix-PAS heterodimer regulated by cellular O2 tension*. Proc Natl Acad Sci U S A, 1995. **92**(12): p. 5510-4.
61. Kaelin, W.G., Jr. and P.J. Ratcliffe, *Oxygen sensing by metazoans: the central role of the HIF hydroxylase pathway*. Mol Cell, 2008. **30**(4): p. 393-402.
62. Dayan, F., et al., *Gene regulation in response to graded hypoxia: The non-redundant roles of the oxygen sensors PHD and FIH in the HIF pathway*. Journal of Theoretical Biology, 2009. **259**(2): p. 304-316.
63. Rey, S. and G.L. Semenza, *Hypoxia-inducible factor-1-dependent mechanisms of vascularization and vascular remodelling*. Cardiovasc Res, 2010. **86**(2): p. 236-42.
64. Semenza, G.L., *Regulation of metabolism by hypoxia-inducible factor 1*. Cold Spring Harb Symp Quant Biol, 2011. **76**: p. 347-53.
65. Bullen, J.W., et al., *Protein kinase A-dependent phosphorylation stimulates the transcriptional activity of hypoxia-inducible factor 1*. Sci Signal, 2016. **9**(430): p. ra56.
66. Klionsky, D.J., *Autophagy: from phenomenology to molecular understanding in less than a decade*. Nature Reviews Molecular Cell Biology, 2007. **8**(11): p. 931-937.
67. Groll, M. and R. Huber, *Substrate access and processing by the 20S proteasome core particle*. Int J Biochem Cell Biol, 2003. **35**(5): p. 606-16.
68. Mizushima, N. and B. Levine, *Autophagy in mammalian development and differentiation*. Nat Cell Biol, 2010. **12**(9): p. 823-30.
69. Dikic, I. and Z. Elazar, *Mechanism and medical implications of mammalian autophagy*. Nat Rev Mol Cell Biol, 2018. **19**(6): p. 349-364.
70. Jiang, P. and N. Mizushima, *Autophagy and human diseases*. Cell Research, 2014. **24**(1): p. 69-79.

71. Deretic, V. and B. Levine, *Autophagy balances inflammation in innate immunity*. Autophagy, 2018. **14**(2): p. 243-251.
72. Murrow, L. and J. Debnath, *Autophagy as a stress-response and quality-control mechanism: implications for cell injury and human disease*. Annu Rev Pathol, 2013. **8**: p. 105-37.
73. Rubinsztein, D.C., G. Mariño, and G. Kroemer, *Autophagy and aging*. Cell, 2011. **146**(5): p. 682-95.
74. Wirth, M., J. Joachim, and S.A. Tooze, *Autophagosome formation--the role of ULK1 and Beclin1-PI3KC3 complexes in setting the stage*. Semin Cancer Biol, 2013. **23**(5): p. 301-9.
75. Wong, P.M., et al., *The ULK1 complex: sensing nutrient signals for autophagy activation*. Autophagy, 2013. **9**(2): p. 124-37.
76. Chang, Y.Y. and T.P. Neufeld, *Autophagy takes flight in Drosophila*. FEBS Lett, 2010. **584**(7): p. 1342-9.
77. Kihara, A., et al., *Two distinct Vps34 phosphatidylinositol 3-kinase complexes function in autophagy and carboxypeptidase Y sorting in Saccharomyces cerevisiae*. J Cell Biol, 2001. **152**(3): p. 519-30.
78. Hailey, D.W., et al., *Mitochondria supply membranes for autophagosome biogenesis during starvation*. Cell, 2010. **141**(4): p. 656-67.
79. Geng, J., et al., *Post-Golgi Sec proteins are required for autophagy in Saccharomyces cerevisiae*. Mol Biol Cell, 2010. **21**(13): p. 2257-69.
80. Ravikumar, B., et al., *Plasma membrane contributes to the formation of pre-autophagosomal structures*. Nat Cell Biol, 2010. **12**(8): p. 747-57.
81. Reggiori, F., *1. Membrane origin for autophagy*. Curr Top Dev Biol, 2006. **74**: p. 1-30.
82. Yen, W.L., et al., *The conserved oligomeric Golgi complex is involved in double-membrane vesicle formation during autophagy*. J Cell Biol, 2010. **188**(1): p. 101-14.
83. Pineda, C.T., et al., *Degradation of AMPK by a cancer-specific ubiquitin ligase*. Cell, 2015. **160**(4): p. 715-728.
84. Muñoz-Sánchez, J. and M.E. Cháñez-Cárdenas, *The use of cobalt chloride as a chemical hypoxia model*. J Appl Toxicol, 2019. **39**(4): p. 556-570.
85. Kido, A., et al., *Effect of mesenchymal stem cells on hypoxia-induced desensitization of  $\beta_2$ -adrenergic receptors in rat osteosarcoma cells*. Oncol Lett, 2012. **4**(4): p. 745-750.
86. Cheong, H.I., et al., *Hypoxia sensing through  $\beta$ -adrenergic receptors*. JCI Insight, 2016. **1**(21): p. e90240.
87. Haupt, Y., et al., *Mdm2 promotes the rapid degradation of p53*. Nature, 1997. **387**(6630): p. 296-9.
88. Girnita, L., A. Girnita, and O. Larsson, *Mdm2-dependent ubiquitination and degradation of the insulin-like growth factor 1 receptor*. 2003. **100**(14): p. 8247-8252.
89. Tang, T., et al., *Galphag reduces cAMP production by decreasing Galphas protein abundance*. Biochem Biophys Res Commun, 2008. **377**(2): p. 679-684.
90. Huttlin, E.L., et al., *The BioPlex Network: A Systematic Exploration of the Human Interactome*. Cell, 2015. **162**(2): p. 425-440.
91. Zhao, K., et al., *Regulation of the Mdm2-p53 pathway by the ubiquitin E3 ligase MARCH7*. EMBO Rep, 2018. **19**(2): p. 305-319.
92. Chen, Y., et al., *MDM2 promotes epithelial-mesenchymal transition and metastasis of ovarian cancer SKOV3 cells*. Br J Cancer, 2017. **117**(8): p. 1192-1201.
93. Prives, C., *Signaling to p53: breaking the MDM2-p53 circuit*. Cell, 1998. **95**(1): p. 5-8.
94. Mantovani, F., L. Collavin, and G. Del Sal, *Mutant p53 as a guardian of the cancer cell*. Cell Death Differ, 2019. **26**(2): p. 199-212.

95. Wedegaertner, P.B., H.R. Bourne, and M. von Zastrow, *Activation-induced subcellular redistribution of Gs alpha*. Mol Biol Cell, 1996. **7**(8): p. 1225-33.
96. Toffoli, S., et al., *Intermittent hypoxia changes HIF-1alpha phosphorylation pattern in endothelial cells: unravelling of a new PKA-dependent regulation of HIF-1alpha*. Biochim Biophys Acta, 2007. **1773**(10): p. 1558-71.
97. Ebert, B.L., J.D. Firth, and P.J. Ratcliffe, *Hypoxia and mitochondrial inhibitors regulate expression of glucose transporter-1 via distinct Cis-acting sequences*. J Biol Chem, 1995. **270**(49): p. 29083-9.
98. Dreos, R., et al., *The Eukaryotic Promoter Database: expansion of EPDnew and new promoter analysis tools*. Nucleic Acids Res, 2015. **43**(Database issue): p. D92-6.
99. Taylor, S.S., et al., *Structural framework for the protein kinase family*. Annu Rev Cell Biol, 1992. **8**: p. 429-62.
100. Taylor, S.S., et al., *Assembly of allosteric macromolecular switches: lessons from PKA*. Nat Rev Mol Cell Biol, 2012. **13**(10): p. 646-58.
101. Gjertsen, B.T., et al., *Novel (Rp)-cAMPS analogs as tools for inhibition of cAMP-kinase in cell culture. Basal cAMP-kinase activity modulates interleukin-1 beta action*. J Biol Chem, 1995. **270**(35): p. 20599-607.
102. Lucia, K., et al., *Hypoxia and the hypoxia inducible factor 1 $\alpha$  activate protein kinase A by repressing RII beta subunit transcription*. Oncogene, 2020. **39**(16): p. 3367-3380.
103. Bernhardt, W.M., et al., *Expression of hypoxia-inducible transcription factors in developing human and rat kidneys*. Kidney Int, 2006. **69**(1): p. 114-22.
104. Kömhoff, M., et al., *Brefeldin A induced dose-dependent changes to Golgi structure and function in the rat exocrine pancreas*. Eur J Cell Biol, 1994. **63**(2): p. 192-207.
105. Pommier, Y., *Topoisomerase I inhibitors: camptothecins and beyond*. Nature Reviews Cancer, 2006. **6**(10): p. 789-802.
106. Babbitt, J.L., et al., *Controversies in optimal anemia management: conclusions from a Kidney Disease: Improving Global Outcomes (KDIGO) Conference*. Kidney Int, 2021. **99**(6): p. 1280-1295.
107. Jayasooriya, R., et al., *Camptothecin enhances c-Myc-mediated endoplasmic reticulum stress and leads to autophagy by activating Ca(2+)-mediated AMPK*. Food Chem Toxicol, 2018. **121**: p. 648-656.
108. Prasad Tharanga Jayasooriya, R.G., et al., *Camptothecin induces G(2)/M phase arrest through the ATM-Chk2-Cdc25C axis as a result of autophagy-induced cytoprotection: Implications of reactive oxygen species*. Oncotarget, 2018. **9**(31): p. 21744-21757.
109. Wick, A.N., et al., *Localization of the primary metabolic block produced by 2-deoxyglucose*. J Biol Chem, 1957. **224**(2): p. 963-9.
110. Chen, W. and M. Guéron, *The inhibition of bovine heart hexokinase by 2-deoxy-D-glucose-6-phosphate: characterization by 31P NMR and metabolic implications*. Biochimie, 1992. **74**(9-10): p. 867-73.
111. Kurtoglu, M., et al., *Under normoxia, 2-deoxy-D-glucose elicits cell death in select tumor types not by inhibition of glycolysis but by interfering with N-linked glycosylation*. Mol Cancer Ther, 2007. **6**(11): p. 3049-58.
112. Ferrandon, S., et al., *Sustained cyclic AMP production by parathyroid hormone receptor endocytosis*. Nat Chem Biol, 2009. **5**(10): p. 734-42.
113. Feinstein, T.N., et al., *Noncanonical control of vasopressin receptor type 2 signaling by retromer and arrestin*. J Biol Chem, 2013. **288**(39): p. 27849-60.
114. Rosciglione, S., et al., *Gas regulates the post-endocytic sorting of G protein-coupled receptors*. Nature Communications, 2014. **5**(1): p. 4556.
115. Li, X., et al., *G $\beta$ 1 protein binds ubiquitin to regulate epidermal growth factor receptor endosomal sorting*. 2017. **114**(51): p. 13477-13482.

116. Ahn, D., et al., *G $\alpha$ 's slow conformational transition upon GTP binding and a novel G $\alpha$ 's regulator*. iScience, 2023. **26**(5).
117. Saini, D.K., M. Chisari, and N. Gautam, *Shuttling and translocation of heterotrimeric G proteins and Ras*. Trends Pharmacol Sci, 2009. **30**(6): p. 278-86.
118. Wedegaertner, P.B., H.R. Bourne, and M.v. Zastrow, *Activation-induced subcellular redistribution of Gs  $\alpha$* . 1996. **7**(8): p. 1225-1233.
119. Thiagarajan, M.M., et al., *Activation-induced subcellular redistribution of G  $\alpha$ (s) is dependent upon its unique N-terminus*. Biochemistry, 2002. **41**(30): p. 9470-84.
120. Allen, J.A., et al.,  *$\beta$ -Adrenergic Receptor Stimulation Promotes Gas Internalization through Lipid Rafts: A Study in Living Cells*. 2005. **67**(5): p. 1493-1504.
121. Yu, J.Z. and M.M. Rasenick, *Real-time visualization of a fluorescent G( $\alpha$ )(s): dissociation of the activated G protein from plasma membrane*. Mol Pharmacol, 2002. **61**(2): p. 352-9.
122. Hynes, T.R., et al., *Live cell imaging of Gs and the beta2-adrenergic receptor demonstrates that both alphas and beta1gamma7 internalize upon stimulation and exhibit similar trafficking patterns that differ from that of the beta2-adrenergic receptor*. J Biol Chem, 2004. **279**(42): p. 44101-12.
123. Marcar, L., et al., *MAGE-A Cancer/Testis Antigens Inhibit MDM2 Ubiquitylation Function and Promote Increased Levels of MDM4*. PLoS One, 2015. **10**(5): p. e0127713.
124. Lefkowitz, R.J., K. Rajagopal, and E.J. Whalen, *New roles for beta-arrestins in cell signaling: not just for seven-transmembrane receptors*. Mol Cell, 2006. **24**(5): p. 643-652.
125. Cheong, H.I., et al., *Hypoxia sensing through  $\beta$ -adrenergic receptors*. JCI Insight, 2017. **1**(21).
126. Hemker, S.L., S. Sims-Lucas, and J. Ho, *Role of hypoxia during nephrogenesis*. Pediatr Nephrol, 2016. **31**(10): p. 1571-7.
127. Rudolph, A.M., et al., *Studies on the Circulation of the Preivable Human Fetus*. 1971. **5**: p. 452-465.
128. Brezis, M. and S. Rosen, *Hypoxia of the renal medulla--its implications for disease*. N Engl J Med, 1995. **332**(10): p. 647-55.
129. Kömhoff, M. and K. Laghmani, *Pathophysiology of antenatal Bartter's syndrome*. Curr Opin Nephrol Hypertens, 2017. **26**(5): p. 419-425.
130. Walker-Gray, R., F. Stengel, and M.G. Gold, *Mechanisms for restraining cAMP-dependent protein kinase revealed by subunit quantitation and cross-linking approaches*. 2017. **114**(39): p. 10414-10419.
131. Sjøberg, K. and B.S. Skålhegg, *The Molecular Basis for Specificity at the Level of the Protein Kinase  $\alpha$  Catalytic Subunit*. Front Endocrinol (Lausanne), 2018. **9**: p. 538.
132. Cadd, G. and G.S. McKnight, *Distinct patterns of cAMP-dependent protein kinase gene expression in mouse brain*. Neuron, 1989. **3**(1): p. 71-9.
133. Simko, V., et al., *Hypoxia induces cancer-associated cAMP/PKA signalling through HIF-mediated transcriptional control of adenylyl cyclases VI and VII*. Sci Rep, 2017. **7**(1): p. 10121.
134. Rieg, T., et al., *Adenylyl Cyclase 6 Enhances NKCC2 Expression and Mediates Vasopressin-Induced Phosphorylation of NKCC2 and NCC*. The American Journal of Pathology, 2013. **182**(1): p. 96-106.
135. Shaikh, D., et al., *cAMP-dependent protein kinase is essential for hypoxia-mediated epithelial-mesenchymal transition, migration, and invasion in lung cancer cells*. Cell Signal, 2012. **24**(12): p. 2396-406.
136. Hill, P., et al., *Inhibition of hypoxia inducible factor hydroxylases protects against renal ischemia-reperfusion injury*. J Am Soc Nephrol, 2008. **19**(1): p. 39-46.
137. Rosenberger, C., et al., *Immunohistochemical detection of hypoxia-inducible factor-1 $\alpha$  in human renal allograft biopsies*. J Am Soc Nephrol, 2007. **18**(1): p. 343-51.

138. Shu, S., et al., *Hypoxia and Hypoxia-Inducible Factors in Kidney Injury and Repair*. Cells, 2019. **8**(3).
139. Fenton, R.A. and M.A. Knepper, *Mouse models and the urinary concentrating mechanism in the new millennium*. Physiol Rev, 2007. **87**(4): p. 1083-112.
140. Zaarour, N., et al., *Multiple evolutionarily conserved Di-leucine like motifs in the carboxyl terminus control the anterograde trafficking of NKCC2*. J Biol Chem, 2012. **287**(51): p. 42642-53.
141. Seayfan, E., et al., *OS9 Protein Interacts with Na-K-2Cl Co-transporter (NKCC2) and Targets Its Immature Form for the Endoplasmic Reticulum-associated Degradation Pathway*. J Biol Chem, 2016. **291**(9): p. 4487-502.
142. Bakhos-Douaihy, D., et al., *Differential Effects of STCH and Stress-Inducible Hsp70 on the Stability and Maturation of NKCC2*. Int J Mol Sci, 2021. **22**(4).
143. Demaretz, S., et al., *Golgi Alpha1,2-Mannosidase IA Promotes Efficient Endoplasmic Reticulum-Associated Degradation of NKCC2*. Cells, 2021. **11**(1).
144. Shaukat, I., et al., *New insights into the role of endoplasmic reticulum-associated degradation in Bartter Syndrome Type 1*. Hum Mutat, 2021. **42**(8): p. 947-968.
145. Fiszer-Kierzkowska, A., et al., *Liposome-based DNA carriers may induce cellular stress response and change gene expression pattern in transfected cells*. BMC Molecular Biology, 2011. **12**(1): p. 27.
146. Casagrande, R., et al., *Degradation of proteins from the ER of S. cerevisiae requires an intact unfolded protein response pathway*. Mol Cell, 2000. **5**(4): p. 729-35.
147. Ju, X., et al., *SARS-CoV-2 main protease cleaves MAGED2 to antagonize host antiviral defense*. mBio, 2023: p. e0137323.
148. Maiuri, M.C., et al., *Autophagy regulation by p53*. Curr Opin Cell Biol, 2010. **22**(2): p. 181-5.
149. Tasdemir, E., et al., *Regulation of autophagy by cytoplasmic p53*. Nature Cell Biology, 2008. **10**(6): p. 676-687.
150. Zhou, Y., et al., *Silencing of NRAGE induces autophagy via AMPK/Ulk1/Atg13 signaling pathway in NSCLC cells*. Tumour Biol, 2017. **39**(6): p. 1010428317709676.
151. Zhang, T., et al., *G-protein-coupled receptors regulate autophagy by ZBTB16-mediated ubiquitination and proteasomal degradation of Atg14L*. Elife, 2015. **4**: p. e06734.
152. Budovskaya, Y.V., et al., *The Ras/cAMP-dependent protein kinase signaling pathway regulates an early step of the autophagy process in Saccharomyces cerevisiae*. J Biol Chem, 2004. **279**(20): p. 20663-71.
153. Palorini, R., et al., *Protein Kinase A Activation Promotes Cancer Cell Resistance to Glucose Starvation and Anoikis*. PLoS Genet, 2016. **12**(3): p. e1005931.
154. Cherra, S.J., 3rd, et al., *Regulation of the autophagy protein LC3 by phosphorylation*. J Cell Biol, 2010. **190**(4): p. 533-9.
155. Jewell, J.L., et al., *GPCR signaling inhibits mTORC1 via PKA phosphorylation of Raptor*. eLife, 2019. **8**: p. e43038.
156. Xie, J., et al., *cAMP inhibits mammalian target of rapamycin complex-1 and -2 (mTORC1 and 2) by promoting complex dissociation and inhibiting mTOR kinase activity*. Cellular Signalling, 2011. **23**(12): p. 1927-1935.
157. Grisan, F., et al., *PKA compartmentalization links cAMP signaling and autophagy*. Cell Death Differ, 2021. **28**(8): p. 2436-2449.
158. Hartleben, B., et al., *Autophagy influences glomerular disease susceptibility and maintains podocyte homeostasis in aging mice*. J Clin Invest, 2010. **120**(4): p. 1084-96.
159. Liu, S., et al., *Autophagy plays a critical role in kidney tubule maintenance, aging and ischemia-reperfusion injury*. Autophagy, 2012. **8**(5): p. 826-837.

160. Tang, C., et al., *Autophagy in kidney homeostasis and disease*. Nat Rev Nephrol, 2020. **16**(9): p. 489-508.
161. Reusch, B., et al., *MAGED2 controls vasopressin-induced aquaporin-2 expression in collecting duct cells*. Journal of Proteomics, 2022. **252**: p. 104424.
162. Khositseth, S., et al., *Autophagic degradation of aquaporin-2 is an early event in hypokalemia-induced nephrogenic diabetes insipidus*. Sci Rep, 2015. **5**: p. 18311.
163. Rosenbaek, L.L., et al., *The thiazide sensitive sodium chloride co-transporter NCC is modulated by site-specific ubiquitylation*. Scientific Reports, 2017. **7**(1): p. 12981.
164. Kumar, V., et al., *Inhibition of Mammalian Target of Rapamycin Complex 1 Attenuates Salt-Induced Hypertension and Kidney Injury in Dahl Salt-Sensitive Rats*. Hypertension, 2017. **70**(4): p. 813-821.
165. Grahammer, F., et al., *mTORC1 maintains renal tubular homeostasis and is essential in response to ischemic stress*. Proc Natl Acad Sci U S A, 2014. **111**(27): p. E2817-26.
166. Kidd, M., et al., *The role of genetic markers--NAP1L1, MAGE-D2, and MTA1--in defining small-intestinal carcinoid neoplasia*. Ann Surg Oncol, 2006. **13**(2): p. 253-62.
167. Kanda, M., et al., *A novel dual-marker expression panel for easy and accurate risk stratification of patients with gastric cancer*. Cancer Med, 2018. **7**(6): p. 2463-2471.
168. Chung, F.Y., et al., *Differential gene expression profile of MAGE family in taiwanese patients with colorectal cancer*. J Surg Oncol, 2010. **102**(2): p. 148-53.
169. Tsai, J.R., et al., *Differential expression profile of MAGE family in non-small-cell lung cancer*. Lung Cancer, 2007. **56**(2): p. 185-92.
170. Jing, X., et al., *Role of hypoxia in cancer therapy by regulating the tumor microenvironment*. Molecular Cancer, 2019. **18**(1): p. 157.
171. Rohwer, N., et al., *The growing complexity of HIF-1 $\alpha$ 's role in tumorigenesis: DNA repair and beyond*. Oncogene, 2013. **32**(31): p. 3569-76.
172. O'Hayre, M., et al., *The emerging mutational landscape of G proteins and G-protein-coupled receptors in cancer*. Nat Rev Cancer, 2013. **13**(6): p. 412-24.
173. Tirosh, A., et al., *Activating genomic alterations in the Gs alpha gene (GNAS) in 274 694 tumors*. Genes Chromosomes Cancer, 2020. **59**(9): p. 503-516.
174. Sorensen, A., et al., *Placental oxygen transport estimated by the hyperoxic placental BOLD MRI response*. Physiol Rep, 2015. **3**(10).
175. Ammon, H.P. and A.B. Müller, *Forskolin: from an ayurvedic remedy to a modern agent*. Planta Med, 1985. **51**(6): p. 473-7.
176. Godard, M.P., B.A. Johnson, and S.R. Richmond, *Body composition and hormonal adaptations associated with forskolin consumption in overweight and obese men*. Obes Res, 2005. **13**(8): p. 1335-43.
177. Henderson, S., et al., *Effects of coleus forskohlii supplementation on body composition and hematological profiles in mildly overweight women*. J Int Soc Sports Nutr, 2005. **2**(2): p. 54-62.
178. González-Sánchez, R., et al., *Forskolin versus sodium cromoglycate for prevention of asthma attacks: a single-blinded clinical trial*. J Int Med Res, 2006. **34**(2): p. 200-7.
179. Salehi, B., et al., *The Therapeutic Potential of the Labdane Diterpenoid Forskolin*. 2019. **9**(19): p. 4089.



## 7. Appendix

### 7.1. List of abbreviations

*MAGED2* \_ Melanoma-associated antigen D2  
tBS \_ Transient antenatal Bartter syndrome  
G $\alpha$ s \_ G-alpha-S  
cAMP \_ Cyclic adenosine monophosphate  
PKA \_ Protein kinase A  
TAL \_ Thick ascending limb  
DCT \_ Distal convoluted tubule  
BS \_ Bartter's syndrome  
NKCC2 \_ Na<sup>+</sup>- K<sup>+</sup> -2Cl<sup>-</sup> cotransport  
ROMK \_ Renal outer medullary (K) channel  
NCC \_ Na<sup>+</sup>- Cl<sup>-</sup> cotransporter  
PTC \_ Premature termination codons  
NMD \_ Nonsense-mediated decay  
MHD \_ MAGE homology domain  
RING \_ Really Interesting New Gene  
HECT \_ Homologous to E6-AP COOH terminus  
ATP \_ Adenosine triphosphate  
E1 \_ Ubiquitin-activating enzyme  
E2 \_ Ubiquitin conjugating enzyme  
E3 \_ Ubiquitin ligase  
G1/S \_ Gap 1, DNA synthesis  
ATM \_ Ataxia-telangiectasia mutated  
ATR \_ ATM-and Rad3-Related  
GC \_ Gastric cancer  
*MDIG* \_ Mineral dust-induced gene

TNBC \_ Triple-negative breast cancer  
 EMT \_ Epithelial-mesenchymal transition  
 H3K36me3 \_ Histone H3 lysine 36 trimethylation  
 KO \_ Knockout  
 TRAIL \_ Tumor necrosis factor-related apoptosis-inducing ligand  
 GPCRs \_ G-protein-coupled receptors  
 RasD \_ Ras-like GTPase domain  
 AHD \_  $\alpha$ -helical domain  
 GDP \_ Guanosine diphosphate  
 GTP \_ Guanosine-5'-triphosphate  
 GEF \_ Guanine nucleotide exchange factor  
 EPAC \_ a GEF for Rap small GTP-binding proteins  
 AKI \_ Acute kidney injury  
 HIF-1 \_ Hypoxia-inducible factor 1  
 PHDs \_ Prolyl hydroxylases  
 VHL \_ von Hippel-Lindau tumor suppressor protein  
 HREs \_ Hypoxia response elements  
*VEGF* \_ Vascular endothelial growth factor  
*EPO* \_ Erythropoietin  
*GLUT* \_ Glucose transporters  
*PK1* \_ Pyruvate dehydrogenase kinase 1  
 αὐτό \_ Self  
 φαγος \_ Devouring  
 UPS \_ Ubiquitin–proteasome system  
 ATGs \_ Autophagy related genes  
 mTORC1 \_ Mechanistic target of rapamycin complex 1  
 PAS \_ Phagophore formation site  
 PtdIns3K \_ Phosphatidylinositol 3-kinase

Vps \_ Vacuolar protein sorting  
 Beclin-1 \_ Mammalian ortholog of the yeast autophagy-related gene 6 (Atg6)  
 ER \_ Endoplasmic reticulum  
 PE \_ Phosphatidylethanolamine  
 AMPK \_ AMP-activated protein kinase  
 TRIM28 \_ Tripartite motif-containing 28  
 $\beta$ 2AR \_  $\beta$ 2-adrenergic receptor  
 Co-IP \_ Co-immunoprecipitation  
 MDM2 \_ Murine double minute 2  
 IBMX \_ 3-isobutyl-1-methylxanthine  
 FSK \_ Forskolin  
 ELISA \_ Enzyme-linked immunoassay  
 CREB1 \_ cAMP responsive element binding protein 1  
 qPCR \_ Quantitative polymerase chain reaction  
 IS \_ Inhibitory sequence  
 R \_ Regulatory subunit  
 C \_ Catalytic subunit  
 p62/SQSTM1 \_ Sequestosome1  
 LC3B \_ Microtubule-associated protein 1A/1B-light chain 3  
 Tun \_ Tunicamycin  
 BFA \_ Brefeldin A  
 CPT \_ Camptothecin  
 2-DG \_ 2-Deoxy-D-glucose  
 G<sub>2</sub>/M \_ Gap 2, Mitosis  
 EGFR \_ Epidermal growth factor receptor  
 ARRB2 \_  $\beta$ -Arrestins  
 ERAD \_ Er retention and associated degradation  
 SARS-CoV-2 \_ Severe acute respiratory syndrome coronavirus 2

N protein \_ Nucleocapsid protein

ZBTB16-Cullin3-Roc1 \_ Phosphorylating zinc finger and BTB domain-containing protein 16-  
Cullin3- Regulator of cullins-1

AQP2 \_ Aquaporin-2

IMCD \_ Inner medullary collecting duct ()

RAPTOR \_ Regulatory associated protein with Mtor

WT \_ Wild type

## 7.2. Curriculum Vitae



### Personal Data

Name	Sadiq Nasrah
Date of birth	30.08.1992
Place of birth	Latakia - Syria
Email	Sadiq.nasrah@uni-marburg.de

### Studies and education

09.2020 - 08.2023 Marburg-Germany	Doctoral thesis in natural science Thesis: MAGED2 essential regulation of GalphaS function and cAMP/PKA activation, which promotes hypoxic induction of HIF-1 $\alpha$ and inhibits stress-induced autophagy. Supervisor: Prof. Dr. Martin Kömhoff
10.2016 - 12.2019 Bremen-Germany	M.Sc. Biochemistry and Molecular Biology, Universität Bremen Thesis: Development of a mutant strain of Azoarcus sp. BH72 to facilitate GWAS analysis for plant-endophyte interactions. Supervisors: Prof. Dr. Barbara Reinhold-Hurek and Prof. Dr. Tilman Achstetter.
09.2009 - 07.2014 Latakia-Syria	Bachelor of Pharmacy and Pharmaceutical Chemistry, Tishreen University

### Work experience

03.2020 - 08.2020 Erlangen-Germany	Internship, Friedrich-Alexander-Universität Erlangen-Nürnberg(FAU) Project title: Identification of the interactome of muscular LAP proteins and their involvement in endocytic recycling at the neuromuscular synapse.
06.2018 - 09.2018 Bremerhaven-Germany	Internship, Alfred Wegener Institute, Helmholtz Center for Polar and Marine Research (AWI) Report title: qPCR computation of genes involved in calcium transport at Dungeness crab.
02.2018 - 05.2018 Bremen-Germany	Internship, Fraunhofer Institut für Fertigungstechnik und angewandte Materialforschung (IFAM) Report title: Optical characterization of antibiotics release from structured titanium surfaces.
08.2014 - 05.2016	Pharmacist, Tishreen University Hospital

Latakia-Syria  08.2014 - 05.2016 Latakia-Syria	Consolidate knowledge about drugs, pharmacodynamics, pharmacokinetics, drugs interactions and adverse drugs reactions. Tutoring Teaching high school students biology, chemistry, physics and math using innovative methods.
---	--

### **Techniques**

- Cell culture, Cell labeling, Transfection, Immunocytochemistry, Cryosection, Muscle dissection, Fiber bundle preparation, Immunohistochemistry.
- Nucleic acid extraction, DNA cloning, PCR, qPCR, Genotyping, Microarray.
- Protein extraction, Blotting techniques, ELISA, Immunoprecipitation (IP/co-IP), Spectrophotometry.
- Bacterial culture, Plant inoculation, Assessment of bacterial colonization.
- Confocal laser scanning microscopy, 3D- image quantification, LAS-3000MINI imager, Typhoon laser-scanner platform, TECAN microplate readers, Chemidoc Imaging system.
- Bioinformatics: NCBI database, BLAST, Expasy, Clone Manager, SnapGene, miRBase, ImageJ, GraphPad Prism, Image Lab.

### **Publications**

- Elie Seaayfan, Sadiq Nasrah, Lea Quell, Maja Kleim, Stefanie Weber, HemmoMeyer, Kamel Laghmani, Martin Kömhoff. (2022) MAGED2 Is Required under Hypoxia for cAMP Signaling by Inhibiting MDM2-DependentEndocytosis of G-Alpha-S. Cells DOI: 10.3390/cells11162546
- Elie Seaayfan, Sadiq Nasrah, Lea Quell, Aline Radi, Maja Kleim, Ralph T Schermuly, Stefanie Weber, Kamel Laghmani, Martin Kömhoff. (2022) Reciprocal Regulation of MAGED2 and HIF-1 $\alpha$  Augments Their Expression under Hypoxia: Role of cAMP and PKA Type II. Cells DOI:10.3390/cells11213424
- A book chapter: Aline Radi, Sadiq Nasrah (2022) Renal Involvement in Localized and Systemic Autoimmunity Diseases with Insights into the Ongoing Therapeutic Approaches. In: Hussein Fayyad Kazan, editor. Immunology and Cancer Biology Hyderabad, India: Vide Leaf. 2022.
- Sadiq Nasrah, Aline Radi, Johanna Daberkow, Helmut H. Hummler, Stefanie Weber, Elie Seaayfan, Martin Kömhoff.

(2023) MAGED2 depletion promotes stress-induced autophagy by impairing the cAMP/PKA pathway. IJMS  
Doi.org/10.3390/ijms241713433

**Languages**

German (Advanced) - English (Professional) - Arabic (Native)

**References**

Prof. Dr. med. Martin Kömhoff  
UKGM- Klinik für Kinder und Jugendmedizin II- Stellv. Direktor  
+49 6421 58 62671  
[martin.koemhoff@uk-gm.de](mailto:martin.koemhoff@uk-gm.de)  
Univ.-Prof. Dr. med. Stefanie Weber  
UKGM- Klinik für Kinder und Jugendmedizin II- Direktorin der Klinik  
+49 6421 58 62671  
[stefanie.weber@med.uni-marburg.de](mailto:stefanie.weber@med.uni-marburg.de)  
Dr. Elie Seaayfan  
UKGM- Klinik für Kinder und Jugendmedizin II  
+49 6421 58-62789  
[elie.seaayfan@uni-marburg.de](mailto:elie.seaayfan@uni-marburg.de)

**Conferences**

- Forschungstagung Pädiatrie Philipps-Universität Marburg  
26.11.2022
- GPN Kongress: 54. Jahrestagung der GPN - UKGM -  
04.05.2023

### 7.3. Academic teachers

#### **Philipps-Universität Marburg**

Prof. Kömhoff

Dr. Seaayfan

Prof. Weber

#### **Universität Bremen**

Prof. Kelm

Prof. Achstetter

Prof. Reinhold-Hurek

Dr. Dietz

Prof. Dotzauer

Prof. Groß-Hardt

Dr. Hurek

Dr. Krause

Prof. Nehls

#### **Fraunhofer Institut für Fertigungstechnik und angewandte Materialforschung (IFAM)**

Dr. Salz

#### **Alfred Wegener Institute, Helmholtz Center for Polar and Marine Research (AWI)**

Dr. Wittmann



#### 7.4. Acknowledgment

I am profoundly grateful to the individuals who have played a significant role in the completion of this PhD thesis. Their unwavering support, guidance, and encouragement have been invaluable throughout this journey.

First and foremost, I extend my heartfelt appreciation to my supervisor, Prof. Martin Kömhoff. Your profound expertise, dedication to research, and insightful guidance have been pivotal in shaping the direction of this thesis. Your mentorship has not only enriched my academic experience but also inspired me to strive for excellence in all aspects of my work.

I am deeply thankful to Dr. Elie Seaayfan for his invaluable contributions to this thesis. Your thoughtful insights, tireless efforts in teaching how to design experiments and analyze the outcomes, and willingness to engage in intellectual discussions have immensely enriched the quality of this research. Your expertise and meticulous approach have enriched the empirical foundation of this study and your positivity made the difference.

I extend my sincere appreciation to Prof. Stefanie Weber for her generous provision of resources and consistent engagement in our weekly discussions. Your constructive critiques have been fundamental in refining and illuminating many aspects of this research.

I am indebted to Ms. Aline Radi, your creativity and devotion to research have significantly enhanced the overall quality of this work. Your exceptional performance in conducting practical experiments has been indispensable.

I would also like to extend my gratitude to Ms. Michelle Auer for her support and assistance during various stages of this research. Your commitment to detail, organizational skills, and willingness to assist have been immensely valuable in ensuring the smooth progression of this project. I am also thankful to Dr. Aparna Renigunta, Ilka Bittorf, Lara Sommer, Sarah Prim, Johanna Daberkow, Lea Quell, Jonas Einloft, Simon Bedenbender and Hendrik Meyer. Your encouragement has been a source of strength, reminding me that challenges can be overcome with resilience and a positive spirit.

Thank you all for your belief in my capabilities. Your impact will be cherished, and I am truly fortunate to have such a wonderful network of individuals around me. I am excited to carry forward the knowledge and skills gained during this journey into the next phase of my academic and professional career.

## 7.5. Full lists of publications

Elie Seaayfan, Sadiq Nasrah, Lea Quell, Maja Kleim, Stefanie Weber, HemmoMeyer, Kamel Laghmani, Martin Kömhoff. (2022) MAGED2 Is Required under Hypoxia for cAMP Signaling by Inhibiting MDM2-Dependent Endocytosis of G-Alpha-S. Cells DOI: 10.3390/cells11162546

Elie Seaayfan, Sadiq Nasrah, Lea Quell, Aline Radi, Maja Kleim, Ralph T Schermuly, Stefanie Weber, Kamel Laghmani, Martin Kömhoff. (2022) Reciprocal Regulation of MAGED2 and HIF-1 $\alpha$  Augments Their Expression under Hypoxia: Role of cAMP and PKA Type II. Cells DOI:10.3390/cells11213424

A book chapter: Aline Radi, Sadiq Nasrah (2022) Renal Involvement in Localized and Systemic Autoimmunity Diseases with Insights into the Ongoing Therapeutic Approaches. In: Hussein Fayyad Kazan, editor. Immunology and Cancer Biology Hyderabad, India: Vide Leaf. 2022.

Sadiq Nasrah, Aline Radi, Johanna Daberkow, Helmut H. Hummler, Stefanie Weber, Elie Seaayfan, Martin Kömhoff. (2023) MAGED2 depletion promotes stress-induced autophagy by impairing the cAMP/PKA pathway. IJMS Doi.org/10.3390/ijms241713433

## 7.6. Contribution to the published papers

- **Paper 1:**

MAGED2 Is Required under Hypoxia for cAMP Signaling by Inhibiting MDM2-Dependent Endocytosis of G-Alpha-S

<https://doi.org/10.3390/cells11162546>

Fig.1

a, b, c: Performed by Lea Quell, repeated and complemented with reoxygenation experiment by Sadiq Nasrah

d: Performed by Sadiq Nasrah

e, f: Performed by Lea Quell, repeated by Sadiq Nasrah during the course of his thesis

Fig.2 Performed by Sadiq Nasrah

Fig.3 Performed by Lea Quell

Fig.4 Performed by Sadiq Nasrah

Fig.5 Performed by Sadiq Nasrah

Fig.6 Working model from the lab

S1. Performed by Sadiq Nasrah

S2. Performed by Sadiq Nasrah

S3. Performed by Sadiq Nasrah

S4. Performed by Sadiq Nasrah

S5. Performed by Lea Quell

S6. Performed by Sadiq Nasrah

- **Paper 2:**

Reciprocal Regulation of MAGED2 and HIF-1 $\alpha$  Augments Their Expression under Hypoxia: Role of cAMP and PKA Type II

<https://doi.org/10.3390/cells11213424>

Fig.1

a, b, c, d: Performed by Lea Quell, repeated by Sadiq Nasrah during the course of his thesis

e: Performed by Sadiq Nasrah

f: Performed by Sadiq Nasrah and Aline Radi

Fig.2

a: Performed by Sadiq Nasrah

b: Performed by Lea Quell, repeated by Sadiq Nasrah during the course of his thesis

Fig.3

a: Performed by Sadiq Nasrah

b: Performed by Lea Quell, repeated by Sadiq Nasrah during the course of his thesis

Fig.4

a, b, c, d, e, f: Performed by Lea Quell, repeated by Sadiq Nasrah during the course of his thesis

g: Performed by Sadiq Nasrah

Fig.5 Performed by Lea Quell, repeated by Sadiq Nasrah during the course of his thesis

Fig.6

a, b, d, e: Performed by Lea Quell, repeated by Sadiq Nasrah during the course of his thesis

c: Performed by Sadiq Nasrah and Aline Radi

Fig.7 Working model from the lab

S1.

a: Performed by Aline Radi

b: Performed by Sadiq Nasrah

S2. Performed by Lea Quell

S3. Performed by Aline Radi

- **Paper 3:**

MAGED2 Depletion Promotes Stress-Induced Autophagy by Impairing the cAMP/PKA Pathway

<https://doi.org/10.3390/ijms241713433>

Fig.1 Performed by Sadiq Nasrah

Fig.2 Performed by Sadiq Nasrah

Fig.3 Performed by Sadiq Nasrah, repeated by Aline Radi

Fig.4 Performed by Sadiq Nasrah

Fig.5 Performed by Sadiq Nasrah

Fig.6 Performed by Sadiq Nasrah

Fig.7 Performed by Sadiq Nasrah

Fig.8 Performed by cooperation of both Sadiq Nasrah and Aline Radi

Fig.9 Working model from the lab

S1. Performed by Sadiq Nasrah

S2. Performed by Sadiq Nasrah

S3. Performed by Sadiq Nasrah

S4. Performed by Sadiq Nasrah

S5. Performed by Sadiq Nasrah

S6. Performed by Aline Radi

#### 7.7. Reprints of original publications

## Article

# MAGED2 Is Required under Hypoxia for cAMP Signaling by Inhibiting MDM2-Dependent Endocytosis of G-Alpha-S

Elie Seaayfan <sup>1</sup>, Sadiq Nasrah <sup>1</sup>, Lea Quell <sup>1</sup>, Maja Kleim <sup>1</sup>, Stefanie Weber <sup>1</sup>, Hemmo Meyer <sup>2</sup>, Kamel Laghmani <sup>3,†</sup> and Martin Kömhoff <sup>1,\*,†</sup>

<sup>1</sup> University Children's Hospital, Philipps University, 35043 Marburg, Germany

<sup>2</sup> Faculty of Biology, University of Duisburg-Essen, 45141 Duisburg, Germany

<sup>3</sup> Centre de Recherche des Cordeliers, Sorbonne Université, Inserm, Université de Paris, CNRS, ERL8228, F-75006 Paris, France

\* Correspondence: koemhoff@staff.uni-marburg.de

† These authors contributed equally to this work.

**Abstract:** Mutations in *MAGED2* cause transient Bartter syndrome characterized by severe renal salt wasting in fetuses and infants, which leads to massive polyhydramnios causing preterm labor, extreme prematurity and perinatal death. Notably, this condition resolves spontaneously in parallel with developmental increase in renal oxygenation. *MAGED2* interacts with G- $\alpha$ -S ( $G_{\alpha s}$ ). Given the role of  $G_{\alpha s}$  in activating adenylyl cyclase at the plasma membrane and consequently generating cAMP to promote renal salt reabsorption via protein kinase A (PKA), we hypothesized that *MAGED2* is required for this signaling pathway under hypoxic conditions such as in fetuses. Consistent with that, under both physical and chemical hypoxia, knockdown of *MAGED2* in renal (HEK293) and cancer (HeLa) cell culture models caused internalization of  $G_{\alpha s}$ , which was fully reversible upon reoxygenation. In contrast to  $G_{\alpha s}$ , cell surface expression of the  $\beta$ 2-adrenergic receptor, which is coupled to  $G_{\alpha s}$ , was not affected by *MAGED2* depletion, demonstrating specific regulation of  $G_{\alpha s}$  by *MAGED2*. Importantly, the internalization of  $G_{\alpha s}$  due to *MAGED2* deficiency significantly reduced cAMP generation and PKA activity. Interestingly, the internalization of  $G_{\alpha s}$  was blocked by preventing its endocytosis with dynasore. Given the role of E3 ubiquitin ligases, which can be regulated by MAGE-proteins, in regulating endocytosis, we assessed the potential role of MDM2-dependent ubiquitination in *MAGED2* deficiency-induced internalization of  $G_{\alpha s}$  under hypoxia. Remarkably, MDM2 depletion or its chemical inhibition fully abolished  $G_{\alpha s}$ -endocytosis following *MAGED2* knockdown. Moreover, endocytosis of  $G_{\alpha s}$  was also blocked by mutation of ubiquitin acceptor sites in  $G_{\alpha s}$ . Thus, we reveal that *MAGED2* is essential for the cAMP/PKA pathway under hypoxia to specifically regulate  $G_{\alpha s}$  endocytosis by blocking MDM2-dependent ubiquitination of  $G_{\alpha s}$ . This may explain, at least in part, the transient nature of Bartter syndrome caused by *MAGED2* mutations and opens new avenues for therapy in these patients.

**Keywords:** *MAGED2*; hypoxia; G- $\alpha$ -S; MDM2; Bartter



**Citation:** Seaayfan, E.; Nasrah, S.; Quell, L.; Kleim, M.; Weber, S.; Meyer, H.; Laghmani, K.; Kömhoff, M. *MAGED2 Is Required under Hypoxia for cAMP Signaling by Inhibiting MDM2-Dependent Endocytosis of G-Alpha-S. Cells* **2022**, *11*, 2546. <https://doi.org/10.3390/cells11162546>

Academic Editors:

M.-Saadeh Suleiman and Igor Khaliulin

Received: 23 July 2022

Accepted: 15 August 2022

Published: 16 August 2022

**Publisher's Note:** MDPI stays neutral with regard to jurisdictional claims in published maps and institutional affiliations.



**Copyright:** © 2022 by the authors. Licensee MDPI, Basel, Switzerland. This article is an open access article distributed under the terms and conditions of the Creative Commons Attribution (CC BY) license (<https://creativecommons.org/licenses/by/4.0/>).

## 1. Introduction

Mutations in *MAGED2* associate with marked renal salt wasting in affected fetuses and newborns leading to extreme prematurity and increased perinatal mortality. Renal salt wasting is accompanied by massive polyuria and caused by defective salt reabsorption in the thick ascending limb of the loop of Henle and is referred to as transient Bartter syndrome (or Bartter V). Intriguingly, although patients with Bartter V are characterized by the most severe presentation due to profound excess fetal urine production causing preterm delivery, renal salt and water wasting resolves rapidly and completely starting at late gestation (30 weeks of gestational age) [1]. The reason for the spontaneous recovery, which occurs despite continuous expression of *MAGED2* in the distal tubule from early

fetal development into adulthood, is not known, suggesting that spontaneous recovery is triggered by an external factor or factors. Resolution of hypoxia may be the relevant external factor [1], because kidneys (both in utero as well as in extremely preterm babies) are subjected to hypoxia as evidenced by the expression of the hypoxia inducible factor (HIF-1 $\alpha$ ) until approximately the 30th week of gestation [2–5]. The renal medulla, where NKCC2, one of the key salt transport proteins (mutated in Bartter I) is expressed, has a low oxygen tension, which is further exacerbated during pregnancy in utero. Remarkably, this period coincides with the onset of recovery from salt and water wasting in transient Bartter syndrome. Furthermore, the notion that the function of MAGED2 is to protect renal salt transport against hypoxic stress is consistent with recent studies demonstrating that MAGE proteins protect against diverse forms of stress (radiation, genotoxic, and nutritional stress) [6] by regulating the activity of ubiquitin E3 ligases [7], of which ca. 650 members are known. E3 ligases are the ultimate enzymes involved in the transfer of ubiquitin to substrate proteins, a process that determines the fate of the modified protein. In this regard, it is worth noting that E3 ligases can promote not only the ubiquitination-dependent degradation of client proteins but also a non-degradative ubiquitination pathway involved in the regulation of proteins' endocytosis and trafficking [8].

We and others have recently demonstrated that MAGED2 protein interacts with G $\alpha$ s [1,9]. G $\alpha$ s transmits activation of G-protein coupled receptors (GPCR) resulting in activation of membranous adenylate cyclase and hence cAMP formation [10]. In the kidney, cAMP generation is downstream of vasopressin and other hormones promoting renal tubular salt and water reabsorption [11]. Of note, NKCC2 (mutated in Bartter I) and NCC are two important renal salt transporters, whose intrarenal expression and function are greatly reduced in Bartter V [1] and are stimulated by cAMP [11].

In this study, we hypothesized that the interaction of MAGED2 and G $\alpha$ s is essential under hypoxic conditions such as in fetal kidneys to allow for sufficient cAMP generation and hence activation of the PKA pathway to promote salt reabsorption. We therefore examined the effects of MAGED2 knockdown on the intracellular localization of G $\alpha$ s, and the cAMP/PKA pathway with and without physical and chemical hypoxia in a renal cell culture system (HEK293) and in a human cancer cell line (HeLa). We found that, under hypoxia, MAGED2 prevents translocation of G $\alpha$ s from the plasma membrane to the cytosol by blocking the E3 ligase MDM2, which triggers endocytosis of G $\alpha$ s. Accordingly, MAGED2 depletion impaired cAMP generation and PKA activity. Thus, we demonstrated that MAGED2 is required for the activation of the cAMP/PKA pathway under hypoxic conditions to regulate G $\alpha$ s endocytosis via MDM2-dependent ubiquitination, thereby explaining, at least in part, the transient nature of transient Bartter syndrome.

## 2. Materials and Methods

### 2.1. Plasmid Constructions and Site Directed Mutagenesis

The V5 tagged G $\alpha$ s was generated by Site-Directed Mutagenesis using the long isoform as template according to the Q5<sup>®</sup> Site-Directed Mutagenesis Kit protocol. To generate K28R, K53R, K88R, K300R, and K305R mutations, the site-directed mutagenesis method was performed using wild-type Long G $\alpha$ s-HA construct as a template according to the QuikChange Multi Site-Directed Mutagenesis Kit protocol. All mutations were confirmed by sequencing.

### 2.2. Cell Culture

Human Embryonic Kidney (HEK293) and HeLa cells (Table 1) were grown in DMEM Glutamax complemented with 10% fetal bovine serum superior (Sigma-Aldrich, Schnellendorf, Germany), penicillin (100 units/mL), and streptomycin (100 units/mL) at 37 °C in a humidified atmosphere containing 5% CO<sub>2</sub>. For chemical treatment experiments, the media of confluent cells was changed to DMEM serum free for 14–16 h. Cells for control and experimental groups are always derived from the same flask and passage and studied on the same day.

**Table 1.** Reagent and tools.

Reagent or Resource	Source	Identifier
<b>Antibodies</b>		
Anti-HIF-1 $\alpha$ rabbit	Cell Signaling	14179
Anti-MAGED2 rabbit	This paper	
Anti-beta 2 Adrenergic Receptor antibody	Abcam	ab182136
Anti-G $\alpha$ s	Sigma Aldrich	06-237
Anti-HA tag mouse	Thermo Fisher Scientific	26183
V5-Tag antibody	Bio-rad	MCA1360GA
Monoclonal ANTI-FLAG <sup>®</sup> M2 antibody produced in mouse	Sigma-Aldrich	F3165
Goat anti-Mouse IgG (H + L), Alexa Fluor Plus 555	Thermo Fisher Scientific	A32727
Streptavidin, Alexa Fluor <sup>™</sup> 488 conjugate	Thermo Fisher Scientific	S11223
StarBright Blue 520 Goat Anti-Rabbit IgG	Bio-rad	12005869
StarBright Blue 700 Goat Anti-Mouse IgG	Bio-rad	12004158
<b>Chemicals, Peptides, and Recombinant Proteins</b>		
EZ-Link <sup>™</sup> Sulfo-NHS-LC-Biotin	Thermo Fisher Scientific	21335
<b>Critical Commercial Assays</b>		
PepTag <sup>®</sup> Non-Radioactive Protein Kinase Assays	Promega	V5340
cAMP Assay Kit (Competitive ELISA)	abcam	Ab133051
Q5 <sup>®</sup> Site-Directed Mutagenesis Kit	New England Biolabs'	E0554S
QuikChange Multi Site-Directed Mutagenesis Kit	Agilent Technologies	200515
<b>Experimental Models: Cell Lines</b>		
HEK293	ATCC	CRL1573
HeLa	Gift from Dr. Vijay Renigunta	
<b>Oligonucleotides</b>		
ON-TARGETplus Non-targeting Control Pool	Dharmacon	D-001810-10-05
UGGUUUACAUGUCGACUAA		
UGGUUUACAUGUUGUGUGA		
UGGUUUACAUGUUUUCUGA		
UGGUUUACAUGUUUUCUA		
ON-TARGETplus Human MAGED2 siRNA—SMARTpool	Dharmacon	L-017284-01-0005
GGACGAAGCUGAUUUCGGA		
GCUAAAGACCAGACGAAGA		
AGGCGAUGGAAGCGGAUUU		
GAAAAGGACAGUAGCUCGA		
ON-TARGETplus Human GNAS siRNA—SMARTpool	Dharmacon	L-010825-00-0005
GCAAGUGGAUCCAGUGCUU		
GCAUGCACCUUCGUCAGUA		
AUGAGGAUCCUGCAUGUUA		
CAACCAAAGUGCAGGACAU		
MDM2 siRNA	Dharmacon	
GACAAAGAAGAGAGUGUGG		[12]
GAAGUUAUAAAGUCUGUU		[13]



Table 1. Cont.

Reagent or Resource	Source	Identifier
GNAS from short to long isoform primer	Sigma-Aldrich	
GCTGCAAGGAGCAACAGCGATGGTGAGAAGGCAACCAAAG		
CTGCGGGTCTCTTCGCCGCCCTCTCCATTAAACCCATTAAAC		
GNAS from HA to V5 tag primer	Sigma-Aldrich	
CTGCTGGGCCTGGATAGCACCTAAACTCGAGTCTAGAGCGGCC		
CGGGTTCGGAATCGGTTTGCCAGAGCCTCCACCCCGAG		
GNAS 5X lysine mutation primer	Sigma-Aldrich	
TGAGGCCAACAAAAAGATCGAGAGGCAGCTGCAGAA		
GGTGCTGGAGAATCTGGTAGAAGCACCATTGTGAAG		
GGAGCAACAGCGATGGTGAGAGGGCAACCAAAG		
AGCAAGATCTGCTCGCTGAGAGAGTCCTTGCTG		
GAAAGTCCTTGCTGGGAGATCGAAGATTGAGGACT		
<b>Recombinant DNA</b>		
G protein alpha S/GNAS cDNA ORF Clone, Human, C-HA tag	Sino Biological Inc.	HG12069-CY
pcDNA3 Flag beta-2-adrenergic-receptor	Gift from Robert Lefkowitz	[14]
Single Ubiquitin HA tag	Gift from Professor Hemmo Meyer	
<b>Software and Algorithms</b>		
ImageJ	Schneider et al., 2012	<a href="https://imagej.nih.gov/ij/">https://imagej.nih.gov/ij/</a> , accessed on 22 July 2022
GraphPad Prism 8	GraphPad	
EndNote X9	Clarivate Analytics	

### 2.3. Chemical Hypoxia

Chemical hypoxia was induced by cobalt chloride (CoCl<sub>2</sub>). For hypoxic incubation, media of confluent cells was changed to DMEM without serum supplemented by 300 µM CoCl<sub>2</sub> or the specified dose for the dose response experiment. Cells were placed in a standard humidified at 37 °C for 14–16 h. Induction of hypoxia was confirmed by Western blotting for HIF-1α protein expression.

### 2.4. Physical Hypoxia

Physical hypoxia of cells was performed in a modular hypoxia incubator chamber (Billups-Rothenberg, Inc., San Diego, CA, USA, Cat. MIC-101). For hypoxic incubation, after cells became confluent, media was changed to DMEM without serum and cells were placed in the center of the chamber, which was sealed shut and connected via a single flow meter (Billups-Rothenberg, Inc., San Diego, CA, USA, Cat. SFM-3001) to a gas tank containing 1% O<sub>2</sub>, 5% CO<sub>2</sub>, and 94% N<sub>2</sub>. The modular chamber was placed in a standard humidified incubator at 37 °C for 14–16 h or the specified time for the time course experiment. For the recovery experiment, 100 µg/mL cycloheximide was added to the cells before being placed outside the hypoxia chamber for 2 h to prevent protein synthesis. A normoxic control was placed in the same incubator outside of the hypoxia chamber. Induction of hypoxia was confirmed by Western blotting for HIF-1α protein expression.

### 2.5. Small Interfering RNA (siRNA) Knockdown and Plasmid Transfection

The siRNAs for control, MAGE-D2, GNAS and MDM2 siRNAs were purchased from Dharmacon as ON-TARGETplus SMARTpools (D-001810-10-05 and L-010825-00-0005). Cells were first transfected with control or specific siRNA with Lipofectamine RNAiMAX (Invitrogen, Dreieich, Germany) by reverse transfection using the manufacturer's specifications. G $\alpha$ s-HA and Flag- $\beta$ 2AR expression plasmids were cotransfected with control or MAGE-D2 siRNAs with lipofectamine 3000 by reverse transfection using the manufacturer's specifications.

### 2.6. Biotinylation

After hypoxia, confluent cells were washed twice with DPBS supplemented by 1 mM MgCl<sub>2</sub> and 0.1 mM CaCl<sub>2</sub> (PBS<sup>++</sup>). Cells were incubated at 4 °C for 30 min in PBS<sup>++</sup> containing 1 mg/mL EZ-Link<sup>TM</sup> Sulfo-NHS-LC-Biotin. Cells were rinsed three times in PBS<sup>++</sup> with 100 mM glycine and reincubated at 4 °C in the same solution for 10 min. Then, they were washed three times with PBS<sup>++</sup>. Washed cells were lysed for 45 min at 4 °C in solubilizing buffer (150 mM NaCl, 5 mM EDTA, 3 mM KCl, 120 mM Tris/Hepes, pH 7.4, 1% (v/v) Triton X-100) containing protease inhibitors (Sigma, Schnellendorf, Germany). After taking an aliquot of the total cell extract from each sample to provide a measure of total expression, the rest of cell lysates were incubated with neutravidin beads (Thermo Scientific<sup>TM</sup>, 63303 Dreieich, Germany) overnight at 4 °C. After overnight incubation, samples were centrifuged at 13,000 rpm for 5 min, and the supernatant (the intracellular fraction) was removed. Neutravidin beads were then washed with solubilizing buffer and then centrifuged for 5 min at 13,000 rpm seven times. Pellets were incubated in Western blot loading buffer for 10 min at 95 °C and stored at −20 °C. Each fraction was subjected to SDS-PAGE and Western blot analysis.

### 2.7. Immunocytochemistry

Cells were fixed after biotinylation with 4% paraformaldehyde in PBS for 20 min at 4 °C, permeabilized with 0.1% Triton X-100 for 5 min at 4 °C and incubated with DAKO (antibody diluent with background-reducing components) for 30 min to block nonspecific antibody binding. Fixed cells were incubated for 1 h at room temperature with the primary antibody mouse anti-HA (1:50) in DAKO. Mouse anti-HA and biotinylated membrane proteins were visualized with Alexa 555-coupled secondary antibody (1:1000), and Alexa 488-coupled neutravidin (1:500), respectively. Cells were then washed three times with PBS and mounted with Vectashield containing Dapi. Cells were visualized using a Leica confocal (SP8i) microscope.

### 2.8. Immunoprecipitation Assay

Cells were lysed in TNTE buffer (20 mM Tris-HCl, pH 7.4, 150 mM NaCl, 5 mM EDTA, 0.5% Triton X-100, and 10% glycerol) in the presence of proteinase inhibitor cocktail (Sigma, Schnellendorf, Germany). Cell lysates' (500  $\mu$ g total) immunoprecipitation was performed with the primary antibody of interest coupled and crosslinked, using the crosslinker BS<sup>3</sup> (bis(sulfosuccinimidyl)suberate), to the protein G magnetic beads (Dynabeads). After incubation with magnetic protein G beads coupled to the indicated antibody for 1 h at room temperature, the immune complex was washed three times in PBS (Invitrogen, Dreieich, Germany). The protein samples were boiled in loading buffer, separated on 7.5% TGX Stain-Free gel, and probed with the primary antibodies of interest and fluorescence conjugated secondary antibodies according to standard procedures.

### 2.9. Ubiquitination Assay

Cells were transfected by control or MAGE-D2 siRNA by reverse transfection using lipofectamine RNAiMAX. The second day, cells were transfected with WT V5 tagged G $\alpha$ s with single ubiquitin tagged HA. Later, cells were exposed overnight to hypoxia and lysed using RIPA buffer (50 mM Tris/HCl, 150 mM NaCl, 1 mM EDTA, 0.1% SDS, 1% Triton

X-100, and 100 mM N-ethylmaleimide). Cell lysates were cleared at  $13,000\times g$  for 15 min. Protein concentrations of the supernatants were determined using a Pierce™ BCA Protein Assay Kit (Thermo Scientific™, Dreieich, Germany). The samples were then subjected to immunoprecipitation using protein G magnetic beads coupled to anti-V5 antibody, as described in the co-immunoprecipitation section.

#### 2.10. Intracellular cAMP Measurement

Cyclic AMP was measured using a cAMP complete in vitro ELISA kit (Abcam, Berlin, Germany, ab133051), in which a goat anti-rabbit immunoglobulin G binds with a cAMP antibody. Cyclic AMP then binds to the antibody in competition with a labelled colorimetric conjugate, which was measured at 405 nm using a microplate reader (Tecan Infinite Pro). Standards of known cAMP concentrations were used to compare to samples. Before the assay, cell lysates samples prepared in 0.1 M HCL containing 0.1% Triton X-100. The homogenate was pelleted, and the supernatant was used for the assay. Two blanks were included, one with substrate only, and the other received all additions except a sample. Control wells were also monitored for non-specific binding and colorimetric maxima.

#### 2.11. PKA Kinase Activity

The PepTag Nonradioactive Protein Kinase Assay Kit (Promega, Madison, WI, USA) was used according to the manufacturer's instructions. Quantification of the phosphorylated peptide substrate was performed by spectrophotometry by comparing the absorbance at 570 nm.

#### 2.12. Western Blotting

After three washes with ice-cold phosphate-buffered saline (PBS), cells were lysed in lysis buffer (50 mM Tris pH 7.4, 5 mM EDTA, 150 mM NaCl, 1% Triton X-100, and protease inhibitors) and cell lysates were cleared at  $13,000\times g$  for 15 min. Protein concentrations of the supernatants were determined using a Pierce™ BCA Protein Assay Kit (Thermo Scientific™, Dreieich, Germany). Proteins were separated in 7.5% TGX Stain Free gels (Bio-rad, Feldkirchen, Germany, Cat. 1610181) and after transferring to nitrocellulose membrane (Bio-rad, Feldkirchen, Germany, Cat. 1704270) using a Trans-Blot Turbo Transfer System (Bio-rad, Feldkirchen, Germany), proteins were detected with fluorescently labeled antibodies StarBright Blue 520 and 700 (Bio-rad, Feldkirchen, Germany). Imaging of the blots were performed using a ChemiDoc MP (Bio-Rad, Feldkirchen, Germany). Gray density of Western blots was measured using ImageJ software (National Institutes of Health, Bethesda, MD, USA).

#### 2.13. Statistical Analyses

Results are expressed as mean  $\pm$  SEM. Differences between means were evaluated using unpaired Student t test. Statistical analyses were performed using GraphPad Prism X9 software.  $p \leq 0.05$  was considered statistically significant (\*),  $p \leq 0.01$  was considered highly significant (\*\*) and  $p \leq 0.001$  was considered very highly significant (\*\*\*).

### 3. Results

#### 3.1. MAGED2 Is Required for the Expression of Gαs at the Plasma Membrane under Hypoxic Condition

We first asked whether MAGED2 regulated the localization and hence function of Gαs. To address this question, we monitored intracellular distribution of transiently expressed Gαs in control- or MAGED2-depleted HeLa cells by immunocytochemistry. The plasma membrane was labelled with a biotinylated fluorophore. As illustrated in Figure 1a, MAGED2 knockdown did not affect the expression of Gαs at the cell surface under normoxia. In contrast, in cells exposed to physical hypoxia (1% oxygen overnight), MAGED2 knockdown resulted in a dramatic change of the subcellular localization of Gαs from the plasma membrane to an intracellular localization (Figures 1a–c and S1), with both a diffuse and a vesicular pattern. Interestingly, similar results were obtained with

overexpressed (Figures 1d and S2) and endogenous (Figure S3)  $G\alpha_s$ , in HEK293 and HeLa cells, when cellular hypoxia was induced chemically for 16 h with 300  $\mu$ M of cobalt chloride ( $\text{CoCl}_2$ ) which acts as a hypoxia mimetic by inhibiting prolyl hydroxylase activity [15]. Notably,  $G\alpha_s$  membrane expression was restored when cells were exposed to normoxia for 2 h. It is worth noting that this restoration occurred in the presence of cycloheximide, a protein synthesis inhibitor, which was added to exclude the potential implication of newly synthesized proteins. Of note, the marked induction of HIF-1 $\alpha$  protein levels by Western blotting in response to physical and chemical hypoxia demonstrates that relative hypoxia was achieved (Figure 1e,f).

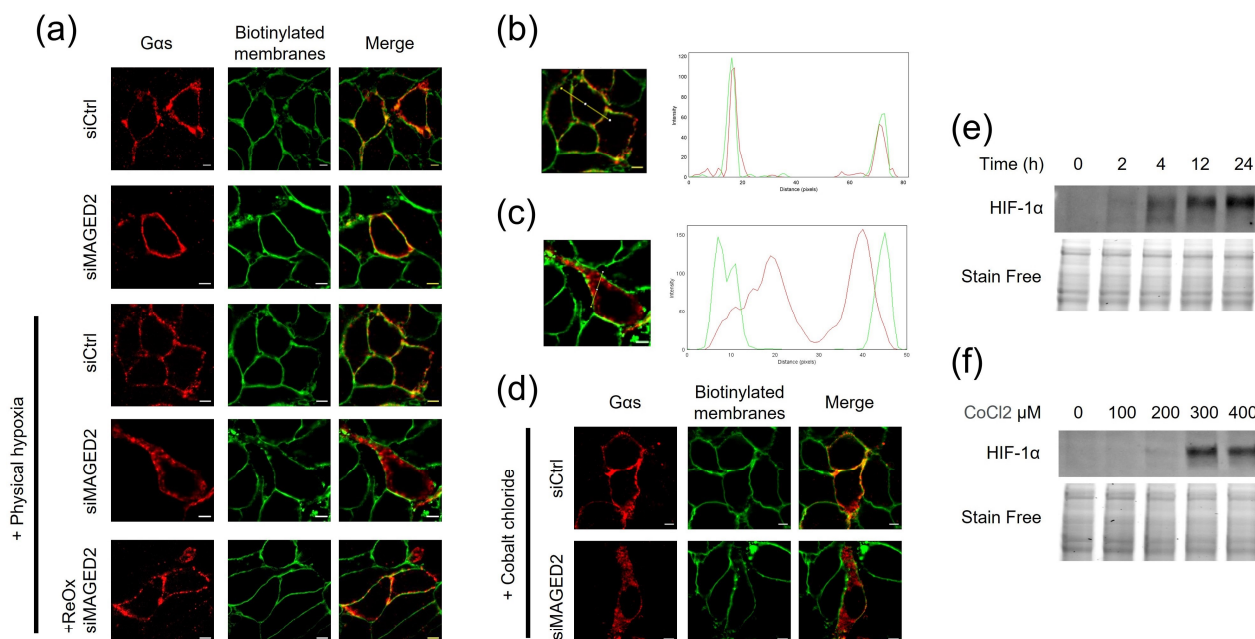


**Figure 1.** MAGED2 prevents internalization of  $G\alpha_s$  under hypoxic condition. **(a)** Immunolocalization studies of  $G\alpha_s$  proteins in presence and absence of MAGED2. HeLa cells were co-transfected with a  $G\alpha_s$ -HA construct and control or MAGED2 siRNA. Forty-eight hours post-transfection, growth medium was replaced by DMEM serum free and cells were exposed to physical hypoxia (1% oxygen overnight), as indicated. Membrane proteins of HeLa cells were biotinylated at 4  $^{\circ}\text{C}$ . Scale bars, 5  $\mu$ m. **(b,c)** Using the “RGB profile plot” plugin in ImageJ, we determined the pattern distribution of  $G\alpha_s$  (red) in comparison to the biotinylated membrane proteins (Green) in the absence **(b)** or presence **(c)** of MAGED2 siRNA under hypoxia. **(d)** Immunolocalization studies of  $G\alpha_s$  proteins in presence and absence of MAGED2 under chemical hypoxia. HeLa cells were co-transfected with a  $G\alpha_s$ -HA construct and control or MAGED2 siRNA. Forty-eight hours post-transfection, growth medium was replaced by DMEM serum free and exposed to chemical hypoxia (300  $\mu$ M  $\text{CoCl}_2$ ), as indicated. Membrane proteins of HeLa cells were biotinylated at 4  $^{\circ}\text{C}$ . Scale bars, 5  $\mu$ m. **(e)** cells were treated with physical hypoxia (1%  $\text{O}_2$ , 5%  $\text{CO}_2$ , 94%  $\text{N}_2$ ) for the specified times. **(f)** cells were treated with chemical hypoxia with the indicated dose of  $\text{CoCl}_2$  for 14–16 h. Chemical hypoxia. **(e,f)** Total cell lysates were separated by SDS-PAGE and probed with anti-HIF-1 $\alpha$  antibodies.

### 3.2. Expression of the $\beta$ 2-Adrenergic Receptor at the Plasma Membrane Is Independent of MAGED2

We next investigated whether the MAGED2 deficiency-induced down regulation of  $G\alpha_s$  cell surface expression under hypoxia can also affect the  $\beta$ 2-adrenergic receptor, which is known to interact physically and functionally with  $G\alpha_s$ . To this end, we assessed endogenous (Figure 2b,c) and transiently (Figure 2a) expressed  $\beta$ 2-adrenergic receptor surface expression using immunocytochemistry and cell surface biotinylation assays. As can be observed in Figure 2a, immunocytochemistry staining shows that MAGED2 knockdown does not affect the cell surface expression of the  $\beta$ 2-adrenergic receptor under normoxic

or hypoxic (physical and chemical hypoxia) conditions as judged by the colocalization of the  $\beta$ 2-adrenergic receptor with biotinylated plasma membrane proteins. As expected, immunoblot analysis shows that, similar to the immunocytochemistry experiments, cell-surface expression of endogenous  $\beta$ 2-adrenergic receptor was not reduced upon MAGED2 knockdown under hypoxia (Figure 2b,c), clearly demonstrating that the effect of MAGED2 knock-down on  $G\alpha_s$  localization under hypoxia is specific. Importantly, we observed internalization the  $\beta$ 2-adrenergic receptor under hypoxic conditions-independently of MAGED2 knockdown, which can be explained by activation of the receptor under hypoxia [16,17].

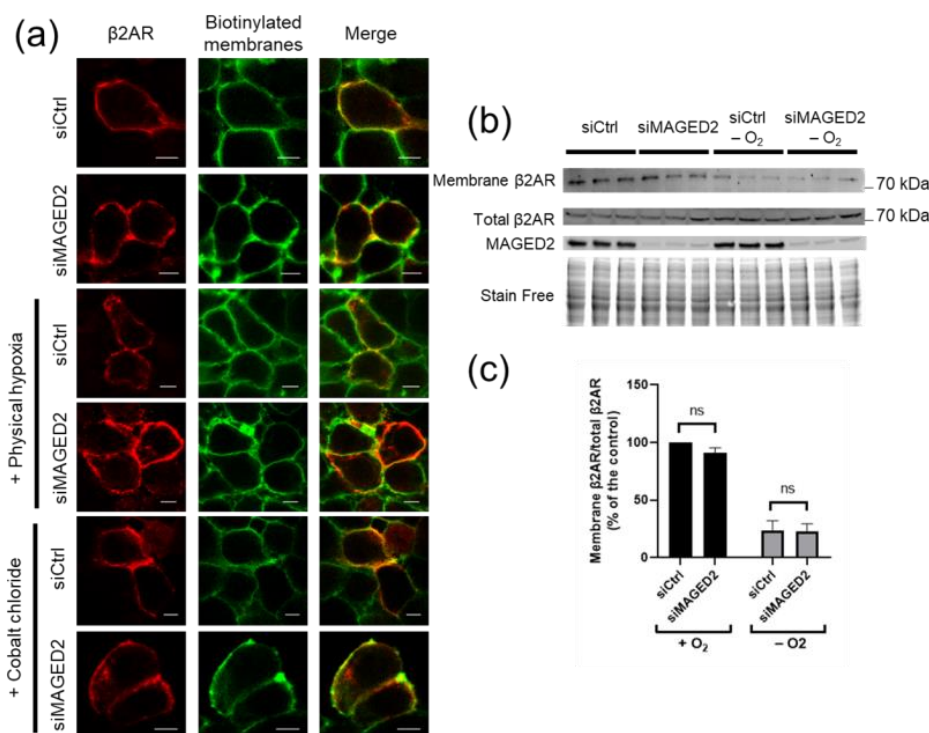


**Figure 2.**  $\beta$ 2-adrenergic receptor internalization is independent of MAGED2 under hypoxic condition. (a) Immunolocalization studies of  $\beta$ 2-adrenergic receptor ( $\beta$ 2AR) in the presence and absence of MAGED2. HeLa cells were co-transfected with a Flag- $\beta$ 2AR construct and control or MAGED2 siRNA. Forty-eight hours post-transfection, growth medium was replaced by DMEM serum free and exposed to physical hypoxia (1% oxygen overnight) or chemical hypoxia (300  $\mu$ M  $\text{CoCl}_2$ ), as indicated. Membrane proteins of HeLa cells were biotinylated at 4  $^{\circ}\text{C}$ . Scale bars, 5  $\mu$ m. (b) HeLa cells were transfected with control and MAGED2 siRNA. In 24–48 h post-transfection, cells were treated with physical hypoxia. Cell surface biotinylated proteins were recovered from cell extracts by precipitation with neutravidin-agarose.  $\beta$ 2AR on the cell surface were detected by Western blotting with a  $\beta$ 2AR antibody. An aliquot of the total cell extract from each sample was also run on a parallel SDS gel and Western blotted for total  $\beta$ 2AR and MAGED2 expression. (c) Densitometric analysis of (b), shown as ratio of membrane  $\beta$ 2AR and total  $\beta$ 2AR immunoblot. Bar graphs show mean  $\pm$  SEM.

### 3.3. MAGED2 Is Required for cAMP Generation and PKA Activity under Hypoxia

$G\alpha_s$  localizes to the plasma membrane to signal GPCR activation to membranous adenylate cyclase in order to promote generation of cAMP and augment PKA activity. Hence both processes could be affected by MAGED2 depletion. We therefore assessed intracellular cAMP levels by ELISA in the different conditions. HeLa and HEK293 cells were transfected by control or MAGED2 siRNA, and subsequently subjected to a hypoxic microenvironment chemically induced by 300  $\mu$ M of  $\text{CoCl}_2$  or physically induced by exposure to 1% oxygen for 16 h. As shown in Figures 3a,b and S4a,c, MAGED2 knockdown decreased basal cAMP levels in HeLa and HEK293 cells, respectively. This decrease was unaffected by the addition of IBMX (Figure S4b), a phosphodiesterase inhibitor, but

reversed by the addition of forskolin, showing that MAGED2 regulates the cAMP level by regulating the localization of  $G_{\alpha s}$  without affecting the activity of adenylate cyclase or phosphodiesterase. Under the same conditions, MAGED2 knockdown reduced PKA activity (Figure 3c,d). In a parallel set of experiments, we analyzed the effect of  $G_{\alpha s}$  knockdown.  $G_{\alpha s}$  knockdown mirrored the effect of MAGED2 depletion, as it reduced basal cAMP levels in both HeLa and HEK293 cells (Figures 3a,b and S4a,b).

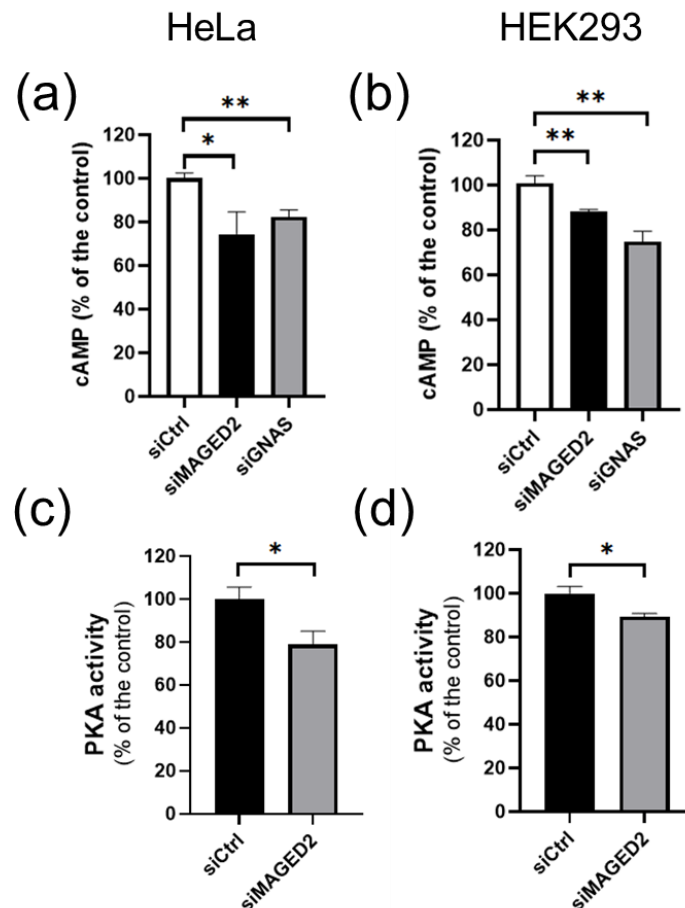


**Figure 3.** MAGED2 depletion decreases cAMP production and PKA activity under hypoxic condition. HeLa (a,c) and HEK293 (b,d) cells were transfected with control, MAGED2 and  $G_{\alpha s}$  siRNA. In 24–48 h post-transfection, growth medium was replaced by DMEM serum free supplemented with 300  $\mu$ M Cobalt chloride ( $CoCl_2$ ). (a,b) Cells were lysed with 0.1 M HCL containing 0.1% Triton X-100 and cAMP was measured by ELISA. (c,d) Cells were lysed with PKA extraction buffer and PKA activity was measured with the PepTag Nonradioactive Protein Kinase Assay Kit. Statistical significance was determined by unpaired two-sided Student's t tests. All data are shown as a representative result from three independent experiments. Bar graphs show mean  $\pm$  SEM. \*  $p \leq 0.05$  and \*\*  $p \leq 0.01$ .

### 3.4. Under Hypoxia, MAGED2 Depletion Promotes Endocytosis of $G_{\alpha s}$ by Enhancing Its MDM2-Dependent Ubiquitination

Because  $G_{\alpha s}$  subcellular redistribution under hypoxia suggests that MAGED2 knockdown enhances  $G_{\alpha s}$  internalization, we first studied the effect of dynasore, a small molecule inhibitor of dynamin mediated endocytosis. As shown in Figure 4a, dynasore treatment fully rescued membrane expression of  $G_{\alpha s}$  upon of MAGED2 depletion. Altogether, the above data provide evidence that the decrease in  $G_{\alpha s}$  cell surface expression was due to an enhanced internalization of the protein, pointing therefore to an inhibitory effect of MAGED2 on endocytosis of  $G_{\alpha s}$  under hypoxia.



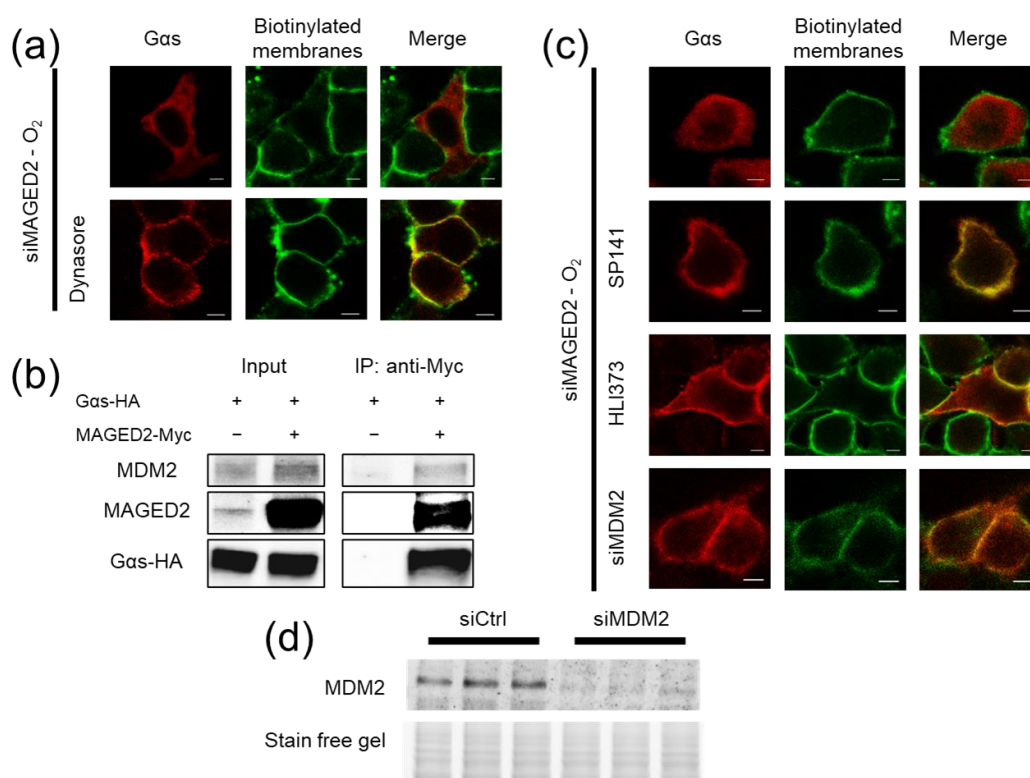


**Figure 4.** MAGED2 prevents MDM2-mediated internalization of Gas under hypoxia. **(a)** HeLa cells were co-transfected with Gas-HA construct and MAGED2 siRNA. Forty-eight hours post-transfection, cells were treated with physical hypoxia overnight in the presence or absence of an endocytosis inhibitor, Dynasore 50  $\mu$ M, as indicated. The stained specimens were evaluated by ApoTome microscopy. Scale bars, 5  $\mu$ m. **(b)** HeLa cells transiently transfected with a Gas-HA construct alone or in combination with a MAGED2-Myc construct were immunoprecipitated (IP) with anti-Myc antibodies. A total of 5% of total cell lysate was loaded for comparison. Co-immunoprecipitated Gas, MAGED2, and MDM2 proteins were detected by immunoblotting using anti-MAGED2, anti-HA, and anti-MDM2 antibodies, respectively. **(c)** HeLa cells were co-transfected with Gas-HA construct and MAGED2 siRNA with or without MDM2 siRNA. Forty-eight hours post-transfection, cells were treated with physical hypoxia overnight in the presence or absence of MDM2 inhibitors, SP141 (1  $\mu$ M), or HLI373 (3  $\mu$ M) as indicated. The stained specimens were evaluated by ApoTome microscopy. Scale bars, 5  $\mu$ m. **(d)** Cells were transfected with control or MDM2 siRNA as indicated. In 24 h post-transfection, cells were lysed in RIPA buffer and cell lysates were separated by SDS-PAGE and probed by anti-MDM2 antibody.

The endocytosis of many proteins is regulated by the action of E3 ubiquitin ligases in a non-degradative fashion by a process called mono or multi-mono ubiquitination [8,18,19]. MAGED2 has been described to interact with both the E3 ubiquitin ligase MDM2 [1,20–22] and Gas [23]. As MDM2 has also been shown to regulate Gas [23], we hypothesized that MAGED2 regulates Gas endocytosis via MDM2. Confirming this notion, we first recapitulated the interaction of MAGED2 to both Gas and MDM2 by Co-IP experiments (Figure 4b). Their interaction is in keeping with the notion that Gas is ubiquitinated by MDM2 in a MAGED2 dependent fashion.

To gain experimental evidence that Gas is ubiquitinated in a MAGED2-dependent fashion, we combined expression of HA-tagged ubiquitin and V5-tagged Gas with knock-down of MAGED2 followed by physical hypoxia (Figure 5a, lower part). Immunoblot analysis of Gas immunoprecipitates using an HA-antibody, revealed increased staining intensity upon knockdown of MAGED2 (Figure 5a, upper part). Given the comparable amounts of immunoprecipitated total V5-Gas proteins (Figure 5a, middle part), our data

strongly indicate that ubiquitination of G $\alpha$ s under hypoxia is markedly increased upon knockdown of MAGED2, which could be confirmed by densitometric analysis (Figure 5b).

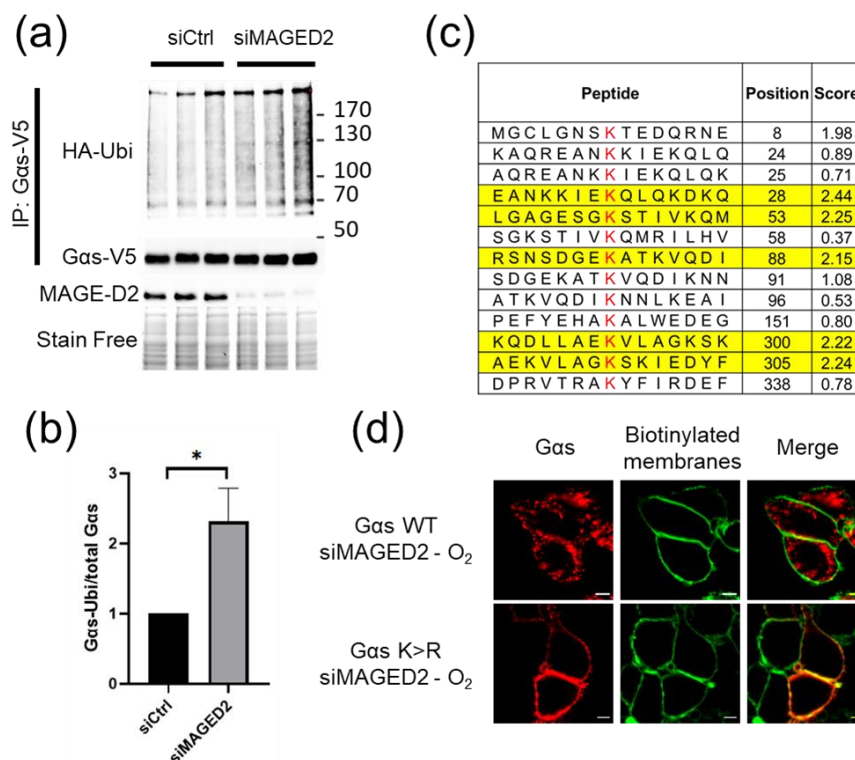


**Figure 5.** MAGED2 inhibits G $\alpha$ s ubiquitination under hypoxic condition. **(a)** MAGED2 regulates G $\alpha$ s ubiquitination. HEK293 cells, transiently transfected with G $\alpha$ s-V5 and ubiquitin-HA, were immunoprecipitated with anti-V5 under denaturing conditions. Ubiquitinated G $\alpha$ s was detected with anti-HA antibody. **(b)** Densitometric analysis of (a), shown as ratio of ubiquitinated G $\alpha$ s and total G $\alpha$ s immunoblot. Statistical significance was determined by unpaired two-sided Student's *t*-tests. Data are shown as a representative result from three independent experiments. Bar graphs show mean  $\pm$  SEM. \* *p*  $\leq$  0.05. **(c)** The ubiquitination sites of G $\alpha$ s were predicted with a Bayesian Discriminant Method [24] and the predicted sites with a score  $\geq 2$  were chosen for mutation (yellow). **(d)** Immunofluorescence microscopy showing distribution of wild type (WT) or a Gas-HA variant harboring 5 lysine-to-arginine substitutions (5 $\times$ K > R) in HeLa cells under physical hypoxia. Cells were stained with mouse anti-HA antibody for G $\alpha$ s (Alexa 555, Red) and plasma membrane biotinylated proteins (Alexa 488, Green). The yellow color (merged image) indicates co-localization of the proteins. Scale bars, 5  $\mu$ m.

After having shown that G $\alpha$ s is ubiquitinated and endocytosed in a MAGED2 dependent fashion, we aimed to gain functional evidence that these processes are indeed regulated by MDM2. Therefore, we inhibited MDM2 by various approaches. As illustrated in Figure 4c, chemical inhibition of MDM2 with either Sp-141 or HLI-373 [25] rescued G $\alpha$ s plasma membrane localization following MAGED2 depletion under hypoxia. Importantly, MDM2 knockdown reproduced the same effect (Figure 4c). Of note, a marked reduction of MDM2 protein levels with siRNA was confirmed by Western blotting (Figure 4d). Consistent with abrogating internalization of G $\alpha$ s in MAGED2-depleted hypoxic cells, Sp-141 treatment also prevented the decrease in cAMP caused by MAGED2 knockdown under physical hypoxia (Figure S4b).

Finally, to prove that ubiquitination of G $\alpha$ s is necessary to allow its endocytosis, we chose five (out of thirteen) lysine residues of G $\alpha$ s protein that could serve as acceptor sites for ubiquitin based on their accessibility and mutated them to arginine (5 $\times$ K > R) (Figure 5c). Immunocytochemistry of cells expressing the 5 $\times$ K > R G $\alpha$ s variant demonstrated that endocytosis triggered by hypoxia and MAGED2 knockdown was suppressed



by the mutations compared to wild type  $G_{\alpha s}$  (Figure 5d). To exclude the possibility that the  $5 \times K > R$   $G_{\alpha s}$  construct is locked in the plasma membrane because of a general defect of internalization, cells were treated with cholera toxin, which induces  $G_{\alpha s}$  internalization by directly activating its GTPase function [26]. As shown in Figure S6, the cholera toxin induced internalization of both wildtype and the mutant  $5 \times K > R$   $G_{\alpha s}$  variant. This finding supports the notion that the blockade of the hypoxia-induced endocytosis of  $G_{\alpha s}$  in MAGED2-depleted cells results specifically from impaired ubiquitination of critical lysine residues and not from a general defect in protein internalization (Figure S6). Taken together, our data clearly demonstrate that MAGED2 deficiency leads to the ubiquitin and MDM2-triggered endocytosis of  $G_{\alpha s}$  under hypoxic conditions.

#### 4. Discussion

The molecular basis of the role of MAGED2 in transient Bartter syndrome, which is characterized by profound fetal salt wasting and polyuria leading to perinatal death and extreme prematurity followed by spontaneous recovery in the survivors, has been unknown. In this study, we demonstrate that MAGED2 acts as a master regulator of cAMP/PKA under hypoxia, by controlling the endocytosis  $G_{\alpha s}$  via MDM2-dependent ubiquitination (Figure 6). Because the essential salt-transporters NKCC2 and NCC require cAMP for proper expression and functioning our finding of  $G_{\alpha s}$  mistargeting and impaired cAMP generation in MAGED2-depleted hypoxic cells may explain, at least in part, the transient nature of antenatal Bartter syndrome caused by MAGED2 mutations and reveal potential strategies of intervention in this disease and beyond.

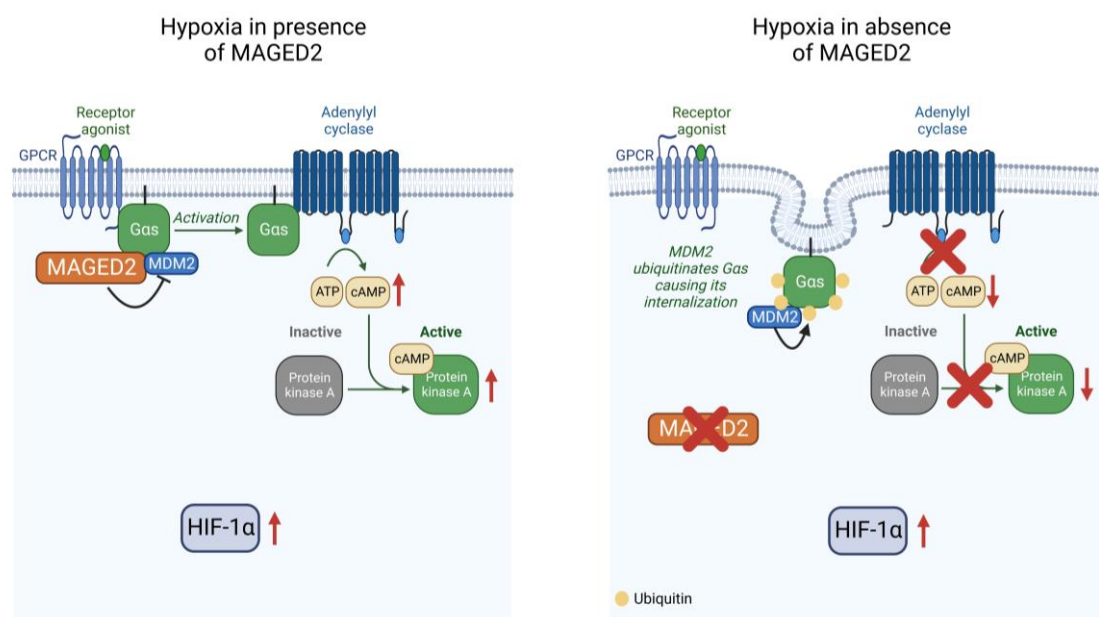


**Figure 6.** Proposed model for MAGED2's role under hypoxia (created with BioRender.com). Under hypoxia, MAGED2 inhibits MDM2 dependent ubiquitination and endocytosis of  $G_{\alpha s}$ . This ensures activation of the adenylate cyclase and cAMP generation and activation of PKA under hypoxia. Reduced cAMP levels impair cAMP-dependent salt reabsorption, explaining salt wasting in transient Bartter syndrome.

On the cell biological level, we now demonstrate that MAGED2 is necessary under hypoxia to prevent ubiquitin-dependent and dynasore-sensitive endocytosis of  $G_{\alpha s}$  by blocking the E3 ubiquitin ligase MDM2. The mechanism how  $G_{\alpha s}$  dissociates from the plasma membrane to enter into the endocytic network, where it engages with GPCRs and the epidermal growth factor receptor (EGFR) to promote signaling [27,28] and sorting [29,30], respectively, is ill defined. The depalmitoylation of  $G_{\alpha s}$  followed by simple diffusion through the cytosol was proposed [31]. Indeed, imaging studies have demonstrated that

internalized G $\alpha$ s can appear to be diffuse in the cytosol [26,32], but association with intracellular vesicles has also been observed [33–35].

Given the well-recognized role of ubiquitination in endocytosis [8] our finding that G $\alpha$ s is internalized in an ubiquitin dependent manner is—although not unexpected—a necessary step to pave the way for subsequent studies, giving more insight into the regulation of the endocytosis of G $\alpha$ s. We demonstrate that MDM2 is the relevant E3 ligase mediating the MAGED2 dependent endocytosis of G $\alpha$ s, which concurs with previous studies demonstrating a physical interaction between MDM2 and MAGED2 [1,22], as well as MAGED2 and G $\alpha$ s [1,9]. Inhibition of ubiquitination and endocytosis of G $\alpha$ s could result from MAGED2 inhibiting the ligase activity of MDM2, a mechanism also proposed for MAGEA2 and MAGEC2 [36,37]. Alternatively, MAGED2 could inhibit ubiquitination of G $\alpha$ s by shielding it from the ligase activity of MDM2. Our data thus corroborate and extend previous studies on the important role of MDM2 in the regulation of GPCR-signaling, which demonstrated that the ubiquitination of  $\beta$ 2-arrestin (ARRB2) by MDM2 promotes the endocytosis of the  $\beta$ 2-adrenergic receptor under normoxia [38]. This demonstrates that MDM2 regulates GPCR signaling in a context and substrate specific way, which can be explained by MAGED2 acting as a specific adaptor of G $\alpha$ s but not for the  $\beta$ 2-adrenergic receptor, as the latter was internalized under hypoxia independently of the presence of MAGED2 (Figure 2). Targeting the cAMP/PKA cascade downstream of G $\alpha$ s should be an ideal treatment for patients with transient Bartter syndrome: It could reactivate renal salt reabsorption to prevent perinatal death or sequelae such as intracerebral hemorrhage resulting from excessive amniotic fluid production causing preterm delivery. Although maternal hyperoxia results in increased oxygenation in the human fetus [39], which could stimulate the cAMP/PKA pathway and hence promote salt reabsorption, the toxicity of oxygen, especially in preterms resulting from the generation of reactive oxygen species, precludes its clinical use. Therefore, direct activators of the cAMP/PKA cascade such as forskolin, which can be given orally and has already been used in human clinical studies [40–44], could be studied in models of transient Bartter syndrome.

Our finding that MAGED2 can block MDM2-dependent internalization of G $\alpha$ s may indicate that this mechanism is regulated in a graded fashion in normal subjects, perhaps by posttranslational modifications of MAGED2 to fine-tune MDM2 ligase activity in order to adjust the diverse functions of G $\alpha$ s (and other substrates of MDM2).

By showing that MAGED2 is dispensable under normoxia (both in vivo and in vitro) but critically important under hypoxia to ensure the G $\alpha$ s-dependent activation of cAMP/PKA pathway, our study adds hypoxia to the growing list of stressors (nutritional, genotoxic, and radiation stress) against which various members of the MAGE family have been shown to protect [6,45]. Of note, especially the renal medulla, where NKCC2, one of the key salt transport proteins, is expressed, has a low oxygen tension. The latter is even more severe in utero [2–4]. However, similar to the previously identified stressors, the molecular switch leading to inhibition of MDM2-dependent ubiquitination under hypoxia is unknown. Rapid relocation of G $\alpha$ s to the plasma membrane upon reoxygenation in the presence of cycloheximide (which blocks protein synthesis) argues that the molecular switch under normoxia is brought about by posttranslational modification (s) of MDM2 and/or its partners.

Of note, MAGED2 is also expressed in many human cancers and is associated with a poor prognosis [4,46–49]. Moreover, the hypoxic microenvironment in cancer cells is the key condition affecting the cellular expression program, leading to chemotherapy resistance [50]. Given the established roles of G $\alpha$ s as oncoprotein in malignancy [51–53], it is conceivable that MAGED2 promotes tumorigenesis by stimulating the cAMP/PKA pathway and could therefore be specifically targeted under hypoxia to inhibit the cAMP/PKA signaling.

The vast majority of patients with transient Bartter syndrome described so far have mutations corresponding to a (functional) knockout of the gene (19 out of 26 patients, please see table one in: [54]. These mutations include two deletions of the entire MAGED2 gene, and 17 mutations in the MAGED2 gene leading to premature termination codons >> 60 basepairs upstream of the 3' most splice-generated exon-exon junction, which elicits nonsense-mediated

decay (NMD). NMD is an essential RNA quality control mechanism that assures the quality of the transcriptome by eliminating transcripts that contain premature termination codons (PTCs) [55]. The remaining seven mutations include four missense mutations and three in frame deletions, which in general reduce the stability of the protein. We therefore think that the depletion of MAGED2 with our siRNA approach is a suitable model to study the function of MAGED2 at the cellular level for the majority of these patients.

As described above, we used HEK293 and HeLa cells instead of tubular renal cells to analyze the function of MAGED2 on  $G_{\alpha s}$  signaling. Given that experiments yielded similar results in both cell lines, we are convinced that our findings can be generalized to human cells. We hypothesize that there is a specific phenotype of MAGED2 deficiency only in the kidney, because the renal medulla of the kidney is known for its low oxygen tension, which in combination with the physiological fetal hypoxia unveil its dependence of MAGED2 for proper  $G_{\alpha s}$  dependent signaling under hypoxia.

In summary, we reveal that MAGED2 regulates ubiquitin dependent endocytosis of  $G_{\alpha s}$  under hypoxia by inhibiting MDM2 and thereby acts a master regulator of the  $G_{\alpha s}$ -dependent activation of the PKA pathway. Whereas activation downstream of  $G_{\alpha s}$  could restore cAMP dependent salt reabsorption in transient Bartter syndrome, inhibition of MAGED2 could target the oncoprotein  $G_{\alpha s}$  specifically in hypoxic tumors without disturbing  $G_{\alpha s}$  signaling in normal tissue.

**Supplementary Materials:** The following supporting information can be downloaded at: <https://www.mdpi.com/article/10.3390/cells11162546/s1>, Figure S1. MAGED2 prevents internalization of  $G_{\alpha s}$  under hypoxic condition; Figure S2. MAGED2 prevents internalization of  $G_{\alpha s}$  under hypoxic condition in renal cells; Figure S3. MAGED2 prevents internalization of endogenous  $G_{\alpha s}$  under hypoxic condition in cells; Figure S4. MAGED2 promotes cAMP production activity under physical hypoxia; Figure S5. Knockdown of MAGED2 and  $G_{\alpha s}$ ; Figure S6.  $G_{\alpha s}$  5K>R variant is sensitive to cholera toxin induced endocytosis.

**Author Contributions:** Conceptualization, E.S. and M.K. (Martin Kömhoff); Methodology, E.S., H.M., K.L. and M.K. (Martin Kömhoff); Investigation, E.S., S.N., L.Q. and M.K. (Maja Kleim); Visualization, E.S. and S.N.; Funding acquisition, E.S. and M.K. (Martin Kömhoff); Project administration, M.K. (Martin Kömhoff); Supervision: M.K. (Martin Kömhoff); Writing—original draft, E.S., H.M., K.L. and M.K. (Martin Kömhoff); Writing—review and editing, S.W. All authors have read and agreed to the published version of the manuscript.

**Funding:** This work was supported by grant: German Research Foundation (DFG) Ko1855/4-1 (MK, Martin Kömhoff), Stiftung P.E. Kempkes 03/2018 (ES), University Medical Center Giessen and Marburg UKGM 15/2021 (ES). Open Access funding provided by the Open Access Publication Fund of Philipps-Universität Marburg with support of the Deutsche Forschungsgemeinschaft (DFG, German Research Foundation).

**Institutional Review Board Statement:** Not applicable.

**Informed Consent Statement:** Not applicable.

**Data Availability Statement:** All data are available in the main text or the Supplementary Materials.

**Acknowledgments:** We thank Michelle Auer for technical support.

**Conflicts of Interest:** Authors declare that they have no competing interest.

## References

1. Laghmani, K.; Beck, B.B.; Yang, S.-S.; Seaayfan, E.; Wenzel, A.; Reusch, B.; Vitzthum, H.; Priem, D.; Demaretz, S.; Bergmann, K.; et al. Polyhydramnios, Transient Antenatal Bartter's Syndrome, and MAGED2 Mutations. *N. Engl. J. Med.* **2016**, *374*, 1853–1863. [[CrossRef](#)] [[PubMed](#)]
2. Rudolph, A.M.; Heymann, M.a.; Teramo, K.a.W.; Barrett, C.T.; Räihä, N.C.R. Studies on the Circulation of the Previabie Human Fetus. *Pediatric Res.* **1971**, *5*, 452–465. [[CrossRef](#)]
3. Brezis, M.; Rosen, S. Hypoxia of the renal medulla—Its implications for disease. *N. Engl. J. Med.* **1995**, *332*, 647–655. [[CrossRef](#)] [[PubMed](#)]

4. Bernhardt, W.M.; Schmitt, R.; Rosenberger, C.; Munchenhagen, P.M.; Grone, H.J.; Frei, U.; Warnecke, C.; Bachmann, S.; Wiesener, M.S.; Willam, C.; et al. Expression of hypoxia-inducible transcription factors in developing human and rat kidneys. *Kidney Int.* **2006**, *69*, 114–122. [CrossRef] [PubMed]
5. Hemker, S.L.; Sims-Lucas, S.; Ho, J. Role of hypoxia during nephrogenesis. *Pediatr. Nephrol.* **2016**, *31*, 1571–1577. [CrossRef]
6. Florke Gee, R.R.; Chen, H.; Lee, A.K.; Daly, C.A.; Wilander, B.A.; Fon Tacer, K.; Potts, P.R. Emerging roles of the MAGE protein family in stress response pathways. *J. Biol. Chem.* **2020**, *295*, 16121–16155. [CrossRef]
7. Doyle, J.M.; Gao, J.; Wang, J.; Yang, M.; Potts, P.R. MAGE-RING protein complexes comprise a family of E3 ubiquitin ligases. *Mol. Cell* **2010**, *39*, 963–974. [CrossRef]
8. Foot, N.; Henshall, T.; Kumar, S. Ubiquitination and the Regulation of Membrane Proteins. *Physiol. Rev.* **2017**, *97*, 253–281. [CrossRef]
9. Huttlin, E.L.; Bruckner, R.J.; Navarrete-Perea, J.; Cannon, J.R.; Baltier, K.; Gebreab, F.; Gygi, M.P.; Thornock, A.; Zarraga, G.; Tam, S.; et al. Dual proteome-scale networks reveal cell-specific remodeling of the human interactome. *Cell* **2021**, *184*, 3022–3040.e3028. [CrossRef]
10. Sassone-Corsi, P. The cyclic AMP pathway. *Cold Spring Harb. Perspect. Biol.* **2012**, *4*, a011148. [CrossRef]
11. Fenton, R.A.; Knepper, M.A. Mouse models and the urinary concentrating mechanism in the new millennium. *Physiol. Rev.* **2007**, *87*, 1083–1112. [CrossRef] [PubMed]
12. Zhang, Y.; Lv, Y.; Zhang, Y.; Gao, H. Regulation of p53 Level by UBE4B in Breast Cancer. *PLoS ONE* **2014**, *9*, e90154. [CrossRef] [PubMed]
13. García-Cano, J.; Sánchez-Tena, S.; Sala-Gaston, J.; Figueras, A.; Viñals, F.; Bartrons, R.; Ventura, F.; Rosa, J.L. Regulation of the MDM2-p53 pathway by the ubiquitin ligase HERC2. *Mol. Oncol.* **2020**, *14*, 69–86. [CrossRef] [PubMed]
14. Tang, Y.; Hu, L.A.; Miller, W.E.; Ringstad, N.; Hall, R.A.; Pitcher, J.A.; DeCamilli, P.; Lefkowitz, R.J. Identification of the endophilins (SH3p4/p8/p13) as novel binding partners for the  $\beta$ 1-adrenergic receptor. *Proc. Natl. Acad. Sci. USA* **1999**, *96*, 12559–12564. [CrossRef] [PubMed]
15. Muñoz-Sánchez, J.; Cháñez-Cárdenas, M.E. The use of cobalt chloride as a chemical hypoxia model. *J. Appl. Toxicol.* **2019**, *39*, 556–570. [CrossRef] [PubMed]
16. Kido, A.; Yoshitani, K.; Shimizu, T.; Akahane, M.; Fujii, H.; Tsukamoto, S.; Kondo, Y.; Honoki, K.; Imano, M.; Tanaka, Y. Effect of mesenchymal stem cells on hypoxia-induced desensitization of  $\beta$ 2-adrenergic receptors in rat osteosarcoma cells. *Oncol. Lett.* **2012**, *4*, 745–750. [CrossRef] [PubMed]
17. Cheong, H.I.; Asosingh, K.; Stephens, O.R.; Queisser, K.A.; Xu, W.; Willard, B.; Hu, B.; Dermawan, J.K.T.; Stark, G.R.; Naga Prasad, S.V.; et al. Hypoxia sensing through  $\beta$ -adrenergic receptors. *JCI Insight* **2016**, *1*, e90240. [CrossRef]
18. Haupt, Y.; Maya, R.; Kazaz, A.; Oren, M. Mdm2 promotes the rapid degradation of p53. *Nature* **1997**, *387*, 296–299. [CrossRef]
19. Girnita, L.; Girnita, A.; Larsson, O. Mdm2-dependent ubiquitination and degradation of the insulin-like growth factor 1 receptor. *Proc. Natl. Acad. Sci. USA* **2003**, *100*, 8247–8252. [CrossRef]
20. Huttlin, E.L.; Ting, L.; Bruckner, R.J.; Gebreab, F.; Gygi, M.P.; Szpyt, J.; Tam, S.; Zarraga, G.; Colby, G.; Baltier, K.; et al. The BioPlex Network: A Systematic Exploration of the Human Interactome. *Cell* **2015**, *162*, 425–440. [CrossRef]
21. Huttlin, E.L.; Bruckner, R.J.; Paulo, J.A.; Cannon, J.R.; Ting, L.; Baltier, K.; Colby, G.; Gebreab, F.; Gygi, M.P.; Parzen, H.; et al. Architecture of the human interactome defines protein communities and disease networks. *Nature* **2017**, *545*, 505–509. [CrossRef] [PubMed]
22. Zhao, K.; Yang, Y.; Zhang, G.; Wang, C.; Wang, D.; Wu, M.; Mei, Y. Regulation of the Mdm2–p53 pathway by the ubiquitin E3 ligase MARCH7. *EMBO Rep.* **2018**, *19*, 305–319. [CrossRef] [PubMed]
23. Tang, T.; Gao, M.H.; Miyano, A.; Hammond, H.K. G $\alpha$ q reduces cAMP production by decreasing G $\alpha$ s protein abundance. *Biochem. Biophys. Res. Commun.* **2008**, *377*, 679–684. [CrossRef] [PubMed]
24. Li, A.; Gao, X.; Ren, J.; Jin, C.; Xue, Y. BDM-PUB: Computational Prediction of Protein Ubiquitination Sites with a Bayesian Discriminant Method. Available online: <http://bmdp.biocuckoo.org/prediction.php> (accessed on 1 June 2021).
25. Chen, Y.; Wang, D.-D.; Wu, Y.-P.; Su, D.; Zhou, T.-Y.; Gai, R.-H.; Fu, Y.-Y.; Zheng, L.; He, Q.-J.; Zhu, H.; et al. MDM2 promotes epithelial-mesenchymal transition and metastasis of ovarian cancer SKOV3 cells. *Br. J. Cancer* **2017**, *117*, 1192–1201. [CrossRef]
26. Wedegaertner, P.B.; Bourne, H.R.; von Zastrow, M. Activation-induced subcellular redistribution of Gs  $\alpha$ . *Mol. Biol. Cell* **1996**, *7*, 1225–1233. [CrossRef]
27. Ferrandon, S.; Feinstein, T.N.; Castro, M.; Wang, B.; Bouley, R.; Potts, J.T.; Gardella, T.J.; Vilardaga, J.P. Sustained cyclic AMP production by parathyroid hormone receptor endocytosis. *Nat. Chem. Biol.* **2009**, *5*, 734–742. [CrossRef]
28. Feinstein, T.N.; Yui, N.; Webber, M.J.; Wehbi, V.L.; Stevenson, H.P.; King, J.D., Jr.; Hallows, K.R.; Brown, D.; Bouley, R.; Vilardaga, J.P. Noncanonical control of vasopressin receptor type 2 signaling by retromer and arrestin. *J. Biol. Chem.* **2013**, *288*, 27849–27860. [CrossRef]
29. Li, X.; Letourneau, D.; Holleran, B.; Leduc, R.; Lavigne, P.; Lavoie, C. Galphas protein binds ubiquitin to regulate epidermal growth factor receptor endosomal sorting. *Proc. Natl. Acad. Sci. USA* **2017**, *114*, 13477–13482. [CrossRef]
30. Rosciglione, S.; Theriault, C.; Boily, M.O.; Paquette, M.; Lavoie, C. Galphas regulates the post-endocytic sorting of G protein-coupled receptors. *Nat. Commun.* **2014**, *5*, 4556. [CrossRef]
31. Saini, D.K.; Chisari, M.; Gautam, N. Shuttling and translocation of heterotrimeric G proteins and Ras. *Trends Pharmacol. Sci.* **2009**, *30*, 278–286. [CrossRef]



32. Thiagarajan, M.M.; Bigras, E.; Van Tol, H.H.; Hébert, T.E.; Evanko, D.S.; Wedegaertner, P.B. Activation-induced subcellular redistribution of G alpha(s) is dependent upon its unique N-terminus. *Biochemistry* **2002**, *41*, 9470–9484. [[CrossRef](#)] [[PubMed](#)]
33. Allen, J.A.; Yu, J.Z.; Donati, R.J.; Rasenick, M.M. Beta-adrenergic receptor stimulation promotes G alpha s internalization through lipid rafts: A study in living cells. *Mol. Pharmacol.* **2005**, *67*, 1493–1504. [[CrossRef](#)] [[PubMed](#)]
34. Hynes, T.R.; Mervine, S.M.; Yost, E.A.; Sabo, J.L.; Berlot, C.H. Live cell imaging of Gs and the beta2-adrenergic receptor demonstrates that both alphas and beta1gamma7 internalize upon stimulation and exhibit similar trafficking patterns that differ from that of the beta2-adrenergic receptor. *J. Biol. Chem.* **2004**, *279*, 44101–44112. [[CrossRef](#)]
35. Yu, J.Z.; Rasenick, M.M. Real-time visualization of a fluorescent G(alpha)(s): Dissociation of the activated G protein from plasma membrane. *Mol. Pharmacol.* **2002**, *61*, 352–359. [[CrossRef](#)] [[PubMed](#)]
36. Hao, J.; Song, X.; Wang, J.; Guo, C.; Li, Y.; Li, B.; Zhang, Y.; Yin, Y. Cancer-testis antigen MAGE-C2 binds Rbx1 and inhibits ubiquitin ligase-mediated turnover of cyclin E. *Oncotarget* **2015**, *6*, 42028–42039. [[CrossRef](#)]
37. Marcar, L.; Ihrig, B.; Hourihan, J.; Bray, S.E.; Quinlan, P.R.; Jordan, L.B.; Thompson, A.M.; Hupp, T.R.; Meek, D.W. MAGE-A Cancer/Testis Antigens Inhibit MDM2 Ubiquitylation Function and Promote Increased Levels of MDM4. *PLoS ONE* **2015**, *10*, e0127713. [[CrossRef](#)]
38. Lefkowitz, R.J.; Rajagopal, K.; Whalen, E.J. New roles for beta-arrestins in cell signaling: Not just for seven-transmembrane receptors. *Mol. Cell* **2006**, *24*, 643–652. [[CrossRef](#)]
39. Sorensen, A.; Sinding, M.; Peters, D.A.; Petersen, A.; Frokjaer, J.B.; Christiansen, O.B.; Uldbjerg, N. Placental oxygen transport estimated by the hyperoxic placental BOLD MRI response. *Physiol. Rep.* **2015**, *3*, e12582. [[CrossRef](#)]
40. Ammon, H.P.T.; Muller, A.B. Forskolin—From an Ayurvedic Remedy to a Modern Agent. *Planta Med.* **1985**, *51*, 473–477. [[CrossRef](#)]
41. Godard, M.P.; Johnson, B.A.; Richmond, S.R. Body Composition and Hormonal Adaptations Associated with Forskolin Consumption in Overweight and Obese Men. *Obes. Res.* **2005**, *13*, 1335–1343. [[CrossRef](#)]
42. Henderson, S.; Magu, B.; Rasmussen, C.; Lancaster, S.; Kersick, C.; Smith, P.; Melton, C.; Cowan, P.; Greenwood, M.; Earnest, C.; et al. Effects of coleus forskohlii supplementation on body composition and hematological profiles in mildly overweight women. *J. Int. Soc. Sports Nutr.* **2005**, *2*, 54–62. [[CrossRef](#)]
43. González-Sánchez, R.; Trujillo, X.; Trujillo-Hernández, B.; Vásquez, C.; Huerta, M.; Elizalde, A. Forskolin versus Sodium Cromoglycate for Prevention of Asthma Attacks: A Single-blinded Clinical Trial. *J. Int. Med. Res.* **2006**, *34*, 200–207. [[CrossRef](#)] [[PubMed](#)]
44. Salehi, B.; Staniak, M.; Czopek, K.; Stepien, A.; Dua, K.; Wadhwa, R.; Chellappan, D.K.; Sytar, O.; Brestic, M.; Bhat, N.G.; et al. The Therapeutic Potential of the Labdane Diterpenoid Forskolin. *Appl. Sci.* **2019**, *9*, 4089. [[CrossRef](#)]
45. Fon Tacer, K.; Montoya, M.C.; Oatley, M.J.; Lord, T.; Oatley, J.M.; Klein, J.; Ravichandran, R.; Tillman, H.; Kim, M.; Connelly, J.P.; et al. MAGE cancer-testis antigens protect the mammalian germline under environmental stress. *Sci. Adv.* **2019**, *5*, eaav4832. [[CrossRef](#)] [[PubMed](#)]
46. Kidd, M.; Modlin, I.M.; Mane, S.M.; Camp, R.L.; Eick, G.; Latich, I. The role of genetic markers—NAP1L1, MAGE-D2, and MTA1—In defining small-intestinal carcinoid neoplasia. *Ann. Surg. Oncol.* **2006**, *13*, 253–262. [[CrossRef](#)] [[PubMed](#)]
47. Kanda, M.; Murotani, K.; Tanaka, H.; Miwa, T.; Umeda, S.; Tanaka, C.; Kobayashi, D.; Hayashi, M.; Hattori, N.; Suenaga, M.; et al. A novel dual-marker expression panel for easy and accurate risk stratification of patients with gastric cancer. *Cancer Med.* **2018**, *7*, 2463–2471. [[CrossRef](#)]
48. Chung, F.Y.; Cheng, T.L.; Chang, H.J.; Chiu, H.H.; Huang, M.Y.; Chang, M.S.; Chen, C.C.; Yang, M.J.; Wang, J.Y.; Lin, S.R. Differential gene expression profile of MAGE family in taiwanese patients with colorectal cancer. *J. Surg. Oncol.* **2010**, *102*, 148–153. [[CrossRef](#)]
49. Tsai, J.R.; Chong, I.W.; Chen, Y.H.; Yang, M.J.; Sheu, C.C.; Chang, H.C.; Hwang, J.J.; Hung, J.Y.; Lin, S.R. Differential expression profile of MAGE family in non-small-cell lung cancer. *Lung Cancer* **2007**, *56*, 185–192. [[CrossRef](#)]
50. Jing, X.; Yang, F.; Shao, C.; Wei, K.; Xie, M.; Shen, H.; Shu, Y. Role of hypoxia in cancer therapy by regulating the tumor microenvironment. *Mol. Cancer* **2019**, *18*, 157. [[CrossRef](#)]
51. Rohwer, N.; Zasada, C.; Kempa, S.; Cramer, T. The growing complexity of HIF-1alpha's role in tumorigenesis: DNA repair and beyond. *Oncogene* **2013**, *32*, 3569–3576. [[CrossRef](#)]
52. O'Hayre, M.; Vázquez-Prado, J.; Kufareva, I.; Stawiski, E.W.; Handel, T.M.; Seshagiri, S.; Gutkind, J.S. The emerging mutational landscape of G proteins and G-protein-coupled receptors in cancer. *Nat. Rev. Cancer* **2013**, *13*, 412–424. [[CrossRef](#)] [[PubMed](#)]
53. Tirosh, A.; Jin, D.X.; De Marco, L.; Laitman, Y.; Friedman, E. Activating genomic alterations in the Gs alpha gene (GNAS) in 274694 tumors. *Genes Chromosomes Cancer* **2020**, *59*, 503–516. [[CrossRef](#)] [[PubMed](#)]
54. Wu, X.; Huang, L.; Luo, C.; Liu, Y.; Niu, J. A Case Report and Literature Review of a Novel Mutation in the MAGED2 Gene of a Patient With Severe Transient Polyhydramnios. *Front. Pediatrics* **2021**, *9*, 778814. [[CrossRef](#)] [[PubMed](#)]
55. Karousis, E.D.; Mühlemann, O. The broader sense of nonsense. *Trends Biochem. Sci.* **2022**. [[CrossRef](#)] [[PubMed](#)]

## Supplementary figures

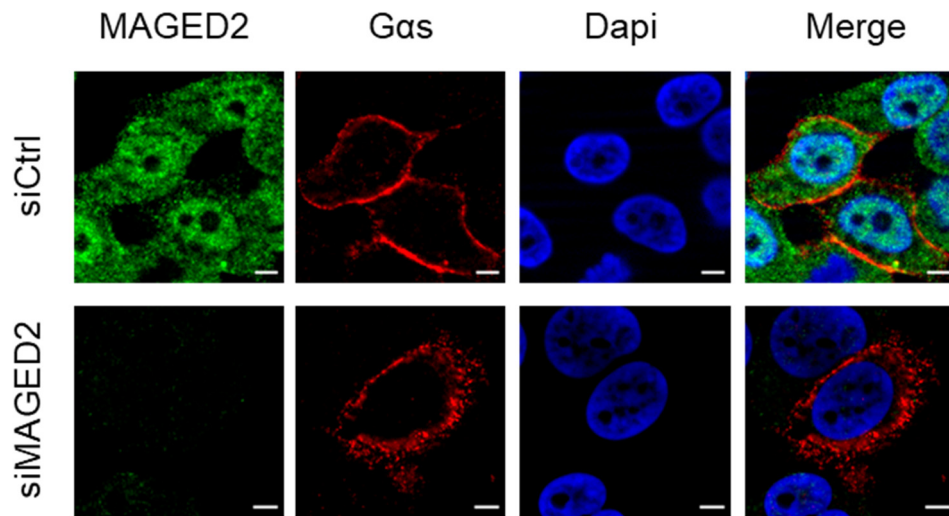


**Figure S1. MAGED2 prevents internalization of Gas under hypoxic condition.** Immunolocalization studies of Gas proteins in presence and absence of MAGED2. HeLa cells were co-transfected with a Gas-HA construct and control or MAGED2 siRNA. Forty-eight hours post-transfection, growth medium was replaced by DMEM serum free and exposed to physical hypoxia (1% oxygen overnight). Scale bars, 5  $\mu$ m.

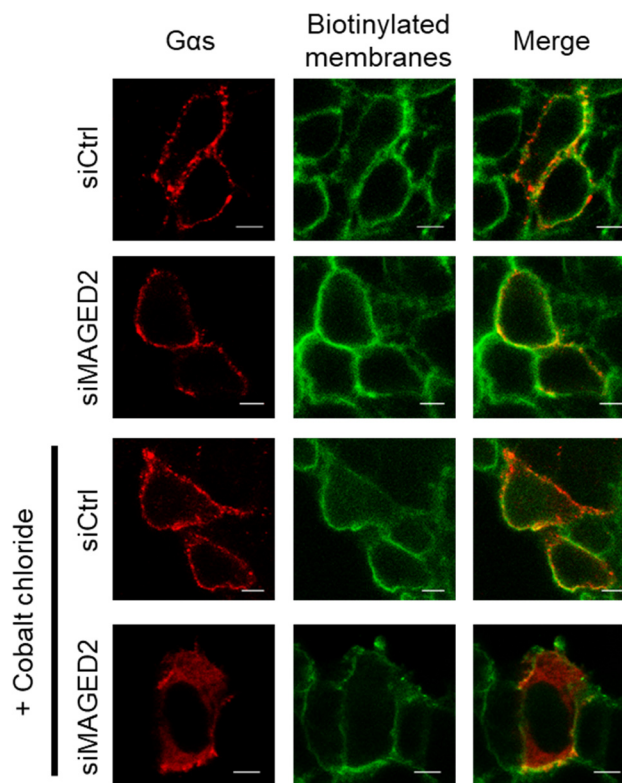


**Figure S2. MAGED2 prevents internalization of Gas under hypoxic condition in renal cells.** Immunolocalization studies of Gas proteins in presence and absence of MAGED2. HEK293 cells were co-transfected with a Gas-HA construct and control or MAGED2 siRNA. Forty-eight hours post-transfection, growth medium was replaced by DMEM serum free and exposed to chemical hypoxia (300  $\mu$ M CoCl<sub>2</sub>), as indicated.

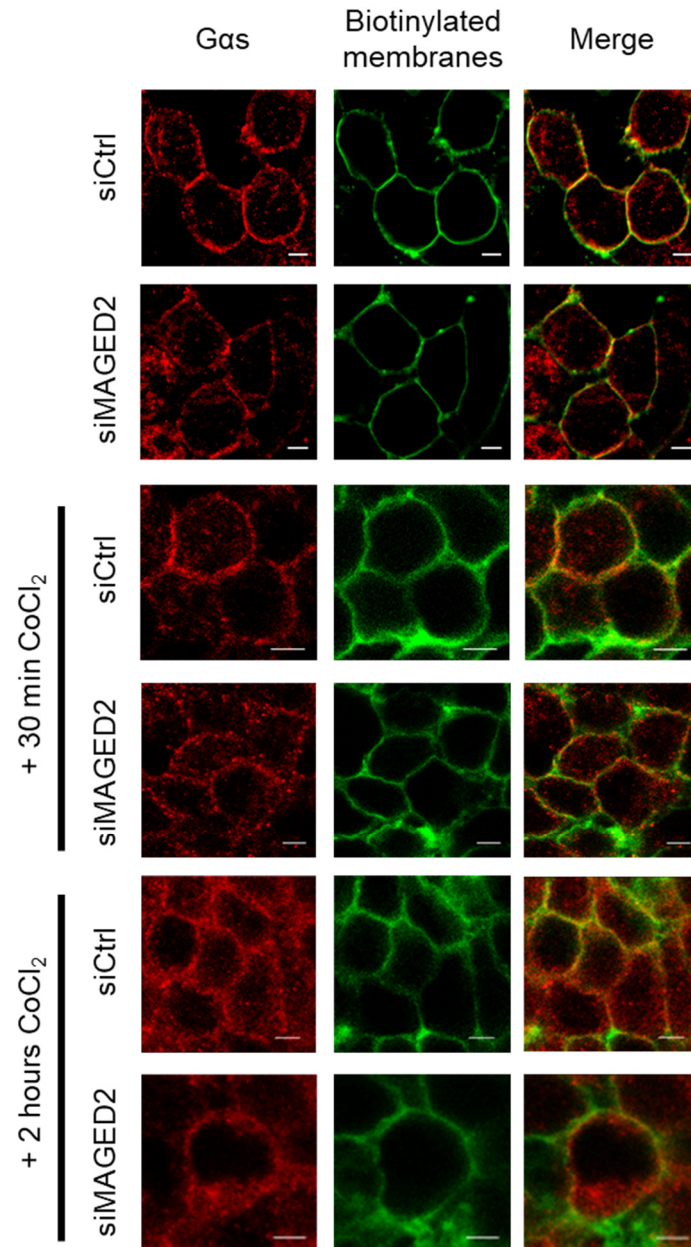


**Figure S3. MAGED2 prevents internalization of endogenous Gas under hypoxic condition in cells.** Immunolocalization studies of Gas proteins in presence and absence of MAGED2. HeLa cells were transfected with a control or MAGED2 siRNA. Forty-eight hours post-transfection, growth medium was replaced by DMEM serum free and exposed to chemical hypoxia (300  $\mu$ M CoCl<sub>2</sub>), as indicated.

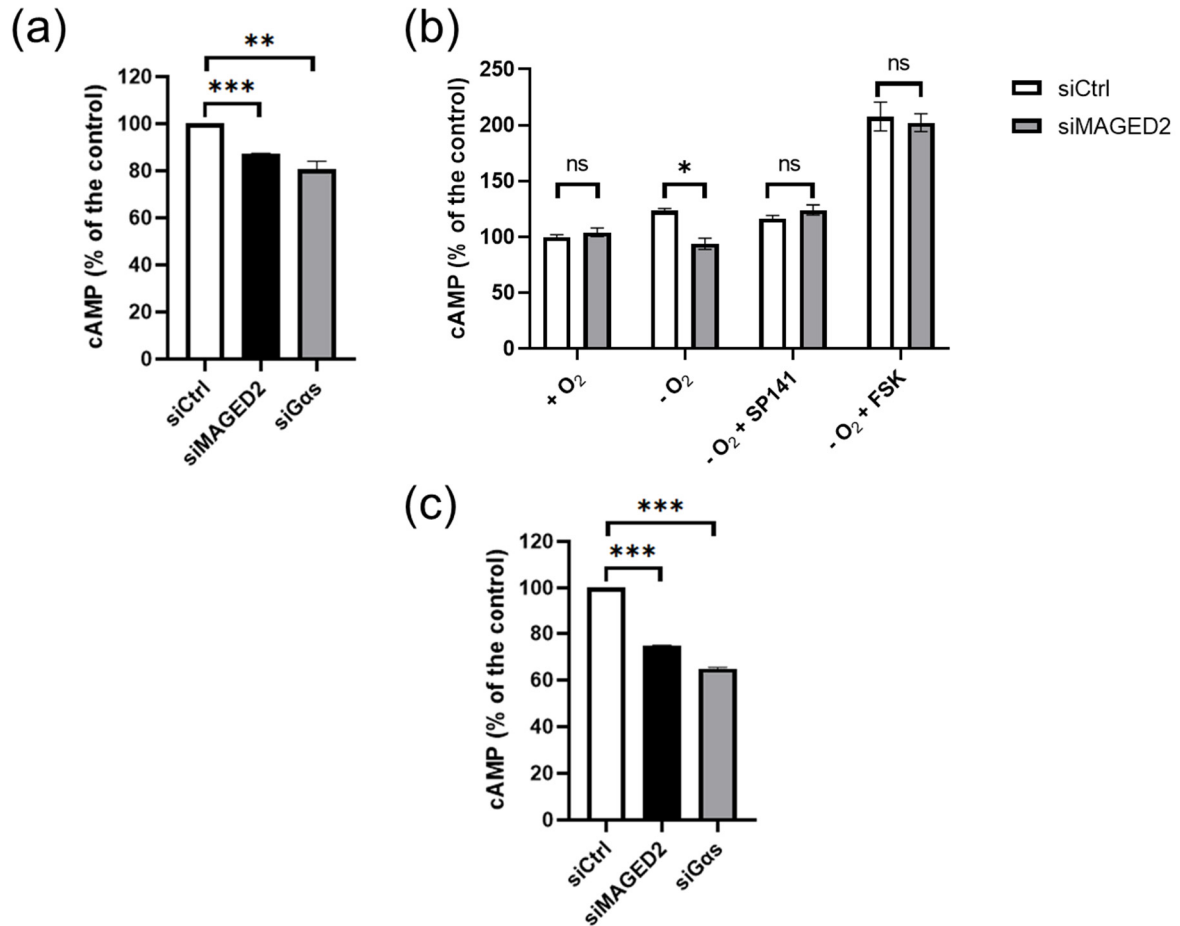


**Figure S4. MAGED2 promotes cAMP production activity under physical hypoxia.** HeLa (a and b) and HEK293 (c) cells were transfected with control, MAGED2 and Gas siRNA. Forty-eight hours post-transfection, cells were treated with physical hypoxia overnight in the presence of the phosphodiesterases inhibitor, IBMX 0.5 mM and in the presence or absence of SP141 1  $\mu$ M or forskolin (FSK) 10  $\mu$ M, as indicated. Cells were lysed with 0.1 M HCL containing 0.1% Triton X-100 and cAMP was measured by ELISA. Statistical significance was determined by unpaired two tailed Student's t tests (a and c) or by two-way ANOVA test (b). All data are shown as a representative result from three independent experiments (a and c) or three biological replicates (b). Bar graphs show mean  $\pm$  SEM. \*  $P \leq 0.05$ , \*\*  $P \leq 0.01$  and \*\*\*  $P \leq 0.001$ .

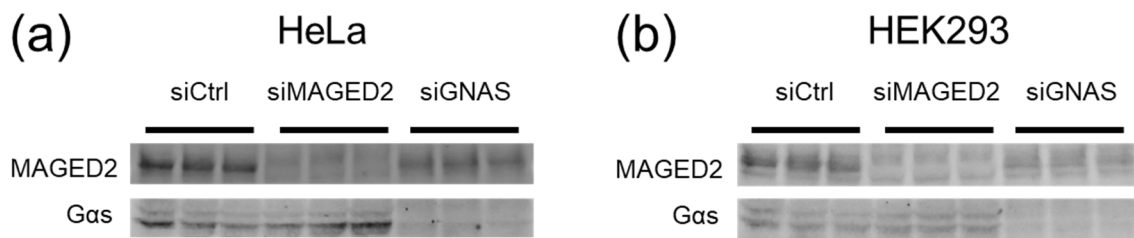


**Figure S5. Knockdown of MAGED2 and Gas markedly reduces expression of MAGED2 and Gas as revealed by western blotting.** These experiments were done in parallel with cAMP and PKA activity measurements (Figure 3 and S4).



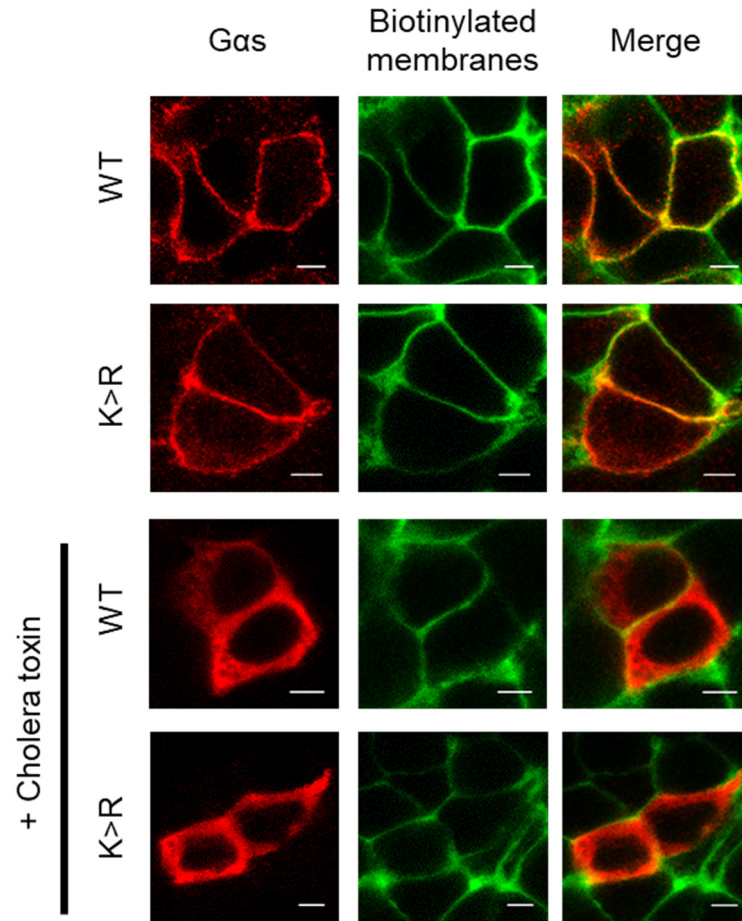


**Figure S6. Gas 5K>R variant is sensitive to cholera toxin induced endocytosis.** HeLa cells were transfected with a Gas-HA WT or 5K>R construct. Forty-eight hours post-transfection, growth medium was replaced by DMEM serum free and exposed to 1  $\mu\text{g/mL}$  of cholera toxin for 4 hours, as indicated. Membrane proteins of HeLa cells were biotinylated at 4  $^{\circ}\text{C}$ . Scale bars, 5  $\mu\text{m}$ .

## Article

# Reciprocal Regulation of MAGED2 and HIF-1 $\alpha$ Augments Their Expression under Hypoxia: Role of cAMP and PKA Type II

Elie Seaayfan <sup>1</sup>, Sadiq Nasrah <sup>1,†</sup>, Lea Quell <sup>1,†</sup>, Aline Radi <sup>1</sup>, Maja Kleim <sup>1</sup>, Ralph T. Schermuly <sup>2</sup>, Stefanie Weber <sup>1</sup>, Kamel Laghmani <sup>3,‡</sup> and Martin Kömhoff <sup>1,\*</sup>

<sup>1</sup> University Children's Hospital, Philipps University, 35043 Marburg, Germany

<sup>2</sup> Department of Internal Medicine, Member of the German Center for Lung Research (DZL), Excellence Cluster Cardio-Pulmonary Institute (CPI), Justus-Liebig-University, 35392 Giessen, Germany

<sup>3</sup> Centre de Recherche des Cordeliers, Sorbonne Université, Inserm, Université de Paris, CNRS, ERL8228, F-75006 Paris, France

\* Correspondence: koemhoff@staff.uni-marburg.de

† These authors contributed equally to this work.

‡ These authors contributed equally to this work.

**Abstract:** Hypoxia stabilizes the transcription factor HIF-1 $\alpha$ , which promotes the transcription of many genes essential to adapt to reduced oxygen levels. Besides proline hydroxylation, expression of HIF-1 $\alpha$  is also regulated by a range of other posttranslational modifications including phosphorylation by cAMP-dependent protein kinase A (PKA), which stabilizes HIF-1 $\alpha$ . We recently demonstrated that MAGED2 is required for cAMP generation under hypoxia and proposed that this regulation may explain the transient nature of antenatal Bartter syndrome (aBS) due to *MAGED2* mutations. Consequently, we sought to determine whether hypoxic induction of HIF-1 $\alpha$  requires also MAGED2. In HEK293 and HeLa cells, MAGED2 knock-down impaired maximal induction of HIF-1 $\alpha$  under physical hypoxia as evidenced by time-course experiments, which showed a significant reduction of HIF-1 $\alpha$  upon MAGED2 depletion. Similarly, using cobalt chloride to induce HIF-1 $\alpha$ , MAGED2 depletion impaired its appropriate induction. Given the known effect of the cAMP/PKA pathway on the hypoxic induction of HIF-1 $\alpha$ , we sought to rescue impaired HIF-1 $\alpha$  induction with isoproterenol and forskolin acting upstream and downstream of G $\alpha$ s, respectively. Importantly, while forskolin induced HIF-1 $\alpha$  above control levels in MAGED2-depleted cells, isoproterenol had no effect. To further delineate which PKA subtype is involved, we analyzed the effect of two PKA inhibitors and identified that PKA type II regulates HIF-1 $\alpha$ . Interestingly, MAGED2 mRNA and protein were also increased under hypoxia by a cAMP mimetic. Moreover, MAGED2 protein expression also required HIF-1 $\alpha$ . Thus, our data provide evidence for reciprocal regulation of MAGED2 and HIF-1 $\alpha$  under hypoxia, revealing therefore a new regulatory mechanism that may further explain the transient nature of aBS caused by MAGED2 mutations.

**Keywords:** MAGED2; hypoxia; HIF-1 $\alpha$ ; GalphaS; PKA type II; Bartter



**Citation:** Seaayfan, E.; Nasrah, S.; Quell, L.; Radi, A.; Kleim, M.; Schermuly, R.T.; Weber, S.; Laghmani, K.; Kömhoff, M. Reciprocal Regulation of MAGED2 and HIF-1 $\alpha$  Augments Their Expression under Hypoxia: Role of cAMP and PKA Type II. *Cells* **2022**, *11*, 3424. <https://doi.org/10.3390/cells11213424>

Academic Editors: Weibo Luo and Yingfei Wang

Received: 30 August 2022

Accepted: 26 October 2022

Published: 29 October 2022

**Publisher's Note:** MDPI stays neutral with regard to jurisdictional claims in published maps and institutional affiliations.



**Copyright:** © 2022 by the authors. Licensee MDPI, Basel, Switzerland. This article is an open access article distributed under the terms and conditions of the Creative Commons Attribution (CC BY) license (<https://creativecommons.org/licenses/by/4.0/>).

## 1. Introduction

During gestation, the fetus is exposed to a very low arterial O<sub>2</sub> tension (~25 mmHg) as compared with that of adults (~95 mmHg) [1]. Despite low oxygen levels, salt and water reabsorption in the renal medulla, which has a much lower supply of oxygen compared with the renal cortex [2–5], is very effective in the fetus, as evidenced by loss of function mutations in NKCC2 (which is expressed in the renal medulla and reabsorbs about 30% of filtered sodium) causing profound renal salt wasting [6]: The latter causes excessive amniotic fluid production and hence polyhydramnios leading to preterm birth and severely increased risk of intraventricular hemorrhage.

We and others have recently shown, that truncating mutations in *MAGED2*, which promotes expression and activity of salt-transporter NKCC2, cause a similar antenatal phenotype during gestation as those in the gene encoding NKCC2 [6–8]. More recently, we demonstrated that *MAGED2* is required under hypoxia to allow for the generation of cAMP, which is essential for the cell surface expression and function of NKCC2, thus explaining, at least in part, the salt loss in patients with *MAGED2* mutations [9]. The idea that *MAGED2* shields renal salt transport from hypoxic stress by allowing cAMP generation needed for NKCC2 expression and function concurs with recent studies demonstrating that many members of the large family of MAGE proteins protect against various forms of stress [10] by modulating activity and substrate specificity of ubiquitin E3 ligases [11]. Ubiquitination denotes a form of posttranslational modification (PTM), which is mediated by enzymes that catalyze ubiquitin activation (E1s), coupling (E2s), and binding to protein targets (E3s), as well as by deubiquitination enzymes, which remove ubiquitin molecules and chains from targets. E3 ubiquitin ligases determine the exact substrate specificity of ubiquitination. Therefore, alterations in E3 activity and subsequent changes in the ubiquitin-proteasome system (UPS), protein quality control, protein trafficking, and other ubiquitin-driven pathways affect all biological processes.

Compensation for fetal hypoxia is of critical importance because it can be aggravated by several internal (maternal anemia, placental insufficiency, umbilical cord pre-eclampsia, cardiac and pulmonary disease) and external factors (smoking 25% of all pregnancies in the United States), exposure to environmental pollutants, and living at high altitude (140 million people worldwide) [1], which may further decrease blood flow to the kidneys [12].

Under normoxia, the transcription factor HIF-1 $\alpha$  is hydroxylated by prolyl hydroxylases (PHD), which targets HIF-1 $\alpha$  for proteasomal degradation by the E3 ubiquitin Ligase Von Hippel Lindau. Hypoxia inhibits PHD and thereby stabilizes HIF-1 $\alpha$ , which promotes the transcription of many genes including erythropoietin and vascular endothelial growth factor (VEGF) [13]. Not surprisingly, HIF-1 $\alpha$  and VEGF are expressed abundantly in the fetal renal medulla [4]. Next to prolyl-hydroxylation and ubiquitination, various other types of PTM including phosphorylation [14,15] regulate HIF-1 $\alpha$  stability. A role of cAMP-mediated signaling was suggested by studies using  $\beta$ -adrenergic receptor ( $\beta$ -AR) blockade which revealed a markedly diminished induction of erythropoietin to hypoxia in animal models [16,17]. In line with these findings, hypoxia was shown to increase cAMP-dependent protein kinase A (PKA) in various human carcinoma cell lines [18,19]. A recent study demonstrated that PKA activates the transcription HIF-1 $\alpha$  gene and that PKA-dependent phosphorylation stabilizes HIF-1 $\alpha$  [20].

The aim of the present study is to identify a potential role of *MAGED2* in the hypoxic induction of HIF-1 $\alpha$ , given that the former is essential for cAMP generation under hypoxia, both of which stabilize HIF-1 $\alpha$  expression. We could demonstrate that maximal and appropriate hypoxic induction HIF-1 $\alpha$  requires *MAGED2* by allowing sufficient cAMP levels. Moreover, we identified PKA Type II as the relevant isoform for this effect. We further revealed that HIF-1 $\alpha$  protein is required for normal *MAGED2* protein levels and conversely, that *MAGED2* expression is stimulated by cAMP mimetics under hypoxia.

Our findings unveil a reciprocal control of *MAGED2* and HIF-1 $\alpha$  to promote their proper expression under hypoxia, which is mediated by cAMP-dependent induction of PKA type II.

## 2. Materials and Methods

### 2.1. Cell Culture

Human embryonic kidney (HEK293) and HeLa cells (Table 1) were cultured at 37 °C in a humidified environment containing 5% CO<sub>2</sub> in DMEM Glutmax complemented with 10% fetal bovine serum superior (Sigma-Aldrich, St. Louis, MO, USA), penicillin (100 units/mL), and streptomycin (100 units/mL). For chemical treatment experiments, the media of confluent cells was changed to DMEM serum-free for 14–16 h, Forskolin (10  $\mu$ M) and Isoproterenol (10  $\mu$ M) were added to the media at the same time as hypoxia treatment, and the PKA

inhibitors, Rp-cAMPS (100  $\mu$ M) and Rp-8-Br-cAMPS (50  $\mu$ M) were administered to the cells 30 min before lysis. The control and experimental groups' cells are always generated from the same flask and passage, and they are studied on the same day.

**Table 1.** Reagents and tools.

Reagent or Resource	Source	Identifier
<b>Antibodies</b>		
Anti-HIF-1 $\alpha$ rabbit	Cell Signaling	14179
Anti-MAGED2 rabbit	This paper	
Anti-RII $\beta$ rabbit	Thermo Fisher Scientific	PA582348
Anti-RII $\alpha$ mouse	Thermo Fisher Scientific	TA501145
Anti-G $\alpha$ s	Sigma Aldrich	06-237
StarBright Blue 520 Goat Anti-Rabbit IgG	Bio-rad	12005869
StarBright Blue 700 Goat Anti-Mouse IgG	Bio-rad	12004158
<b>Chemicals, Peptides, and Recombinant Proteins</b>		
Forskolin	Sigma-Aldrich	F6886-10MG
(–)-Isoproterenol hydrochloride	Sigma-Aldrich	I6504-100MG
Rp-cAMPS	Sigma-Aldrich	116814-5UMOL
Rp-8-Br-cAMPS	Sigma-Aldrich	116816-5UMOL
<b>Critical Commercial Assays</b>		
SingleShot Cell Lysis Kit	Bio-rad	1725080
iScript Advanced cDNA Synthesis Kit for RT-qPCR	Bio-rad	1725038
SsoAdvanced Universal SYBR Green Supermix	Bio-rad	1725271
<b>Experimental Models: Cell Lines</b>		
HEK293	ATCC	CRL1573
HeLa	Gift from Dr. Vijay Renigunta	
<b>Oligonucleotides</b>		
ON-TARGETplus Non-targeting Control Pool	Dharmacon	D-001810-10-05
UGGUUUACAUGUCGACUAA		
UGGUUUACAUGUUGUGUGA		
UGGUUUACAUGUUUCUGA		
UGGUUUACAUGUUUCCUA		
ON-TARGETplus Human MAGED2 siRNA—SMARTpool	Dharmacon	L-017284-01-0005
GGACGAAGCUGAUUCGGA		
GCUAAAGACCAGACGAAGA		
AGGCGAUGGAAGCGGAUUU		
GAAAAGGACAGUAGCUCGA		
ON-TARGETplus Human GNAS siRNA—SMARTpool	Dharmacon	L-010825-00-0005
GCAAGUGGAUCCAGUGCUU		
GCAUGCACCUUCGUCAGUA		
AUGAGGAUCCUGCAUGUUA		
CAACCAAAGUGCAGGACAU		

Table 1. Cont.

Reagent or Resource	Source	Identifier
ON-TARGETplus Human HIF-1 $\alpha$ siRNA-SMARTpool	Dharmacon	L-004018-00-0005
GAACAAUACAUGGGAUUA		
AGAAUGAAGUGUACCCUAA		
GAUGGAAGCACUAGACAAA		
CAAGUAGCCUCUUUGACAA		
GAPD, Human GAPDH, Real-Time PCR Primer Set	Biomol	VHPS-3541
GAGTCAACGGATTGGTCGT		
TTGATTITGGAGGGATCTCG		
MAGED2, Human melanoma antigen family D, 2, Real-Time PCR Primer Set	Biomol	VHPS-5486
TTTTGGCTAAAGACCAGACG		
AATAGCCTGCTCGTTCAATG		
GLUT1, Real-Time PCR Primer Set	Sigma-Aldrich	[21]
TCACTGTGCTCCTGGTTCTG		
CCTGTGCTGAGAGATCC		
<b>Software and Algorithms</b>		
ImageJ	Schneider et al., 2012	<a href="https://imagej.nih.gov/ij/">https://imagej.nih.gov/ij/</a>
GraphPad Prism 9	GraphPad	
EndNote X9	Clarivate Analytics	

## 2.2. Cobalt Chloride Treatment

Cobalt chloride (CoCl<sub>2</sub>), a hypoxia mimetic was used to induce HIF-1 $\alpha$  in the cells (“chemical hypoxia” [22]). The media of confluent cells was changed to DMEM without serum with 300  $\mu$ M CoCl<sub>2</sub> or the desired dose for the dose–response experiment for hypoxia incubation. For 14–16 h, cells were placed in a standard humidified incubator at 37 °C. A Western blot for HIF-1 $\alpha$  protein expression was used to assess hypoxia.

## 2.3. Physical Hypoxia

In a modular hypoxia incubator chamber, cells were exposed to physical hypoxia (Billups-Rothenberg, Inc., San Diego, CA, USA; Cat. MIC-101). After the cells had reached ~100% confluence, the media was changed to DMEM without serum, and the cells were put in the center of the chamber, which was sealed shut and linked to a gas tank containing 1% O<sub>2</sub>, 5% CO<sub>2</sub>, and 94% N<sub>2</sub> through a single flow meter (Billups-Rothenberg, Inc., San Diego, CA, USA; Cat. SFM-3001). The hypoxia chamber was placed in a standard incubator humidified at 37 °C for 14–16 h or the time indicated for the time course experiment. Outside the hypoxia chamber, a normoxic control was placed in the same incubator. A Western blot for HIF-1 $\alpha$  protein expression was used to assess hypoxia.

## 2.4. Small Interfering RNA (siRNA) Transfection

Control, MAGE-D2, GNAS, and HIF-1 $\alpha$  siRNAs were purchased as ON-TARGETplus SMARTpools from Dharmacon (D-001810-10-05, L-017284-01-0005, L-010825-00-0005, and L-004018-00-0005). By reverse transfection, cells were initially transfected with control or specific siRNA using Lipofectamine RNAiMAX (Invitrogen, Waltham, MA, USA) according to the manufacturer’s instructions.

### 2.5. Western Blotting

Cells were lysed in lysis buffer (50 mM Tris pH 7.4, 5 mM EDTA, 150 mM NaCl, 1 percent Triton X-100, and protease inhibitors) after three washes with ice-cold phosphate-buffered saline (PBS), and cell lysates were cleared at 13,000 g for 15 min at 4 °C. A Pierce™ BCA Protein Assay Kit (Thermo Scientific™, Waltham, MA, USA) was used to determine the protein contents in the supernatants. Proteins were separated on 7.5% TGX Stain Free gels (Bio-rad, Hercules, CA, USA; Cat. 1610181) and transferred to nitrocellulose membranes (Bio-rad, Cat. 1704270) using a Trans-Blot Turbo Transfer System (Bio-rad). Fluorescence antibodies StarBright Blue 520 and 700 were used to identify the proteins (Bio-rad). The blots were imaged with a ChemiDoc MP imaging system (Bio-Rad). ImageJ software was used to determine the gray density of Western blots (National Institutes of Health, Bethesda, MD, USA).

### 2.6. Quantitative Real-Time Reverse Transcription PCR (qRT-PCR)

The mRNA amount of MAGE-D2 was determined by quantitative real-time RT-PCR (qRT-PCR) and the GAPDH gene was used as the internal control. The total RNA of cells was isolated using the SingleShot Cell Lysis Kit (Bio-rad) and transcribed to complementary DNA (cDNA) with the iScript™ Advanced cDNA Synthesis Kit (Bio-rad). PCR was carried out with SsoAdvanced Universal SYBR Green Supermix (Bio-rad) on a 7500 Real-Time PCR System (Applied Biosystems, Waltham, MA, USA). Cycle threshold values were normalized to amplification of GAPDH.

### 2.7. Statistical Analyses

Results are expressed as mean  $\pm$  SEM. Differences between means were evaluated using unpaired Student *t*-test or two-way ANOVA test. Statistical analyses were performed using GraphPad Prism X9 software.  $p \leq 0.05$  was considered statistically significant (\*),  $p \leq 0.01$  was considered highly significant (\*\*), and  $p \leq 0.001$  was considered very highly significant (\*\*\*)

## 3. Results

### 3.1. MAGED2 Is Required for Hypoxic Induction of HIF-1 $\alpha$

As activation of the cAMP/PKA pathway stabilizes HIF-1 $\alpha$  by phosphorylation and enhances its transcriptional activity [20,23], we analyzed the effect of MAGED2 knockdown on the induction of HIF-1 $\alpha$  using physical hypoxia (Figures 1a,c and S1a) or CoCl<sub>2</sub> (Figure 1b,d) to induce HIF-1 $\alpha$  in HeLa cells. As expected, physical hypoxia induced HIF-1 $\alpha$  expression in a time-dependent manner (Figures 1a,c and S1a). Interestingly, as can be seen in Figures 1a,c and S1a, MAGED2 knockdown significantly reduced the induction of HIF-1 $\alpha$  by physical hypoxia. Likewise, the same effect was observed with CoCl<sub>2</sub> given that MAGED2 knockdown reduced again HIF-1 $\alpha$  expression (Figure 1b,d). As PKA-dependent phosphorylation has been shown to reduce proteasomal degradation of HIF-1 $\alpha$  [20], we analyzed the effect of the proteasome inhibitor MG132 on HIF-1 $\alpha$  (Figure 1e). We revealed that this compound neutralized the negative effect of MAGE2 depletion on HIF-1 $\alpha$  expression, which supports the notion, that PKA-dependent phosphorylation impairs proteasomal degradation of HIF-1 $\alpha$  in MAGED2 depleted cells. We next asked if reduced HIF-1 $\alpha$  protein expression translated into decreased mRNA levels of GLUT1, a classical HIF-1 $\alpha$  transcriptional target [24]. As shown in Figure 1f, MAGED2 depletion did indeed reduce GLUT1 mRNA abundance.

### 3.2. MAGED2 Is Required for Hypoxic Induction of HIF-1 $\alpha$ Independently of the Expression System

As protein regulations and subcellular distributions may be cell-dependent and therefore depend on the expression system used, we sought to confirm our findings by conducting the experiments in another cell line, the HEK293 cells. As illustrated in Figures 2 and S1b, similar to HeLa cells, MAGED2 depletion in HEK293 cells significantly



impaired the induction of HIF-1 $\alpha$  by physical hypoxia and CoCl<sub>2</sub>. Taken in concert, these data confirm our observation that MAGED2 is required for maximal induction of HIF-1 $\alpha$  under hypoxia and clearly indicate that the MAGED2 effect on HIF-1 $\alpha$  is independent of the expression system.

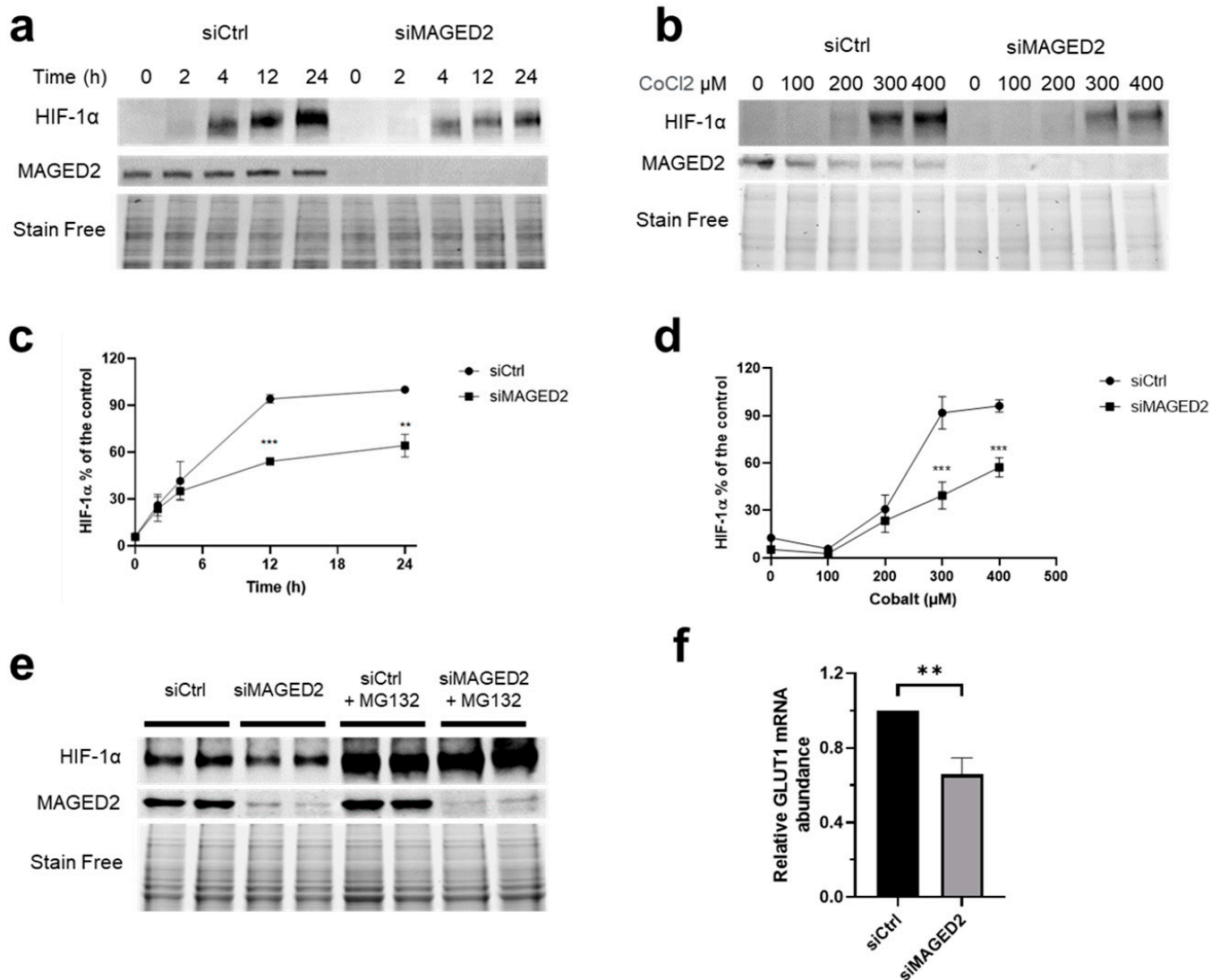


**Figure 1.** MAGED2 promotes hypoxic HIF-1 $\alpha$  protein expression in HeLa cells. HeLa cells were transfected with control (siCtrl), MAGED2 (siMAGED2). Briefly, 24–48 h post-transfection, cells were exposed to physical hypoxia (a,e) or to the hypoxia mimetic CoCl<sub>2</sub> (b): (a) Cells were exposed to physical hypoxia (1% O<sub>2</sub>, 5% CO<sub>2</sub>, 94% N<sub>2</sub>) for the specified times. (b) Cells were exposed to CoCl<sub>2</sub> with the indicated dose of CoCl<sub>2</sub> for 14–16 h. Total cell lysates were separated by SDS-PAGE and probed with anti-HIF-1 $\alpha$  and MAGED2 antibodies. (c,d) Densitometric analysis of HIF-1 $\alpha$  immunoblot is presented in (a,d), respectively. (e) Cells were exposed to physical hypoxia and treated with the proteasome inhibitor, 10  $\mu$ M MG132. (f) Cells were exposed to physical hypoxia for 14 h. Total RNA was extracted, and the relative mRNA amount of GLUT1 was determined by qRT-PCR. Statistical significance was determined by two-way ANOVA test (c,d) or unpaired two-sided Student's *t*-test (f). All Western blots shown are from the same experiment, which is a representative example of three independent experiments. Bar graphs show mean  $\pm$  SEM. \*\* *p*  $\leq$  0.01 and \*\*\* *p*  $\leq$  0.001.

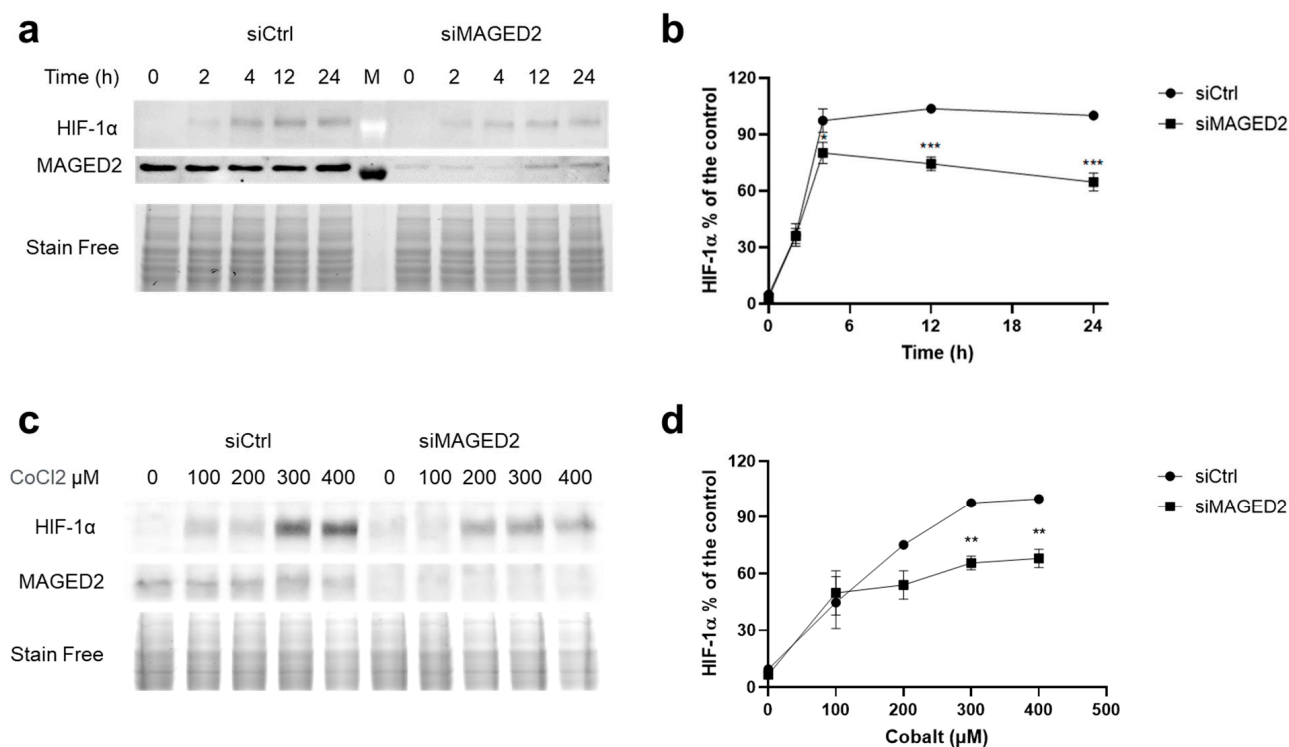


**Figure 2.** MAGED2 promotes hypoxic HIF-1α protein expression in HEK293 cells. HEK293 cells were transfected with control (siCtrl), and MAGED2 (siMAGED2). Briefly, 24–48 h post-transfection, cells were exposed to physical hypoxia (a) or to the hypoxia mimetic CoCl<sub>2</sub> (c): (a) Cells were exposed to physical hypoxia (1% O<sub>2</sub>, 5% CO<sub>2</sub>, 94% N<sub>2</sub>) for the specified times. (c) Cells were exposed to CoCl<sub>2</sub> with the indicated dose for 14–16 h. Total cell lysates were separated by SDS-PAGE and probed with anti-HIF-1α and MAGED2 antibodies. (b,d) Densitometric analysis of HIF-1α immunoblot is presented in (a,c), respectively. Statistical significance was determined by two-way ANOVA test. All Western blots shown are from the same experiment, which is a representative example of three independent experiments. Bar graphs show mean ± SEM. \*  $p \leq 0.05$ , \*\*  $p \leq 0.01$  and \*\*\*  $p \leq 0.001$ .

### 3.3. Similar to MAGED2, Gαs Is Required for Hypoxic Induction of HIF-1α

We have shown previously that MAGED2 depletion inhibits the functioning of Gαs by causing its MDM2 and ubiquitin-dependent internalization, which precludes activation of membrane-bound adenylate cyclase and hence cAMP generation [9]. To investigate if the effects of the MAGED2 knockdown on HIF-1α expression are indeed caused by inhibiting Gαs, we analyzed also the effect of GNAS knockdown on hypoxic HIF-1α induction by exposing cells to physical hypoxia (Figure 3a,b) or to the hypoxia mimetic CoCl<sub>2</sub> (Figure 3c,d). Similar to MAGED2 knockdown, Gαs knockdown decreased also the induction of HIF-1α to a comparable degree under both conditions. Thus, these data strongly suggest not only that MAGED2 is required for full and appropriate hypoxic induction of HIF-1α, but also that the positive effect of MAGED2 on HIF-1α protein expression involves the cAMP/PKA pathway initiated upstream by Gαs.

### 3.4. Activation of the cAMP/PKA Pathway Reversed the Effect of MAGED2 Knockdown on Hypoxic HIF-1α Induction

To independently confirm that MAGED2 acts via Gαs to induce the expression of HIF-1α, we compared the effects of isoproterenol and forskolin on the expression of HIF-1α induced by CoCl<sub>2</sub> in HeLa cells. Isoproterenol is a β<sub>2</sub>-adrenergic receptor agonist acting upstream of Gαs, whereas forskolin, is an activator of membrane-bound adenylate cyclase, acting downstream of Gαs. As shown in Figures 4a–d and S3, isoproterenol was unable to reverse the effect of MAGED2 knockdown on HIF-1α protein expression. In contrast,



forskolin reversed the impaired induction of HIF-1 $\alpha$  caused by MAGED2 knockdown. Together, these results confirm that MAGED2 is essential for promoting the expression of HIF-1 $\alpha$  via the cAMP/PKA pathway under hypoxia, and that regulation occurs at the level of G $\alpha$ s.

As expected, forskolin also reversed the effect of MAGED2 knockdown on HIF-1 $\alpha$  protein expression in HEK293 cells (Figure S2).

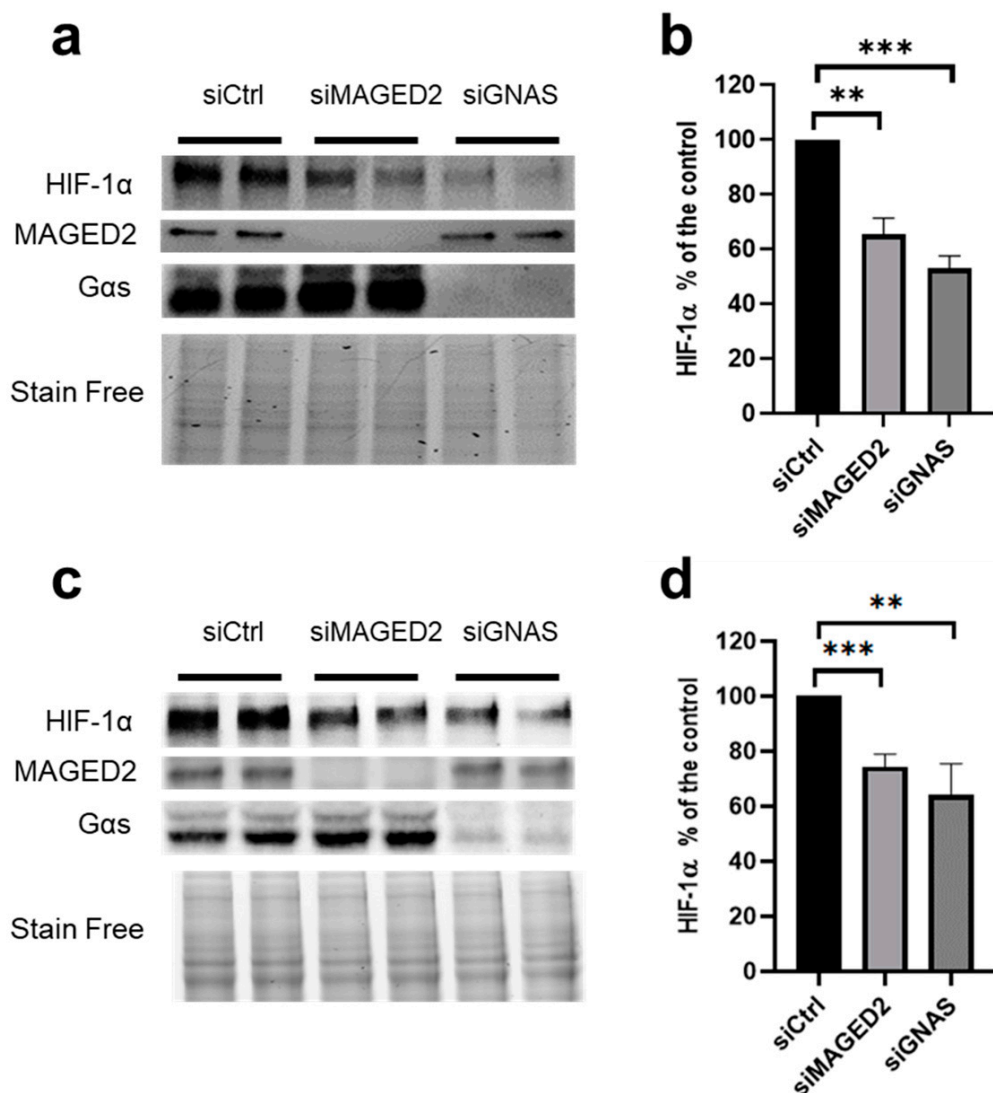


**Figure 3.** MAGED2 and G $\alpha$ s promote hypoxic HIF-1 $\alpha$  protein expression in HeLa cells. HeLa cells were transfected with control (siCtrl), MAGED2 (siMAGED2) or GNAS (siGNAS) siRNA. Briefly, 24–48 h post-transfection, cells were exposed to physical hypoxia (a) or 300 $\mu$ M CoCl<sub>2</sub> (c) for 14–16 h. Total cell lysates were separated by SDS-PAGE and probed with anti-HIF-1 $\alpha$ , MAGED2, and G $\alpha$ s antibodies. (b,d) Densitometric analysis of HIF-1 $\alpha$  immunoblot is presented in (a,c). Statistical significance was determined by unpaired two-sided Student's *t*-test (b,d). All Western blots shown are from the same experiment, which is a representative example of three independent experiments. Bar graphs show mean  $\pm$  SEM. \*\*  $p \leq 0.01$  and \*\*\*  $p \leq 0.001$ .

### 3.5. Activation of the cAMP/PKA Pathway Increased MAGED2 mRNA and Protein Abundance

Interestingly, we noticed that forskolin increased MAGED2 protein levels under hypoxic conditions (Figure 4a,b,e,f). As the MAGED2 promoter contains four CREB1 (cAMP responsive element binding protein 1) binding sites at the positions-122, -1311, -1468, and -1980 relative to the transcription start site (<https://epd.epfl.ch//index.php>, accessed on 15 July 2019, [25]) we asked if activation of the cAMP/PKA pathway may induce transcrip-

tion of the MAGED2 gene via enhanced binding of the transcription factor CREB to the four CREB1 sites. To address this question, we analyzed MAGED2 mRNA levels in HEK293 cells exposed to  $\text{CoCl}_2$  and treated with forskolin. As illustrated in Figure 4g, forskolin increased MAGED2 mRNA abundance under hypoxia, which is in agreement with our finding of enhanced MAGED2 protein expression under the same experimental conditions.

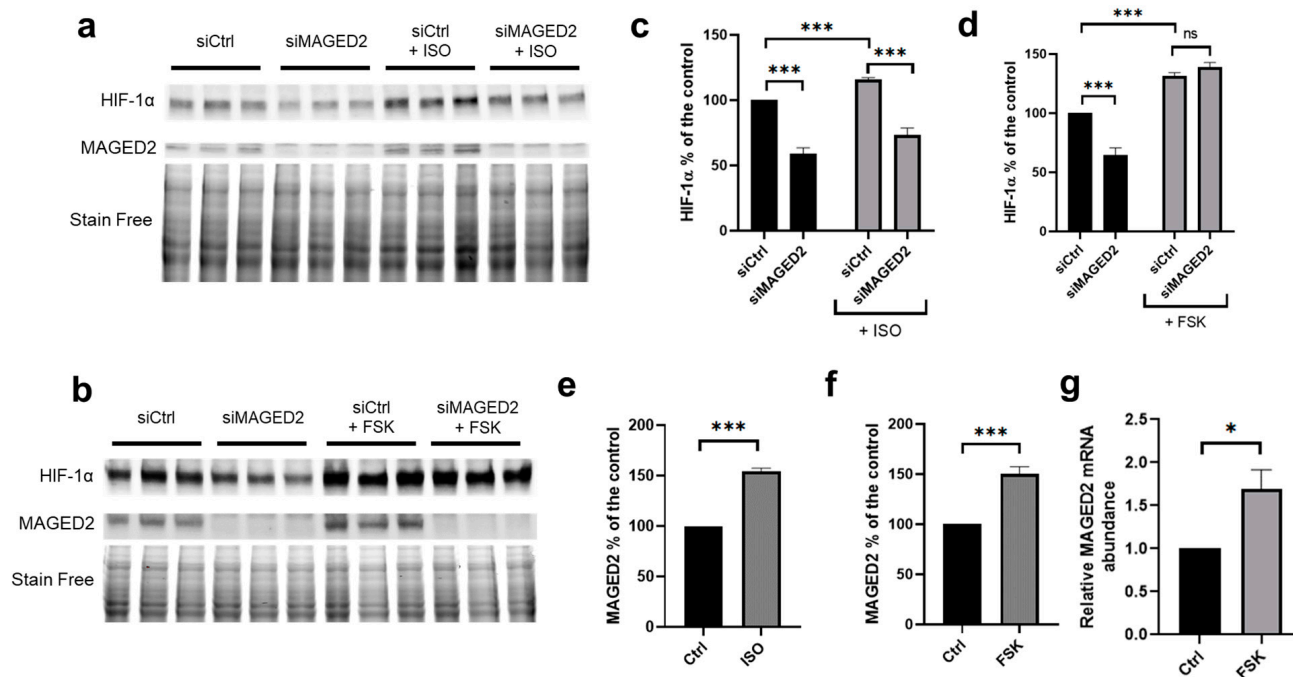


**Figure 4.** Forskolin reverses the effect of MAGED2 knockdown on hypoxic HIF-1α induction and induces MAGED2 transcription: (a,b) HeLa cells were transfected with control (siCtrl) or MAGED2 (siMAGED2) siRNA. Cells were exposed to the hypoxia mimetic  $\text{CoCl}_2$  (300 μM) and with (a) 10 μM isoproterenol (ISO) or (b) 10 μM forskolin (FSK) for 14–16 h. Total cell lysates were separated by SDS-PAGE and probed with anti-HIF-1α and MAGED2 antibodies. (c,d) Densitometric analysis of HIF-1α immunoblot presented in (a,b), respectively. (e,f) Densitometric analysis of MAGED2 immunoblot presented in (a,b), respectively. (g) HEK293 cells were treated with  $\text{CoCl}_2$  for 14 h and then treated with DMSO or Forskolin 10 μM for 2 h. Total RNA was extracted, and the relative mRNA amount of MAGED2 was determined by qRT-PCR. Statistical significance was determined by unpaired two-sided Student's *t*-test (c–g). All Western blots shown are from the same experiment, which is a representative example of three independent experiments. Bar graphs show mean ± SEM. \*  $p \leq 0.05$  and \*\*\*  $p \leq 0.001$ .

### 3.6. PKA type II Regulates the Expression of HIF-1α

To determine which type of PKA regulates the expression of HIF-1α under hypoxic conditions, we treated cells with a non-selective PKA inhibitor (Rp-cAMPS, 100 μM) or a selective PKA type I inhibitor (Rp-8-Br-cAMPS, 50 μM). Rp-cAMPS slightly lowered HIF-1α protein abundance (Figure 5a,c). As expected, the selective PKA type I inhibitor Rp-8-Br-cAMPS, which activates PKA type II at 50 μM [26], had the opposite effect and increased HIF-1α expression (Figure 5b,d). Accordingly, we observed a decreased abundance of the regulatory subunits RIIα and RIIβ (Figure 5b), reflecting PKA type II activation. Together, these findings indicate that PKA type II is the PKA isoform involved in the regulation of HIF-1α. In line with these findings, MAGED2 knockdown increased RIIα and RIIβ expression under hypoxic conditions reflecting a decrease in PKA type II activity (Figure 5e).

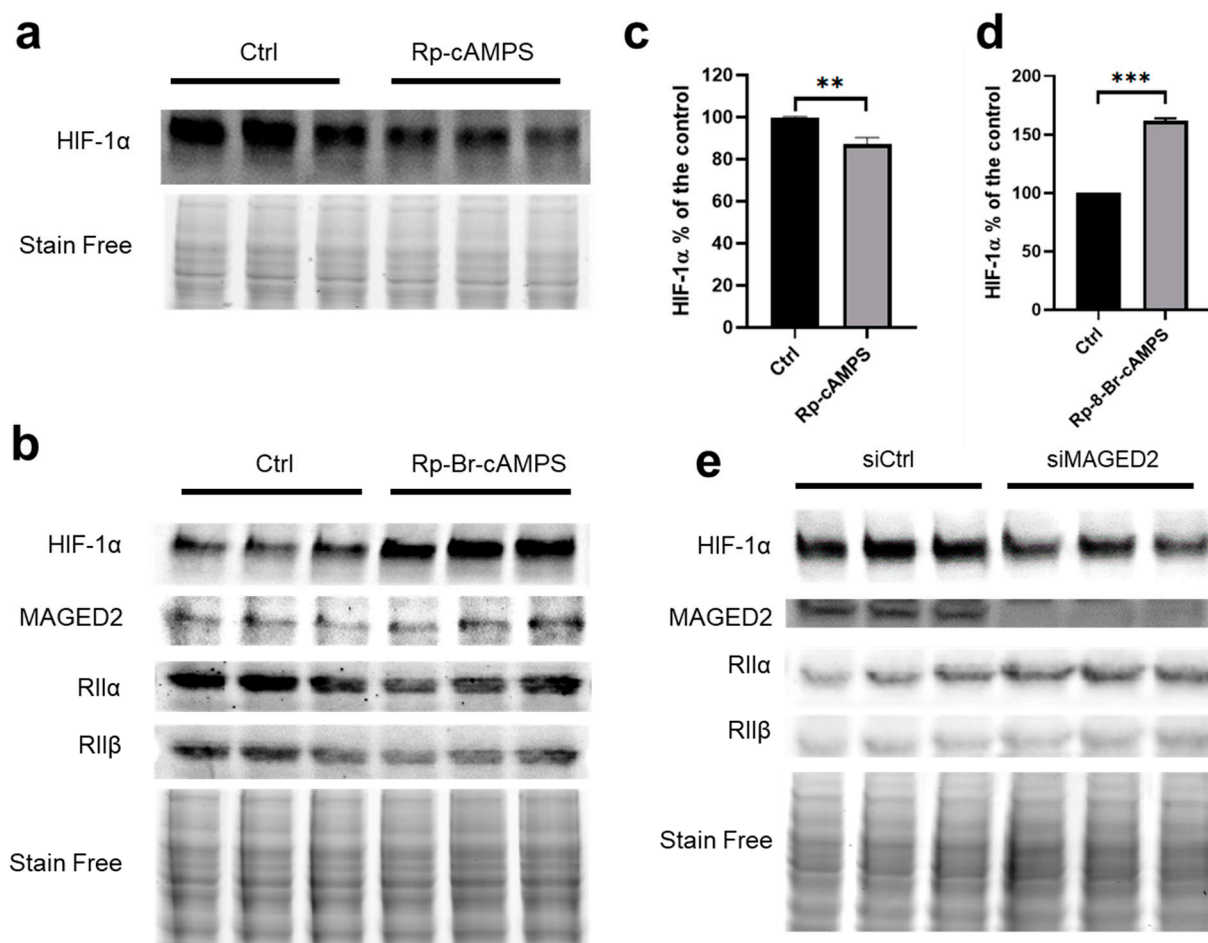


**Figure 5.** PKA type II regulates HIF-1α protein abundance: (a,b) HEK293 cells were treated with the non-selective PKA inhibitor (Rp-cAMPS, 100 μM) or the selective PKA type I inhibitor (Rp-8-Br-cAMPS, 50 μM) for 30 min under CoCl<sub>2</sub>. Total cell lysates were separated by SDS-PAGE and probed with anti-HIF-1α, MAGED2, RIIα, or RIIβ antibodies. (c,d) Densitometric analysis of HIF-1α immunoblot presented in (a,b), respectively. (e) cells were transfected with control (siCtrl) or MAGED2 (siMAGED2) siRNA. Cells were exposed to 300 μM CoCl<sub>2</sub> for 14–16 h. Total cell lysates were separated by SDS-PAGE and probed with anti-HIF-1α, MAGED2, RIIα, and RIIβ antibodies. Statistical significance was determined by unpaired two-sided Student's *t*-test (c,d). All Western blots shown are from the same experiment, which is a representative example of three independent experiments. Bar graphs show mean ± SEM. \*\* *p* ≤ 0.01 and \*\*\* *p* ≤ 0.001.

### 3.7. HIF-1α Promotes MAGED2 Expression under Hypoxia

As HIF-1α was previously shown to increase PKA activity under hypoxia [27] and our finding that forskolin increases MAGED2 mRNA levels and protein levels under hypoxia (Figure 4), we hypothesized that HIF-1α is essential for the induction of MAGED2 protein expression. To this end, we analyzed the effect of HIF-1α knockdown under hypoxia in HEK293 and HeLa cells. As illustrated in Figure 6, HIF-1α knockdown decreases MAGED2 protein expression in HeLa (Figure 6a,b) and HEK293 cells (Figure 6d,e) exposed to CoCl<sub>2</sub> demonstrating that HIF-1α is required for expression of MAGED2 protein under these conditions. Likewise, using physical hypoxia in HIF-1α depleted HeLa cells, a significant reduction of MAGED2 mRNA was observed (Figure 6c).

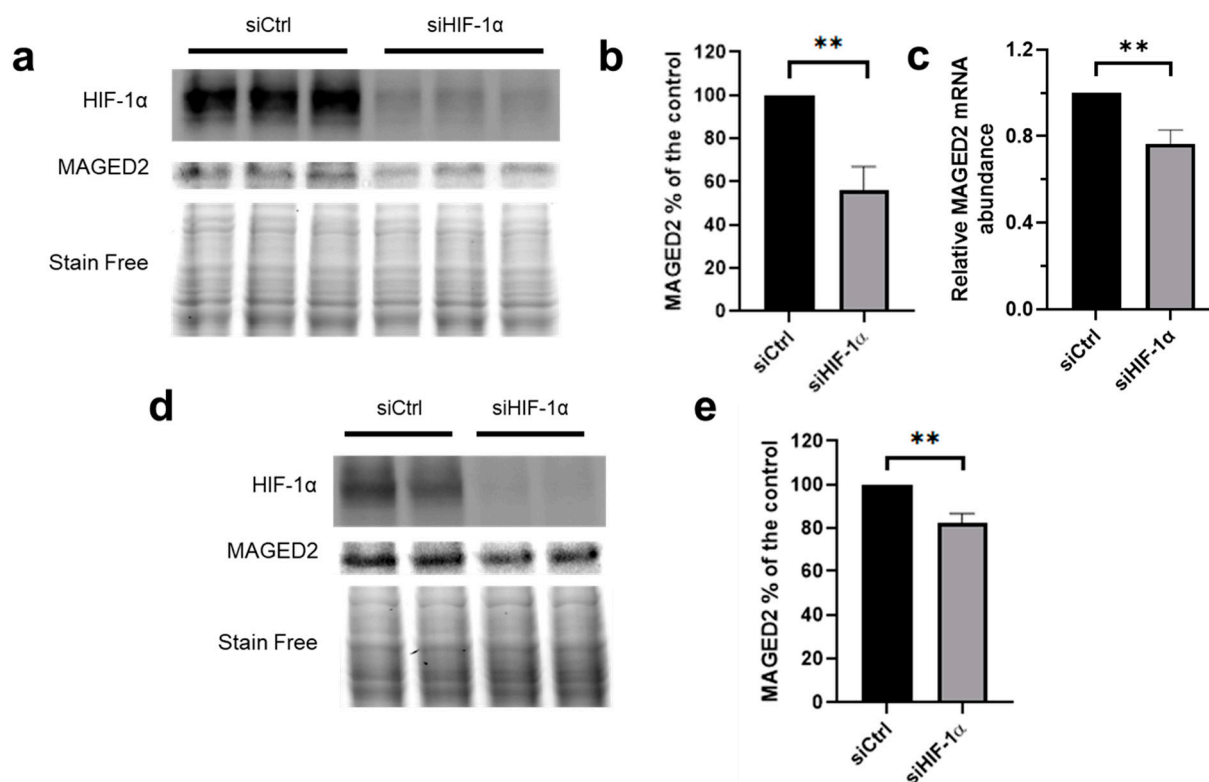


**Figure 6.** HIF-1 $\alpha$  knockdown reduces MAGED2 expression under hypoxia. HeLa (a,c) and HEK293 (d) cells were transfected with control or HIF-1 $\alpha$  siRNA. cells were treated with 300  $\mu$ M CoCl<sub>2</sub> for 14–16 h: (a,d) Total cell lysates were separated by SDS-PAGE and probed by anti-HIF-1 $\alpha$  and MAGED2 antibodies. (b,e) densitometric analysis of HIF-1 $\alpha$  immunoblot presented in (a,d), respectively. (c) HeLa cells were exposed to physical hypoxia for 14 h. Total RNA was extracted, and the relative mRNA amount of MAGED2 was determined by qRT-PCR. Statistical significance was determined by unpaired two-sided Student's *t*-test (b,c,d). All Western blots shown are from the same experiment, which is a representative example of three independent experiments. Bar graphs show mean  $\pm$  SEM. \*\*  $p \leq 0.01$ .

#### 4. Discussion

The key finding of this study is that MAGED2 is required under both physical hypoxia and treatment with the hypoxia mimetic CoCl<sub>2</sub> to fully induce HIF-1 $\alpha$  in renal (HEK293) and cancer (HeLa) cell culture models. Our finding of interdependent regulation of MAGED2 and HIF-1 $\alpha$  via PKA type II under hypoxia provides a mechanism for how MAGED2 through induction of HIF-1 $\alpha$  promotes cAMP generation, which is essential in the hypoxic fetal kidneys to promote salt reabsorption. Thus, the lack of the MAGED2 and HIF-1 $\alpha$  amplification loop compromises cAMP generation, which leads to renal salt-wasting in transient Bartter syndrome, caused by truncating mutations in *MAGED2*.

Our data with PKA subtype-specific agents indicate that PKA type II is the relevant PKA isoform involved in the regulation of HIF-1 $\alpha$ . This notion was further corroborated by the observation that the regulatory subunits RII $\alpha$  and RII $\beta$  (which- together with the catalytic subunits- constitute PKA type II) were increased in hypoxia with the knockdown of MAGED2, (Figure 5e). In agreement with our findings, PKA type II was shown to be expressed in the majority of organs [28,29] whereas PKA type I is mainly expressed in the brain [30]. In addition, the notion that PKA type II is involved in the hypoxic induction of HIF-1 $\alpha$  is in line with the study from Lucia and coworkers, who demonstrated that the hypoxic induction of PKA type II is mediated by hypoxic repression of RII $\beta$  gene transcription [27].

Of interest, our studies under hypoxia also revealed that isoproterenol and forskolin increased MAGED2 protein abundance and that *GNAS* knockdown elicits the opposite effect. This clearly indicates that the  $G_{\alpha s}$ /cAMP/PKA pathway promotes MAGED2 expression under hypoxic conditions. To further support this notion, we also showed that forskolin increases the abundance of MAGED2 transcript under hypoxic conditions, which is in agreement with the presence of four CRE sites in the 2000 bp of the MAGED2 promoter. The lack of effect of isoproterenol in MAGED2-depleted cells on the hypoxic induction of HIF-1 $\alpha$  concurs with our previous study showing that MAGED2 is essential for  $G_{\alpha s}$  dependent activation of membrane-bound adenylate cyclase [9] thereby explaining that agents acting upstream of  $G_{\alpha s}$  such as isoproterenol are ineffective in MAGED2-depleted cells.

In light of the interdependence between MAGED2,  $G_{\alpha s}$ /cAMP/PKA, and HIF-1 $\alpha$  shown in this study we asked if HIF-1 $\alpha$  also regulates MAGED2 expression. We could indeed show that HIF-1 $\alpha$  was necessary for maximal MAGED2 protein expression. Given that the MAGED2 promoter does not contain HRE elements, which precludes direct activation of the MAGED2 promoter by HIF-1 $\alpha$ , we speculate that reduced MAGED2 expression resulted from reduced PKA activity possibly by increased PRKAR2B gene transcription under hypoxic conditions [27], which represses PKA type II activity and hence reduces MAGED2 mRNA levels. To this end, we suggest that under hypoxic conditions, MAGED2 inhibits  $G_{\alpha s}$  endocytosis. This ensures the activation of adenylate cyclase and cAMP and the activation of PKA type II, which enhances HIF-1 $\alpha$  expression under hypoxic conditions. The latter increases (similar to forskolin) MAGED2 mRNA levels. Thus, MAGED2 depletion impairs the cAMP/PKA pathway and HIF-1 $\alpha$  induction. Decreased cAMP level explains, at least in part, the salt loss in transient Bartter syndrome (Figure 7). This model is further supported by our finding that MAGED2 stabilizes HIF-1 $\alpha$  by inhibiting its proteasomal degradation in a PKA-dependent manner. The functional importance of this pathway is demonstrated by reduced GLUT1 mRNA levels, a classical transcriptional target of HIF-1 $\alpha$ .

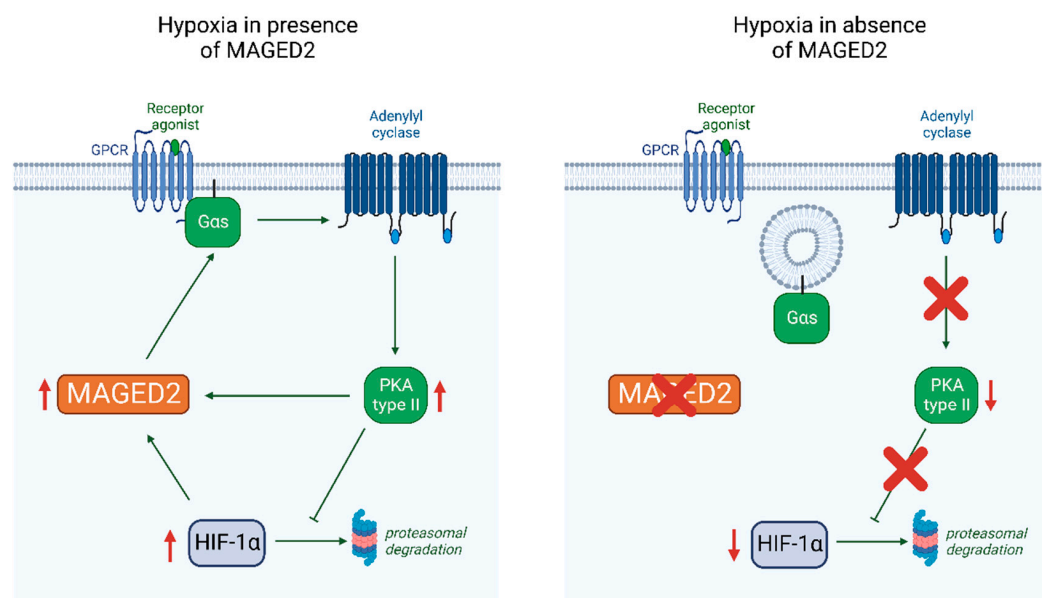


**Figure 7.** Proposed model for MAGED2's role under hypoxia (created with BioRender.com). Under hypoxia, MAGED2 inhibits  $G_{\alpha s}$  endocytosis. This ensures activation of the adenylate cyclase and cAMP generation and activation of PKA, which enhances expression of HIF-1 $\alpha$  under hypoxia by inhibiting its proteasomal degradation. The latter amplifies together with forskolin MAGED2 mRNA levels. Hence, depletion of MAGED2 impairs the cAMP/PKA pathway and induction of HIF-1 $\alpha$ . Reduced cAMP levels explain salt loss in transient Bartter syndrome.

The biological implications of MAGED2's role in amplifying hypoxic induction of HIF-1 $\alpha$  are broad because MAGED2 is expressed in many adult tissues where it could play



a critical role under hypoxic conditions (i.e., high altitude, inflamed hypoxic tissue, acute kidney injury, and cancer). Although our study was conducted in cell culture, it is likely that this reciprocal regulation of MAGED2 and HIF-1 $\alpha$ , could also take place in native tissues, in particular the kidney, and play a crucial role in the chronic renal adaptations to physiological or pathological challenges: Of note, MAGED2 protein is constitutively expressed in the distal tubule [8,31] while HIF-1 $\alpha$  protein is absent in adult kidney, both are induced in the distal tubule of the kidney in rodent models of acute kidney injury (AKI) [31–33]. HIF-1 $\alpha$  protein has also been demonstrated in humans with renal transplant failure [34]. In conjunction with our data, it is conceivable that MAGED2 is required for proper induction of HIF-1 $\alpha$  in the distal tubule. As several research groups have demonstrated a protective effect in animal models of AKI by exogenous induction of HIF1 either by small molecules or by genetic techniques (Table 2 in [32]), activation of MAGED2 might be an additional route to increase HIF-1 $\alpha$  activity. Moreover, we previously showed that MAGED2 mutations cause transient Bartter syndrome characterized by severe renal salt wasting and polyuria in fetuses, by heavily altering the expression of two critical renal salt-transporters, NKCC2, and NCC. It is also conceivable that physiological or pathological changes in the expression level of HIF-1 $\alpha$  and/or MAGED2 may affect the activity of NKCC2 and/or NCC, therefore altering the water balance and sodium homeostasis, not only during pregnancy but also during adult life.

In regard to the transient nature of aBS caused by MAGED2 mutations (tBS5), which denotes spontaneous recovery from salt-wasting in parallel with a developmental increase in renal oxygenation, we hypothesized that MAGED2 function is required mainly under physiological hypoxic conditions such as in fetuses. Given the well-established link between HIF-1 $\alpha$  and cAMP/PKA and by showing in the present study that MAGED2 is also required for hypoxic induction of HIF-1 $\alpha$ , the finding of the present study may further explain the transient nature of this kidney disease. However, the effect of MAGED2 on cAMP and HIF-1 $\alpha$  pathways, may still not entirely explain the profound salt wasting caused by impaired NKCC2 and NCC post-Golgi regulation and targeting to the cell surface. Indeed, one cannot exclude that, in MAGED2-depleted hypoxic cells, other molecular mechanisms such as ER retention and associated degradation of the cotransporters due to ER stress induced by hypoxia, are also involved. In line with this idea, we previously showed that export from the ER constitutes the limiting step in NKCC2 maturation and cell surface expression and that WT NKCC2 and its disease-causing mutants are subject to regulation by endoplasmic reticulum-associated degradation (ERAD), in particular under ER stress conditions [35–39].

Importantly, our previous studies showed that MAGED2 depletion impaired the maturation of the transiently expressed key renal transport proteins and membrane proteins NKCC2 and NCC in HEK293 cells [8]. Given that transient overexpression induces ER stress [40], especially when overexpressing transmembrane proteins [41], we speculate that this stress rendered the maturation of NKCC2 and NCC MAGED2 sensitive. Along these lines, it is conceivable that the effects of MAGED2 depletion on HIF-1 $\alpha$  induction and G $\alpha$ s localization seen with cobalt chloride results from redox stress [9]. Taken together, we speculate that MAGED2 protects against various forms of stress, namely hypoxic stress, ER stress, and redox stress.

MAGED2 is also expressed in many human cancers and is associated with a poor prognosis [4,42–45]. Moreover, the hypoxic microenvironment in cancer cells is the key condition affecting the cellular expression program leading to chemotherapy resistance [46]. Given the established roles of G $\alpha$ s and HIF-1 $\alpha$  as oncoproteins in malignancy [47–49], it is conceivable that MAGED2 promotes tumorigenesis by stimulating the cAMP/PKA-HIF-1 $\alpha$  pathway.

Our data significantly extend previous studies, which uncovered unidirectional links between cAMP/PKA and HIF-1 $\alpha$  and vice versa but not their reciprocal interactions governed by MAGED2 acting as a master regulator: Starting with the finding that  $\beta$ -blockers reduce expression of the HIF-1 $\alpha$  dependent gene erythropoietin more than 40 years

ago, various groups reported unidirectional connections between hypoxia, HIF-1 $\alpha$ , and the cAMP/PKA pathway. In a sequential order starting at the plasma membrane, all these studies identified the following links between the HIF-1 $\alpha$  and the cAMP/PKA pathways: A hypoxia-specific phosphorylation of the  $\beta$ -receptor is essential for HIF-1 $\alpha$  activation [50], adenylyl cyclase VI and VII are induced by HIF-1 $\alpha$  [19], hypoxia increases PKA activity [18,27], and PKA stabilizes HIF-1 $\alpha$  by phosphorylation [20,23]. Our study now adds substantially to the above findings because we identified MAGED2 as a master regulator, which is connected to HIF-1 $\alpha$  and the cAMP/PKA pathways in a multidirectional fashion through multiple and partly independent ways.

In summary, we identified that MAGED2 acts as a master regulator for the hypoxic induction of HIF-1 $\alpha$  by controlling G $\alpha$ s dependent activation of PKA type II. In terms of therapeutic applications, inhibition of MAGED2 could target the oncoproteins G $\alpha$ s and HIF-1 $\alpha$  specifically in hypoxic tumors, and its activation may enhance HIF-1 $\alpha$  induction in kidney disease.

**Supplementary Materials:** The following supporting information can be downloaded at: <https://www.mdpi.com/article/10.3390/cells11213424/s1>.

**Author Contributions:** Conceptualization, E.S., K.L. and M.K. (Martin Kömhoff); Methodology, E.S. and M.K. (Martin Kömhoff); Investigation, E.S., S.N., L.Q., A.R. and M.K. (Maja Kleim); Visualization, E.S. and S.N.; Funding acquisition, M.K. (Martin Kömhoff); Project administration, M.K. (Martin Kömhoff); Supervision: M.K. (Martin Kömhoff); Writing—original draft preparation, E.S., K.L. and M.K. (Martin Kömhoff); Writing—review and editing, S.W. and R.T.S. All authors have read and agreed to the published version of the manuscript.

**Funding:** This work was supported by a grant from the German Research Foundation (DFG) Ko1855/4-1 and Behring Röntgen Foundation, grant 67-0061 (MK, Martin Kömhoff). Open Access funding provided by the Open Access Publication Fund of Philipps-Universität Marburg with support of the Deutsche Forschungsgemeinschaft (DFG, German Research Foundation).

**Institutional Review Board Statement:** Not applicable.

**Informed Consent Statement:** Not applicable.

**Data Availability Statement:** All data are available in the main text or the Supplementary Materials.

**Acknowledgments:** We thank Michelle Auer for technical support.

**Conflicts of Interest:** Authors declare that they have no competing interests.

## References

1. Ducsay, C.A.; Goyal, R.; Pearce, W.J.; Wilson, S.; Hu, X.Q.; Zhang, L. Gestational Hypoxia and Developmental Plasticity. *Physiol. Rev.* **2018**, *98*, 1241–1334. [CrossRef] [PubMed]
2. Hemker, S.L.; Sims-Lucas, S.; Ho, J. Role of hypoxia during nephrogenesis. *Pediatr. Nephrol.* **2016**, *31*, 1571–1577. [CrossRef] [PubMed]
3. Rudolph, A.M.; Heymann, M.A.; Teramo, K.A.W.; Barrett, C.T.; Räihä, N.C.R. Studies on the Circulation of the Previabie Human Fetus. *Pediatr. Res.* **1971**, *5*, 452–465. [CrossRef]
4. Bernhardt, W.M.; Schmitt, R.; Rosenberger, C.; Munchenhagen, P.M.; Grone, H.J.; Frei, U.; Warnecke, C.; Bachmann, S.; Wiesener, M.S.; Willam, C.; et al. Expression of hypoxia-inducible transcription factors in developing human and rat kidneys. *Kidney Int.* **2006**, *69*, 114–122. [CrossRef]
5. Brezis, M.; Rosen, S. Hypoxia of the renal medulla—Its implications for disease. *N. Engl. J. Med.* **1995**, *332*, 647–655. [CrossRef] [PubMed]
6. Komhoff, M.; Laghmani, K. Pathophysiology of antenatal Bartter’s syndrome. *Curr. Opin. Nephrol. Hypertens.* **2017**, *26*, 419–425. [CrossRef]
7. Legrand, A.; Treard, C.; Roncelin, I.; Dreux, S.; Bertholet-Thomas, A.; Broux, F.; Bruno, D.; Decramer, S.; Deschenes, G.; Djeddi, D.; et al. Prevalence of Novel MAGED2 Mutations in Antenatal Bartter Syndrome. *Clin. J. Am. Soc. Nephrol.* **2018**, *13*, 242–250. [CrossRef] [PubMed]
8. Laghmani, K.; Beck, B.B.; Yang, S.S.; Seaayfan, E.; Wenzel, A.; Reusch, B.; Vitzthum, H.; Priem, D.; Demarets, S.; Bergmann, K.; et al. Polyhydramnios, Transient Antenatal Bartter’s Syndrome, and MAGED2 Mutations. *N. Engl. J. Med.* **2016**, *374*, 1853–1863. [CrossRef]

9. Seaayfan, E.; Nasrah, S.; Quell, L.; Kleim, M.; Weber, S.; Meyer, H.; Laghmani, K.; Kömhoff, M. MAGED2 Is Required under Hypoxia for cAMP Signaling by Inhibiting MDM2-Dependent Endocytosis of G-Alpha-S. *Cells* **2022**, *11*, 2546. [[CrossRef](#)] [[PubMed](#)]
10. Gee, R.R.F.; Chen, H.; Lee, A.K.; Daly, C.A.; Wilander, B.A.; Fon Tacer, K.; Potts, P.R. Emerging roles of the MAGE protein family in stress response pathways. *J. Biol. Chem.* **2020**, *295*, 16121–16155. [[CrossRef](#)]
11. Doyle, J.M.; Gao, J.; Wang, J.; Yang, M.; Potts, P.R. MAGE-RING protein complexes comprise a family of E3 ubiquitin ligases. *Mol. Cell* **2010**, *39*, 963–974. [[CrossRef](#)]
12. Kamitomo, M.; Alonso, J.G.; Okai, T.; Longo, L.D.; Gilbert, R.D. Effects of long-term, high-altitude hypoxemia on ovine fetal cardiac output and blood flow distribution. *Am. J. Obstet. Gynecol.* **1993**, *169*, 701–707. [[CrossRef](#)]
13. Semenza, G.L. Hypoxia-inducible factors in physiology and medicine. *Cell* **2012**, *148*, 399–408. [[CrossRef](#)]
14. Brahimi-Horn, C.; Mazure, N.; Pouyssegur, J. Signalling via the hypoxia-inducible factor-1alpha requires multiple posttranslational modifications. *Cell Signal.* **2005**, *17*, 1–9. [[CrossRef](#)] [[PubMed](#)]
15. Albanese, A.; Daly, L.A.; Mennerich, D.; Kietzmann, T.; Sée, V. The Role of Hypoxia-Inducible Factor Post-Translational Modifications in Regulating Its Localisation, Stability, and Activity. *Int. J. Mol. Sci.* **2021**, *22*, 268. [[CrossRef](#)] [[PubMed](#)]
16. Živný, J.; Ostádal, B.; Neuwirt, J.; Procházka, J.; Pelouch, V. Effect of beta adrenergic blocking agents on erythropoiesis in rats. *J. Pharmacol. Exp. Ther.* **1983**, *226*, 222–225. [[PubMed](#)]
17. Fink, G.D.; Paulo, L.G.; Fisher, J.W. Effects of beta adrenergic blocking agents on erythropoietin production in rabbits exposed to hypoxia. *J. Pharmacol. Exp. Ther.* **1975**, *193*, 176–181. [[PubMed](#)]
18. Shaikh, D.; Zhou, Q.; Chen, T.; Ibe, J.C.; Raj, J.U.; Zhou, G. cAMP-dependent protein kinase is essential for hypoxia-mediated epithelial-mesenchymal transition, migration, and invasion in lung cancer cells. *Cell Signal.* **2012**, *24*, 2396–2406. [[CrossRef](#)]
19. Simko, V.; Iuliano, F.; Sevcikova, A.; Labudova, M.; Barathova, M.; Radvak, P.; Pastorekova, S.; Pastorek, J.; Csaderova, L. Hypoxia induces cancer-associated cAMP/PKA signalling through HIF-mediated transcriptional control of adenylyl cyclases VI and VII. *Sci. Rep.* **2017**, *7*, 10121. [[CrossRef](#)] [[PubMed](#)]
20. Bullen, J.W.; Tchernyshyov, I.; Holewinski, R.J.; DeVine, L.; Wu, F.; Venkatraman, V.; Kass, D.L.; Cole, R.N.; Van Eyk, J.; Semenza, G.L. Protein kinase A-dependent phosphorylation stimulates the transcriptional activity of hypoxia-inducible factor 1. *Sci. Signal.* **2016**, *9*, ra56. [[CrossRef](#)] [[PubMed](#)]
21. De Backer, J.; Maric, D.; Bosman, M.; Dewilde, S.; Hoogewijs, D. A reliable set of reference genes to normalize oxygen-dependent cytoglobin gene expression levels in melanoma. *Sci. Rep.* **2021**, *11*, 10879. [[CrossRef](#)] [[PubMed](#)]
22. Munoz-Sanchez, J.; Chanez-Cardenas, M.E. The use of cobalt chloride as a chemical hypoxia model. *J. Appl. Toxicol.* **2019**, *39*, 556–570. [[CrossRef](#)] [[PubMed](#)]
23. Toffoli, S.; Feron, O.; Raes, M.; Michiels, C. Intermittent hypoxia changes HIF-1alpha phosphorylation pattern in endothelial cells: Unravelling of a new PKA-dependent regulation of HIF-1alpha. *Biochim. Et Biophys. Acta* **2007**, *1773*, 1558–1571. [[CrossRef](#)] [[PubMed](#)]
24. Ebert, B.L.; Firth, J.D.; Ratcliffe, P.J. Hypoxia and mitochondrial inhibitors regulate expression of glucose transporter-1 via distinct Cis-acting sequences. *J. Biol. Chem.* **1995**, *270*, 29083–29089. [[CrossRef](#)] [[PubMed](#)]
25. Dreos, R.; Ambrosini, G.; Perier, R.C.; Bucher, P. The Eukaryotic Promoter Database: Expansion of EPDnew and new promoter analysis tools. *Nucleic Acids Res.* **2015**, *43*, D92–D96. [[CrossRef](#)] [[PubMed](#)]
26. Gjertsen, B.; Mellgren, G.; Otten, A.; Maronde, E.; Genieser, H.-G.; Jastorff, B.; Vintermyr, O.K.; McKnight, G.S.; DøSkeland, S.O. Novel (Rp)-cAMPS Analogs as Tools for Inhibition of cAMP-Kinase in Cell Culture: Basal cAMP-Kinase Activity Modulates Interleukin-1 $\beta$  Action. *J. Biol. Chem.* **1995**, *270*, 20599–20607. [[CrossRef](#)] [[PubMed](#)]
27. Lucia, K.; Wu, Y.; Garcia, J.M.; Barlier, A.; Buchfelder, M.; Saeger, W.; Renner, U.; Stalla, G.K.; Theodoropoulou, M. Hypoxia and the hypoxia inducible factor 1alpha activate protein kinase A by repressing RII beta subunit transcription. *Oncogene* **2020**, *39*, 3367–3380. [[CrossRef](#)]
28. Walker-Gray, R.; Stengel, F.; Gold, M.G. Mechanisms for restraining cAMP-dependent protein kinase revealed by subunit quantitation and cross-linking approaches. *Proc. Natl. Acad. Sci. USA* **2017**, *114*, 10414–10419. [[CrossRef](#)]
29. Søberg, K.; Skålhegg, B.S. The Molecular Basis for Specificity at the Level of the Protein Kinase A Catalytic Subunit. *Front. Endocrinol.* **2018**, *9*, 538. [[CrossRef](#)] [[PubMed](#)]
30. Cadd, G.; McKnight, G.S. Distinct patterns of cAMP-dependent protein kinase gene expression in mouse brain. *Neuron* **1989**, *3*, 71–79. [[CrossRef](#)]
31. Valiño-Rivas, L.; Cuarental, L.; Agustin, M.; Husi, H.; Cannata-Ortiz, P.; Sanz, A.B.; Mischak, H.; Ortiz, A.; Sanchez-Niño, M.D. MAGE genes in the kidney: Identification of MAGED2 as upregulated during kidney injury and in stressed tubular cells. *Nephrol. Dial. Transplant.* **2019**, *34*, 1498–1507. [[CrossRef](#)] [[PubMed](#)]
32. Shu, S.; Wang, Y.; Zheng, M.; Liu, Z.; Cai, J.; Tang, C.; Dong, Z. Hypoxia and Hypoxia-Inducible Factors in Kidney Injury and Repair. *Cells* **2019**, *8*, 207. [[CrossRef](#)] [[PubMed](#)]
33. Hill, P.; Shukla, D.; Tran, M.G.; Aragones, J.; Cook, H.T.; Carmeliet, P.; Maxwell, P.H. Inhibition of hypoxia inducible factor hydroxylases protects against renal ischemia-reperfusion injury. *J. Am. Soc. Nephrol.* **2008**, *19*, 39–46. [[CrossRef](#)]
34. Rosenberger, C.; Pratschke, J.; Rudolph, B.; Heyman, S.N.; Schindler, R.; Babel, N.; Eckardt, K.U.; Frei, U.; Rosen, S.; Reinke, P. Immunohistochemical detection of hypoxia-inducible factor-1alpha in human renal allograft biopsies. *J. Am. Soc. Nephrol.* **2007**, *18*, 343–351. [[CrossRef](#)]



35. Zaarour, N.; Demaretz, S.; Defontaine, N.; Zhu, Y.; Laghmani, K. Multiple evolutionarily conserved Di-leucine like motifs in the carboxyl terminus control the anterograde trafficking of NKCC2. *J. Biol. Chem.* **2012**, *287*, 42642–42653. [\[CrossRef\]](#)
36. Seaayfan, E.; Defontaine, N.; Demaretz, S.; Zaarour, N.; Laghmani, K. OS9 Protein Interacts with Na-K-2Cl Co-transporter (NKCC2) and Targets Its Immature Form for the Endoplasmic Reticulum-associated Degradation Pathway. *J. Biol. Chem.* **2016**, *291*, 4487–4502. [\[CrossRef\]](#)
37. Bakhos-Douaihy, D.; Seaayfan, E.; Demaretz, S.; Komhoff, M.; Laghmani, K. Differential Effects of STCH and Stress-Inducible Hsp70 on the Stability and Maturation of NKCC2. *Int. J. Mol. Sci.* **2021**, *22*, 2207. [\[CrossRef\]](#)
38. Demaretz, S.; Seaayfan, E.; Bakhos-Douaihy, D.; Frachon, N.; Komhoff, M.; Laghmani, K. Golgi Alpha1,2-Mannosidase IA Promotes Efficient Endoplasmic Reticulum-Associated Degradation of NKCC2. *Cells* **2021**, *11*, 101. [\[CrossRef\]](#)
39. Shaukat, I.; Bakhos-Douaihy, D.; Zhu, Y.; Seaayfan, E.; Demaretz, S.; Frachon, N.; Weber, S.; Komhoff, M.; Vargas-Poussou, R.; Laghmani, K. New insights into the role of endoplasmic reticulum-associated degradation in Bartter Syndrome Type 1. *Hum. Mutat.* **2021**, *42*, 947–968. [\[CrossRef\]](#)
40. Fiszer-Kierzkowska, A.; Vydra, N.; Wysocka-Wycisk, A.; Kronekova, Z.; Jarzab, M.; Lisowska, K.M.; Krawczyk, Z. Liposome-based DNA carriers may induce cellular stress response and change gene expression pattern in transfected cells. *BMC Mol. Biol.* **2011**, *12*, 27. [\[CrossRef\]](#)
41. Casagrande, R.; Stern, P.; Diehn, M.; Shamu, C.; Osario, M.; Zúñiga, M.; Brown, P.O.; Ploegh, H. Degradation of Proteins from the ER of *S. cerevisiae* Requires an Intact Unfolded Protein Response Pathway. *Mol. Cell* **2000**, *5*, 729–735. [\[CrossRef\]](#)
42. Kidd, M.; Modlin, I.M.; Mane, S.M.; Camp, R.L.; Eick, G.; Latich, I. The role of genetic markers–NAP1L1, MAGE-D2, and MTA1–in defining small-intestinal carcinoid neoplasia. *Ann. Surg. Oncol.* **2006**, *13*, 253–262. [\[CrossRef\]](#) [\[PubMed\]](#)
43. Kanda, M.; Murotani, K.; Tanaka, H.; Miwa, T.; Umeda, S.; Tanaka, C.; Kobayashi, D.; Hayashi, M.; Hattori, N.; Suenaga, M.; et al. A novel dual-marker expression panel for easy and accurate risk stratification of patients with gastric cancer. *Cancer Med.* **2018**, *7*, 2463–2471. [\[CrossRef\]](#)
44. Chung, F.Y.; Cheng, T.L.; Chang, H.J.; Chiu, H.H.; Huang, M.Y.; Chang, M.S.; Chen, C.C.; Yang, M.J.; Wang, J.Y.; Lin, S.R. Differential gene expression profile of MAGE family in taiwanese patients with colorectal cancer. *J. Surg. Oncol.* **2010**, *102*, 148–153. [\[CrossRef\]](#)
45. Tsai, J.R.; Chong, I.W.; Chen, Y.H.; Yang, M.J.; Sheu, C.C.; Chang, H.C.; Hwang, J.J.; Hung, J.Y.; Lin, S.R. Differential expression profile of MAGE family in non-small-cell lung cancer. *Lung Cancer* **2007**, *56*, 185–192. [\[CrossRef\]](#)
46. Jing, X.; Yang, F.; Shao, C.; Wei, K.; Xie, M.; Shen, H.; Shu, Y. Role of hypoxia in cancer therapy by regulating the tumor microenvironment. *Mol. Cancer* **2019**, *18*, 157. [\[CrossRef\]](#)
47. Rohwer, N.; Zasada, C.; Kempa, S.; Cramer, T. The growing complexity of HIF-1alpha's role in tumorigenesis: DNA repair and beyond. *Oncogene* **2013**, *32*, 3569–3576. [\[CrossRef\]](#)
48. O'Hayre, M.; Vazquez-Prado, J.; Kufareva, I.; Stawiski, E.W.; Handel, T.M.; Seshagiri, S.; Gutkind, J.S. The emerging mutational landscape of G proteins and G-protein-coupled receptors in cancer. *Nat. Rev. Cancer* **2013**, *13*, 412–424. [\[CrossRef\]](#)
49. Tirosh, A.; Jin, D.X.; De Marco, L.; Laitman, Y.; Friedman, E. Activating genomic alterations in the Gs alpha gene (GNAS) in 274 694 tumors. *Genes Chromosomes Cancer* **2020**, *59*, 503–516. [\[CrossRef\]](#)
50. Cheong, H.I.; Asosingh, K.; Stephens, O.R.; Queisser, K.A.; Xu, W.; Willard, B.; Hu, B.; Dermawan, J.K.; Stark, G.R.; Naga Prasad, S.V.; et al. Hypoxia sensing through beta-adrenergic receptors. *JCI Insight* **2016**, *1*, e90240. [\[CrossRef\]](#)

# Supplementary figures

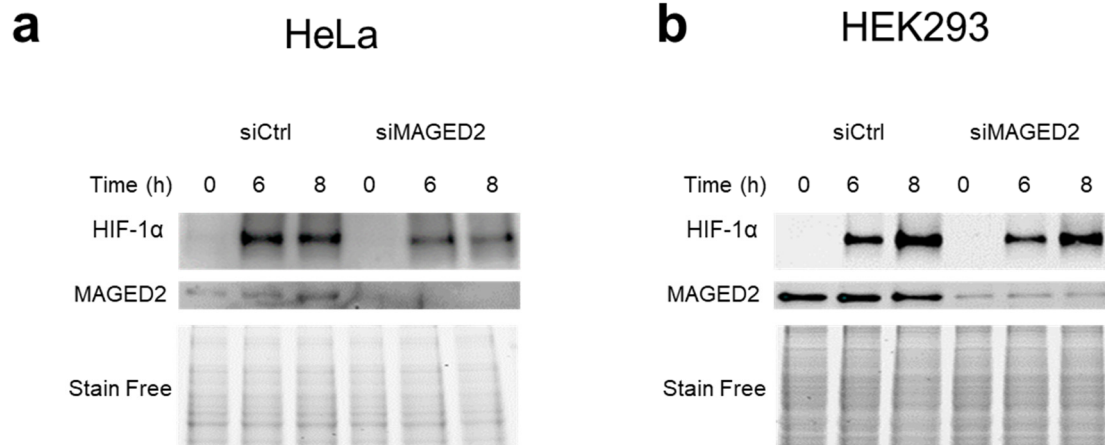


**Figure S1. MAGED2 promotes hypoxic HIF-1 $\alpha$  protein expression in HeLa and HEK293 cells:** HeLa (a) and HEK293 (b) cells were transfected with control (siCtrl), MAGED2 (siMAGED2). Briefly, 24 - 48 h post-transfection, cells were exposed to physical hypoxia. Cells were exposed to physical hypoxia (1% O<sub>2</sub>, 5% CO<sub>2</sub>, 94% N<sub>2</sub>) for the specified times. Total cell lysates were separated by SDS-PAGE and probed with an-ti-HIF-1 $\alpha$  and MAGED2 antibodies.

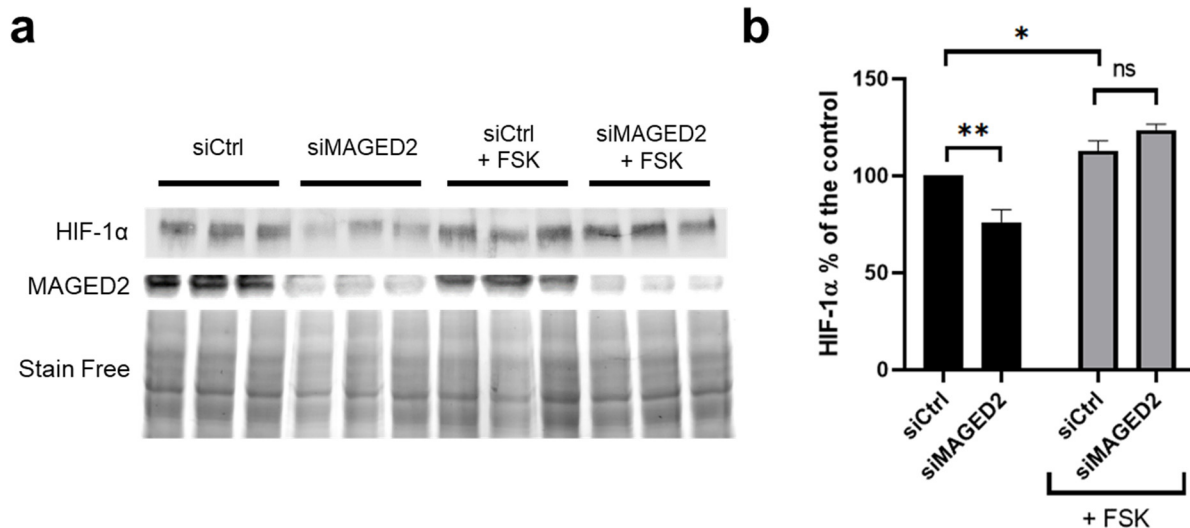


**Figure S2. Forskolin reverses the effect of MAGED2 knock-down on hypoxic HIF-1 $\alpha$  induction in HEK293 cells:** (a) HEK293 cells were transfected with control, or MAGED2 (M) siRNA cells were treated with chemical hypoxia (300 $\mu$ M CoCl<sub>2</sub>) with 10 $\mu$ M forskolin (FSK) for 14 - 16 h. Total cell lysates were separated by SDS-PAGE and probed with anti-HIF-1 $\alpha$  and MAGED2 antibodies. (b) Densitometric analysis of HIF-1 $\alpha$  immunoblot is presented in (a). Statistical significance was determined by unpaired two-sided Student's t-tests (b). Bar graphs show mean  $\pm$  SEM. \*P  $\leq$  0.05 and \*\* P  $\leq$  0.01.

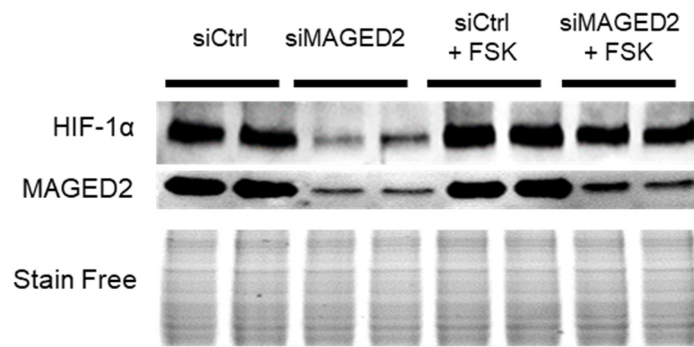



**Figure S3. Forskolin reverses the effect of MAGED2 knockdown on hypoxic HIF-1 $\alpha$  induction.** HeLa cells were transfected with control (siCtrl) or MAGED2 (siMAGED2) siRNA. Cells were exposed to physical hypoxia and with 10 $\mu$ M forskolin (FSK) for 14 - 16 h. Total cell lysates were separated by SDS-PAGE and probed with anti-HIF-1 $\alpha$  and MAGED2 antibodies.



Article

# MAGED2 Depletion Promotes Stress-Induced Autophagy by Impairing the cAMP/PKA Pathway

Sadiq Nasrah <sup>1</sup>, Aline Radi <sup>1</sup>, Johanna K. Daberkow <sup>2</sup>, Helmut Hummler <sup>1</sup>, Stefanie Weber <sup>1</sup>, Elie Seaayfan <sup>1,\*</sup>,<sup>†</sup> and Martin Kömhoff <sup>1,\*</sup>,<sup>†</sup> 

<sup>1</sup> Department of Pediatrics, University Hospital Giessen and Marburg, Philipps University Marburg, 35043 Marburg, Germany; sadiq.nasrah@uni-marburg.de (S.N.); radi@staff.uni-marburg.de (A.R.); hummler@staff.uni-marburg.de (H.H.); stefanie.weber@med.uni-marburg.de (S.W.)

<sup>2</sup> Faculty of Medicine, Justus Liebig University Giessen, 35392 Giessen, Germany; johanna.k.daberkow@med.uni-giessen.de

\* Correspondence: elie.seaayfan@uni-marburg.de (E.S.); koemhoff@staff.uni-marburg.de (M.K.)

<sup>†</sup> These authors contributed equally to this work.

**Abstract:** Melanoma-associated antigen D2 (MAGED2) plays an essential role in activating the cAMP/PKA pathway under hypoxic conditions, which is crucial for stimulating renal salt reabsorption and thus explaining the transient variant of Bartter's syndrome. The cAMP/PKA pathway is also known to regulate autophagy, a lysosomal degradation process induced by cellular stress. Previous studies showed that two members of the melanoma-associated antigens MAGE-family inhibit autophagy. To explore the potential role of MAGED2 in stress-induced autophagy, specific MAGED2-siRNA were used in HEK293 cells under physical hypoxia and oxidative stress (cobalt chloride, hypoxia mimetic). Depletion of MAGED2 resulted in reduced p62 levels and upregulation of both the autophagy-related genes (ATG5 and ATG12) as well as the autophagosome marker LC3II compared to control siRNA. The increase in the autophagy markers in MAGED2-depleted cells was further confirmed by leupeptin-based assay which concurred with the highest LC3II accumulation. Likewise, under hypoxia, immunofluorescence in HEK293, HeLa and U2OS cell lines demonstrated a pronounced accumulation of LC3B puncta upon MAGED2 depletion. Moreover, LC3B puncta were absent in human fetal control kidneys but markedly expressed in a fetal kidney from a MAGED2-deficient subject. Induction of autophagy with both physical hypoxia and oxidative stress suggests a potentially general role of MAGED2 under stress conditions. Various other cellular stressors (brefeldin A, tunicamycin, 2-deoxy-D-glucose, and camptothecin) were analyzed, which all induced autophagy in the absence of MAGED2. Forskolin (FSK) inhibited, whereas GNAS knock-down induced autophagy under hypoxia. In contrast to other MAGE proteins, MAGED2 has an inhibitory role on autophagy only under stress conditions. Hence, a prominent role of MAGED2 in the regulation of autophagy under stress conditions is evident, which may also contribute to impaired fetal renal salt reabsorption by promoting autophagy of salt-transporters in patients with MAGED2 mutation.

**Keywords:** MAGED2; autophagy; cellular stress; cAMP; G-alpha-S; Bartter's syndrome; hypoxia nephrogenesis



**Citation:** Nasrah, S.; Radi, A.; Daberkow, J.K.; Hummler, H.; Weber, S.; Seaayfan, E.; Kömhoff, M. MAGED2 Depletion Promotes Stress-Induced Autophagy by Impairing the cAMP/PKA Pathway. *Int. J. Mol. Sci.* **2023**, *24*, 13433. <https://doi.org/10.3390/ijms241713433>

Academic Editor: Maria Ines Vaccaro

Received: 26 July 2023

Revised: 22 August 2023

Accepted: 28 August 2023

Published: 30 August 2023



**Copyright:** © 2023 by the authors. Licensee MDPI, Basel, Switzerland. This article is an open access article distributed under the terms and conditions of the Creative Commons Attribution (CC BY) license (<https://creativecommons.org/licenses/by/4.0/>).

## 1. Introduction

Bartter's syndrome (BS) is a rare inherited disease caused by mutations in the salt transporters of the thick ascending limb of the loop of Henle (TAL) and/or their regulatory subunits: *SLC12A1* encoding NKCC2 (BS 1), *KCNJ1* encoding ROMK (BS 2), *CLCNKB* encoding CLC-Kb (BS 3), *BSND* encoding Barttin (BS 4a), and *CLCNKA* and *CLCNKB* encoding CLC-Ka, CLC-Kb, respectively (BS 4b) and *MAGED2* encoding MAGED2 (BS 5) [1]. BS is characterized by polyuria, hypokalemia, hypercalciuria, alkalosis, nephrocalcinosis

and low to normal blood pressure. Aside from the majority of cases of BS3, all other types of BS present with polyhydramnios, due to the limited capacity of the placenta to reabsorb electrolytes [2]. In contrast to Bartter's syndromes 1–4, Bartter's syndrome 5 resolves spontaneously despite its most severe initial presentation [3,4].

Our research provides an explanation for the transient character of Bartter's syndrome 5 by showing that under hypoxic conditions, MAGED2 functions as a master regulator of the cAMP/PKA pathway by regulating the endocytosis of G $\alpha$ s through MDM2-dependent ubiquitination [5,6], which in turn is required for renal salt reabsorption by NKCC2 and NCC [7,8]. Hence, the spontaneous resolution of transient Bartter's syndrome caused by MAGED2 mutations may result from a developmental increase in oxygen supply to the kidney, which renders MAGED2 dispensable as G $\alpha$ s can function independently under normoxia [1]. MAGED2 is a member of the melanoma-associated antigens (MAGE) gene family, which is evolutionarily conserved in eukaryotes [9] and is considered the ancestral member of the entire family of approximately 40 members in humans [10]. The human MAGE gene family is divided into two subfamilies: Type I MAGEs (MAGEs A–C), which are mainly expressed in testes and cancer, and Type II MAGEs (MAGEs D–G), which are expressed ubiquitously. MAGE proteins regulate the activity of E3 ubiquitin ligases [11] through the MAGE homology domain (MHD) [12]. There are >700 different E3 ligases, which affect client proteins through non-degradative ubiquitination (such as protein trafficking) or degradative (“proteasomal”) ubiquitination [13]. Apart from that, MAGE proteins also exhibit additional biochemical functions that are independent of E3 ubiquitin ligases [9], and ongoing research is discovering new functions of these proteins. The role of MAGED2 in the protection against hypoxic stress fits well with previous reports showing diverse members of the MAGE-gene family protecting against diverse stressors. For example, Mage-A2/A6/A8 knockout (KO) mice have compromised spermatogenesis following genotoxic or nutritional stress [14]. Moreover, expression of MAGEA3/6 is restricted to germline cells but is re-expressed in tumor cells following demethylation of the promoter, where it promotes proteasomal degradation of AMPK via the E3 ubiquitin ligases TRIM28. The latter inhibits AMPK-dependent autophagy, enhances proliferation downstream of mTORC1, and thereby promotes tumorigenicity [15].

Based on our previous finding that MAGED2 protects against hypoxic stress [5], a known inducer of autophagy, the effects of MAGED2 depletion on the induction of autophagy under different stressors in vitro were analyzed. We showed that MAGED2 blocks autophagy in three different cell lines exposed to physical and chemical hypoxia. Importantly, the markedly increased expression of LC3B in a fetal kidney from a patient with truncating mutations in MAGED2 but not in two corresponding age-matched control kidneys confirms the relevance of our in vitro findings under hypoxia. Because chemical hypoxia stresses cells by different pathways compared to physical hypoxia, we tested endoplasmic-reticulum-, nutritional- and genotoxic stressors, which all induced autophagy in MAGED2 depleted cells. Finally, we revealed that under hypoxia, MAGED2 depletion promotes autophagy by inhibiting the cAMP/PKA pathway. This effect was reversed by forskolin (a cAMP/PKA pathway activator), in contrast to GNAS knockdown (cAMP/PKA pathway inhibition), which promoted it.

## 2. Results

### 2.1. Induction of Autophagy upon MAGED2 Depletion under Hypoxia

To investigate the regulatory role of MAGED2 on autophagy under hypoxic stress, HEK293 cells were transfected with control or MAGED2 siRNAs and exposed at confluency to normoxia or physical hypoxia (1% O $_2$ , 5% CO $_2$ , 94% N $_2$ ) overnight. Immunoblotting confirmed induction of HIF-1 $\alpha$  under hypoxia. Under normoxia, the depletion of MAGED2 had no effect on ATG5-ATG12 conjugate levels, which alongside ATG16 are essential for autophagosome formation, nor on LC3II abundance. In contrast, physical hypoxia induced the expression of ATG5-ATG12 conjugates and led to a statistically significantly increased LC3II abundance in MAGED2-depleted cells, as shown by immunoblotting



(Figures S1 and 1A,B). The autophagy flux was further assayed using p62 and leupeptin, the protease inhibitor which blocks autophagy substrate degradation and allows monitoring LC3B turnover. Indeed, knocking down MAGED2 in HEK293 cells concurred with reduced p62 levels and the highest LC3II accumulation when treating with leupeptin (Figure 1A,B). The measurement of ATG5 and ATG12 mRNA level by RT-qPCR showed an increase in its expression when MAGED2 was depleted (Figure 1D). To independently confirm this observation, accumulation of LC3B puncta was analyzed by immunocytochemistry as demonstrated in Figure 1C; the abundance of puncta was markedly elevated in MAGED2-depleted cells.

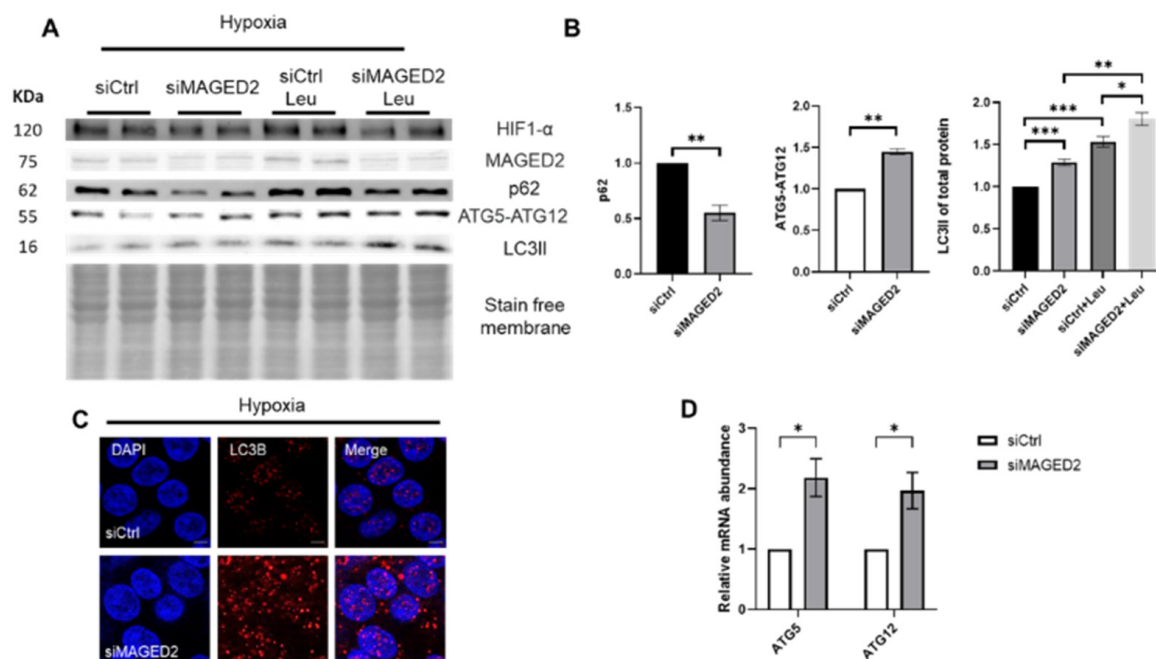


**Figure 1.** MAGED2 depletion induces autophagy under hypoxic conditions. HEK293 cells were transfected with control or MAGED2 siRNAs. Upon confluency 24–48 h post transfection, cells were exposed to physical hypoxia overnight. Total cell lysates were separated by SDS-PAGE and blotted for p62, ATGs and LC3B detection. Blotting for HIF-1 $\alpha$ - was carried out to confirm its induction under hypoxia. Immunocytochemistry was carried out in parallel in HEK293 cells transfected and stressed similarly prior to incubation with LC3B antibody. (A) Representative Western blot images demonstrate decreased p62 levels, elevated ATG5-ATG12 complex levels and a higher LC3II abundance upon MAGED2 depletion in the presence of physical hypoxia. Leupeptin assay confirmed the induced autophagy where the highest LC3II accumulation corresponded to cells where MAGED2 is knocked down. (B) Densitometric analysis of p62, ATG5-ATG12 conjugate and LC3II from the immunoblot A. All samples shown on individual blots are from the same experiment and each blot represents an example of three independent experiments. (C) Representative immunofluorescence images displaying LC3B staining in control and MAGED2-transfected HEK293 cells under physical hypoxia. Scale bar 5  $\mu$ m. (D) This notion was further supported by qRT-PCR, where the quantity of ATG5 and ATG12 was determined in HEK293 cells transfected with control or MAGED2 siRNAs and exposed to hypoxia. Total mRNA was isolated, and the relative mRNA amounts of both genes were measured. Statistical significance was determined by unpaired Student's *t*-test. Bar graphs show mean  $\pm$  SEM, \*  $p \leq 0.05$ , \*\*  $p \leq 0.01$ , \*\*\*  $p \leq 0.001$ .

Induction of autophagy upon MAGED2 depletion in response to hypoxic stress was validated in HeLa (Figure S2A,B) and U2OS (Figure S2C,D) cells (U2OS harbors endogenous wild-type p53 in contrast to HeLa and HEK293 cells), thereby excluding the possibility that induction of autophagy in HeLa and HEK293 cells results from a lack of p53, which could induce or inhibit autophagy by regulating the AMPK/mTOR pathway. A significantly



induced autophagic response as judged by immunoblotting and immunocytochemistry upon MAGED2 depletion was detected, thus validating the potential inhibitory role of MAGED2 on autophagy independently of p53.

Similar to physical hypoxia, cobalt chloride, an oxidative stress inducer, significantly induced autophagy (Figure 2A,B) and led to marked abundance of LC3B puncta (Figure 2C, Figures S3A and S4A) as judged by immunocytochemistry upon MAGED2 depletion. These findings show the important role that MAGED2 plays in inhibiting autophagy under oxidative stress conditions.

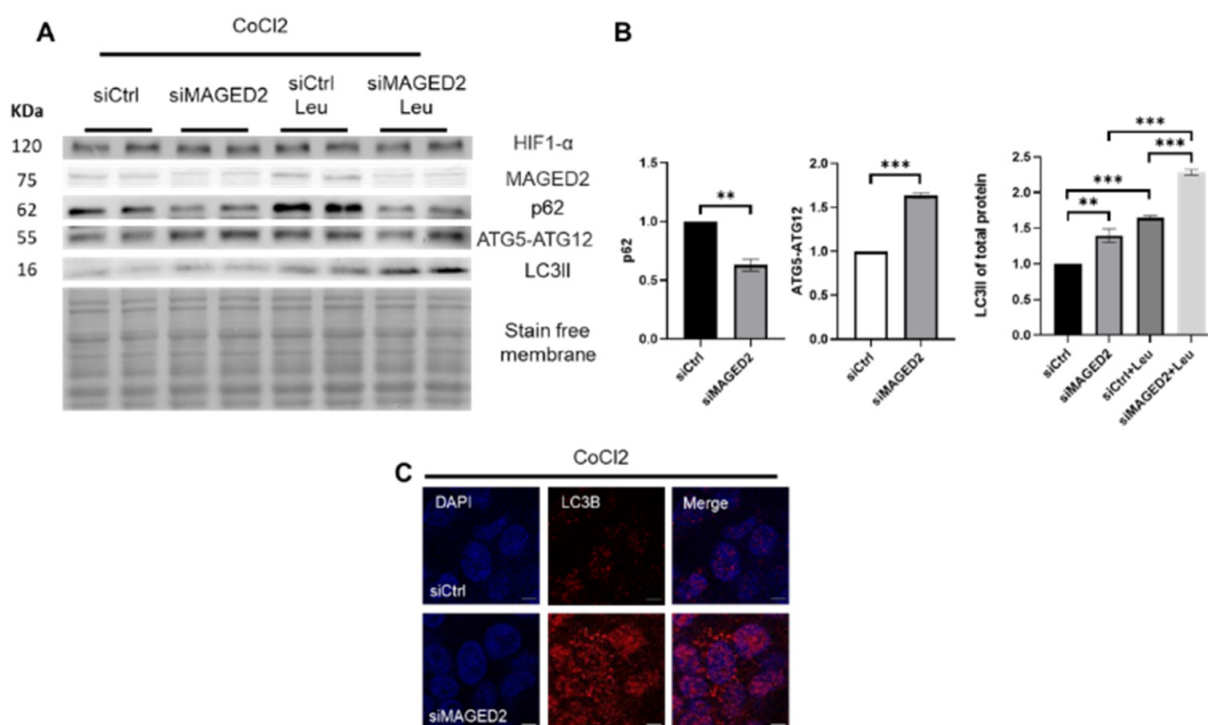


**Figure 2.** Cobalt chloride induces autophagy in MAGED2-depleted HEK293 cells. HEK293 cells were transfected with control or MAGED2 siRNAs. Upon confluency 24–48 h post transfection, cells were treated with cobalt chloride (“chemical hypoxia”,  $\text{CoCl}_2$ , 300  $\mu\text{M}$ ) for 14–16 h. Total cell lysates were separated by SDS-PAGE and blotted for p62, ATGs and LC3B detection. Of note, HIF-1 $\alpha$  immunoblotting confirmed the hypoxic condition. Immunocytochemistry was carried out in parallel in HEK293 cells transfected and stressed similarly prior to incubation with LC3B antibody. (A) Representative Western blot images from HEK293 cells demonstrate reduced p62 levels, increased ATG5-ATG12 conjugate levels and a higher LC3II prevalence upon MAGED2 depletion. Coincubation with leupeptin (100  $\mu\text{M}$ ) led to an increased LC3II accumulation, which confirmed induction of autophagy. (B) Densitometric analysis of p62, ATG5-ATG12 conjugate and LC3II from immunoblot A. All samples shown on individual blots are from the same experiment, and each blot represents an example of three independent experiments. Bar graphs show mean  $\pm$  SEM, \*\*  $p \leq 0.01$ , \*\*\*  $p \leq 0.001$ . (C) Representative immunofluorescence images displaying LC3B staining in control and MAGED2-transfected HEK293 cells treated with  $\text{CoCl}_2$ . Scale bar 5  $\mu\text{M}$ .

## 2.2. Increased Abundance of LC3B in a Fetal Kidney from a Patient with a Truncating Mutation in MAGED2

To independently validate the relevance of our findings of enhanced autophagy in MAGED2-depleted hypoxic cells in vitro, the expression of LC3B was analyzed ex vivo in fetal kidneys from a developmental stage, which is characterized by abundant expression of the hypoxia-marker HIF-1 $\alpha$  (hypoxia inducible factor 1 $\alpha$ ) [16]. In two individual fetal control kidneys (at 20 and 23 weeks of gestation, respectively) LC3B immunoreactivity was barely noticeable. In contrast, in a fetal kidney from a patient who died in utero at

22 weeks of gestation with transient Bartter's syndrome caused by a truncating mutation (c.1038C→G; p.Y346\*), LC3B immunoreactivity was abundantly detected primarily in the epithelia of medullary collecting ducts (co-labeled with cytokeratin) and to a lesser extent in the surrounding interstitial cells (Figure 3).

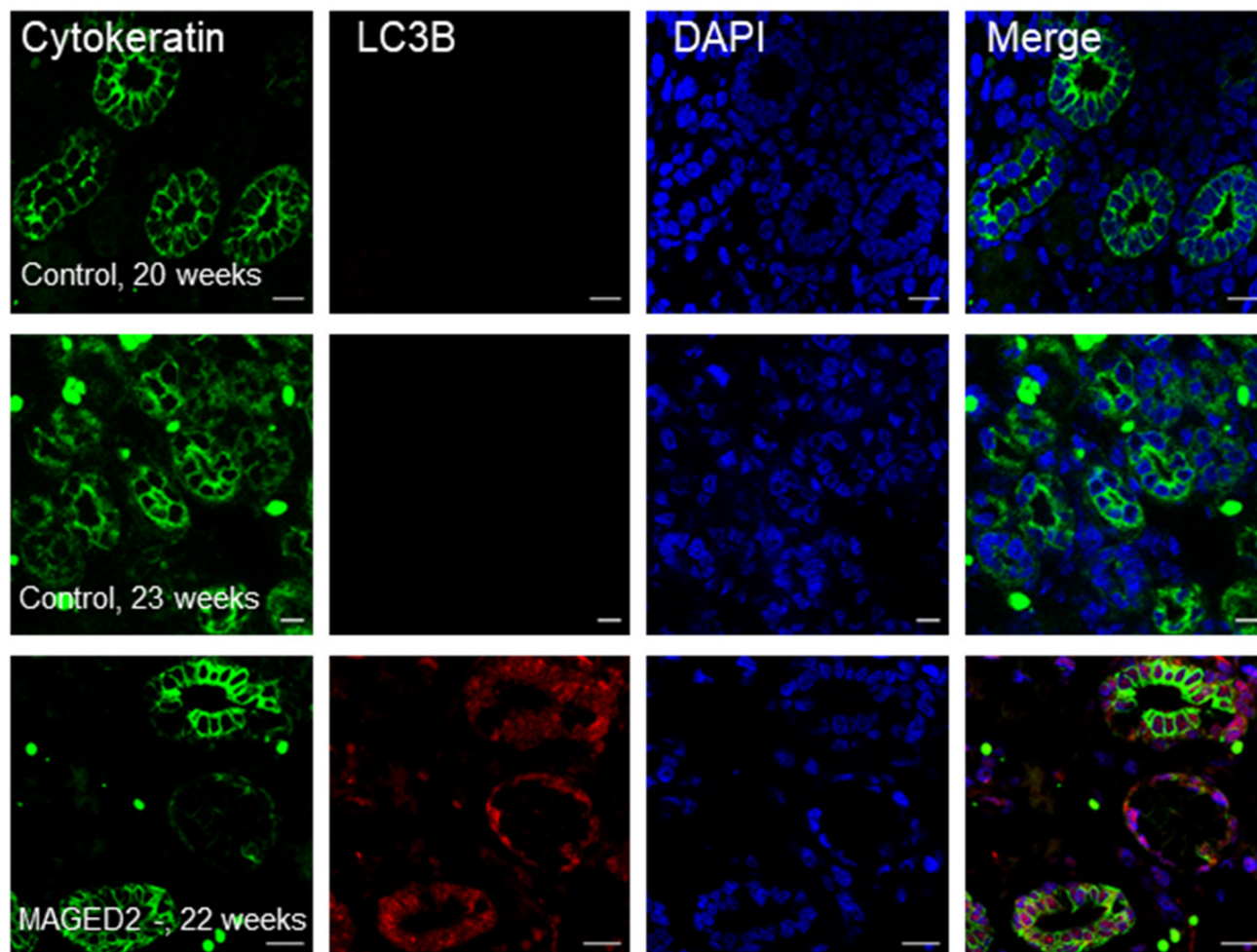


**Figure 3.** Enhanced expression of LC3B in the kidney from a fetus with transient Bartter's syndrome compared to age-matched controls. Representative immunostaining of LC3B in fetal kidney sections from aborted cases. Staining was performed using LC3B and cytokeratin antibodies visualized Alexa 555, red, and Alexa 488, green, respectively. Scale bar 20  $\mu$ M.

### 2.3. ER-Stressors Induce Autophagy upon MAGED2 Depletion

The fact that both physical hypoxia and cobalt chloride, which stress cells very differently but both cause endoplasmic reticulum stress, induce autophagy suggests that other cellular stressors may also induce autophagy in MAGED2-depleted cells. Hence, we studied the effects of two endoplasmic reticulum stress inducers, namely tunicamycin, which disturbs the secretory pathway by inhibiting N-linked glycosylation, and brefeldin A (BFA), which blocks the exit of secretory proteins from the ER, thereby disintegrating the Golgi-apparatus [17].

HEK293 cells were transfected with control or MAGED2 siRNA and treated with tunicamycin overnight. Immunoblotting showed a significantly higher LC3II abundance and ATG5-ATG12 complex expression in MAGED2-depleted cells along with reduced p62 levels (Figure 4A,B). Immunocytochemistry for LC3B puncta confirmed that autophagy was remarkably higher in MAGED2-depleted cells compared to control cells (Figures 4C, S3B and S4B).

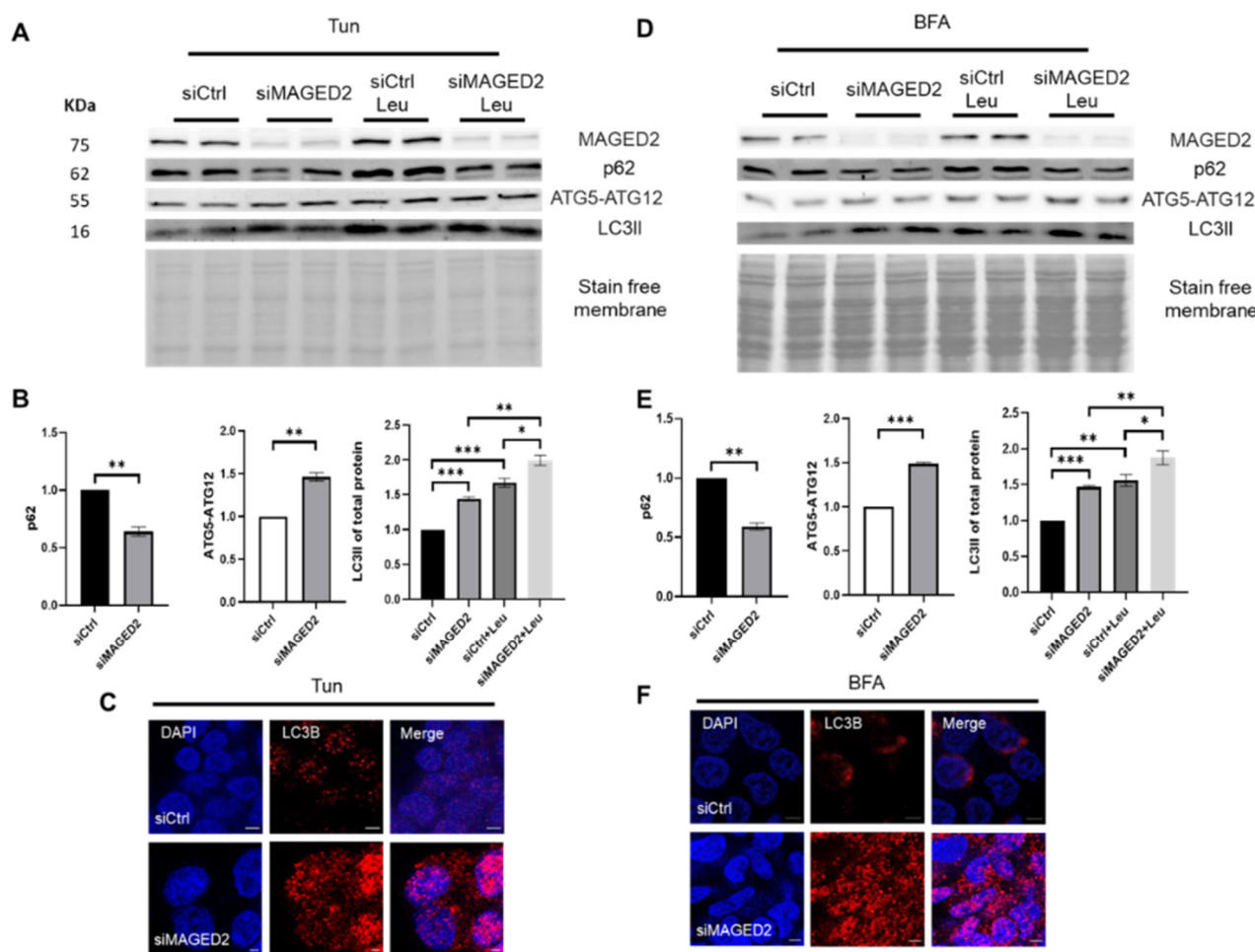


**Figure 4.** Autophagy is significantly induced by classical ER-stressors in MAGED2-depleted cells. Control or MAGED2 siRNAs were transfected into HEK293 cells. At 24–48 h post-transfection, cells were treated with the ER stressors 600 nM tunicamycin (Tun) overnight or 10  $\mu$ M brefeldin A (BFA) for 2 h. SDS-PAGE was used to separate total cell lysates before blotting for p62, LC3B and ATGs detection. Immunocytochemistry was conducted in parallel, and HEK293 cells were stained for the accumulation of LC3B puncta after being transfected and treated with ER stressors. Representative Western blot images from HEK293 cells treated with tunicamycin (**A**) or BFA (**D**) show reduced p62 levels combined with increased levels of ATG5-ATG12 complex and higher LC3II abundance in MAGED2-depleted cells. Leupeptin treatment led to the highest LC3II accumulation because of blocked autophagic flux. (**B,E**) Densitometric analysis of p62, ATG5-ATG12 conjugate and LC3II of the immunoblots (**A,D**) respectively. All blots are from the same experiment, and each represents an example of three independent experiments. Bar graphs show mean  $\pm$  SEM, \*  $p \leq 0.05$ , \*\*  $p \leq 0.01$ , \*\*\*  $p \leq 0.001$ . (**C,F**) LC3B staining in control and MAGED2-transfected HEK 293 cells treated with tunicamycin or BFA, respectively. The scale bar is 5  $\mu$ M.

Similarly, HEK293 cells were treated with BFA for 2 h. Western blotting and immunocytochemistry experiments showed that MAGED2 depletion promotes autophagy in the presence of BFA (Figures 4D–F, S3C and S4B). These findings support the idea that ER stress promotes autophagy in the absence of MAGED2.

#### 2.4. Genotoxic Stress Promotes Autophagy in MAGED2 Depleted Cells

Camptothecin (CPT) stabilizes the topoisomerase I cleavage complex [18] and induces cellular stress beyond DNA damage. It was shown that it elevates ER stress in various cancer cell lines [19,20] and enhances G<sub>2</sub>/M phase cell cycle arrest mediated by reactive oxygen species (ROS) [21]. The aim was to study its effects on autophagy in MAGED2-

depleted cells. Similar to the other stressors, HEK293 cells showed higher induction of autophagy upon CPT treatment, as evidenced by significantly decreased p62 in conjugation with elevated LC3II and ATG5-ATG12 complex levels (Figure 5A,B) and markedly more LC3B puncta (Figure 5C) in MAGED2-depleted cells. Similar effects were observed in HeLa (Figure S3D) and U2OS (Figure S4D) cells.

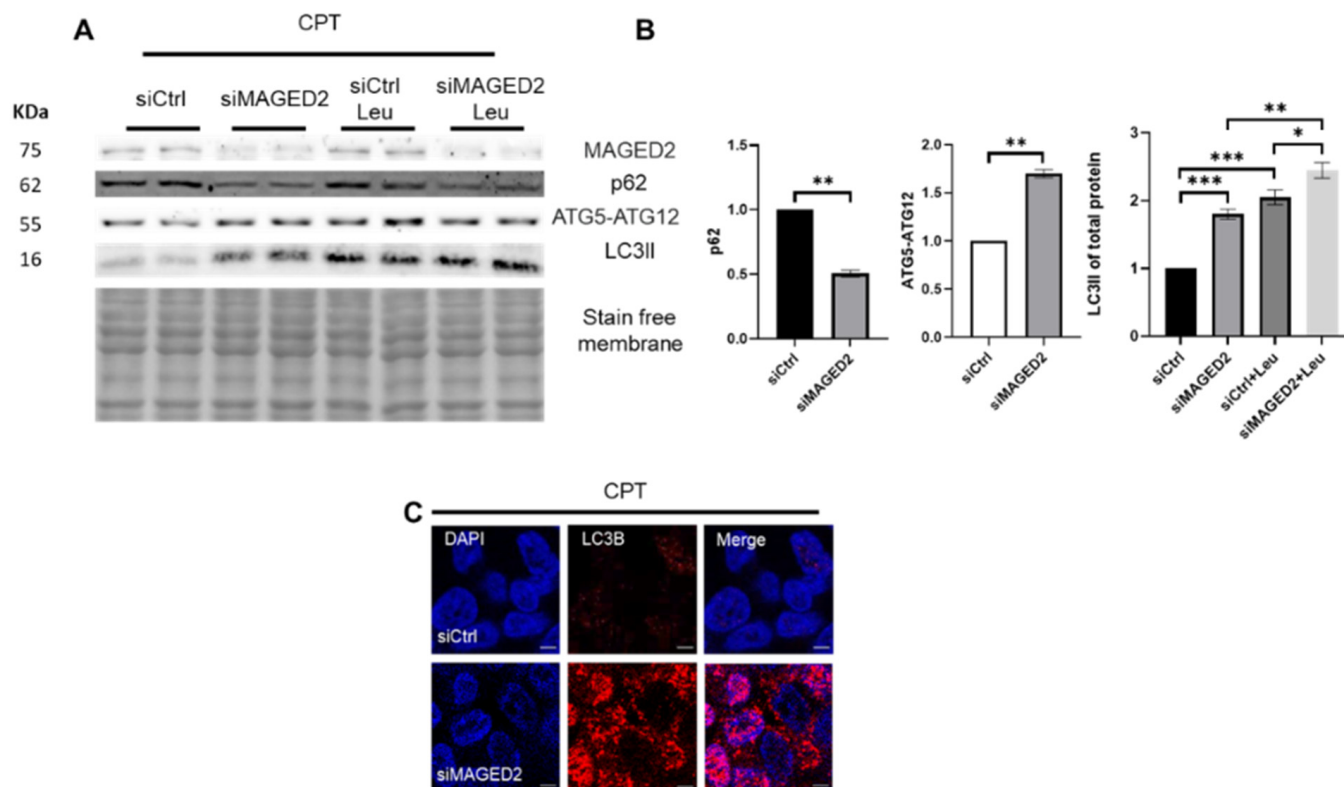


**Figure 5.** Genotoxic stress enhances autophagy in MAGED2-depleted cells. HEK293 cells were transfected with control or MAGED2 siRNAs. Cells were treated 24–48 h post-transfection with 10  $\mu$ M camptothecin (CPT) overnight. Total cell proteins were separated using SDS-PAGE and then immunoblotted for p62, ATGs and LC3B detection. In parallel, immunocytochemistry for HEK293 cells was carried out to stain for LC3B puncta following the same protocol. (A) Representative Western blot images from HEK293 cells treated with CPT show decreased p62 expression, increased levels of ATG5-ATG12 complex and higher LC3II abundance upon MAGED2 depletion. Treatment with leupeptin blocked the autophagic flux and resulted in the highest LC3II accumulation when MAGED2 was depleted. (B) Densitometric analysis of p62, ATG5-ATG12 complex and LC3II from the immunoblots in (A). All blots are from the same experiment, and each represents an example of three independent experiments. Bar graphs show mean  $\pm$  SEM, \*  $p \leq 0.05$ , \*\*  $p \leq 0.01$ , \*\*\*  $p \leq 0.001$ . (C) Representative immunofluorescence images showing LC3B staining in control and MAGED2-transfected HEK293 cells upon CPT treatment. Scale bar 5  $\mu$ m.

### 2.5. Nutritional Stress Promotes Autophagy in MAGED2-Depleted Cells

2-Deoxy-D-glucose (2-DG) is a glucose analog, which induces nutritional stress by inhibiting glycolysis [22,23], thereby reducing cellular ATP. Due to its structural similarity with mannose, it also interferes with oligosaccharide synthesis, causing abnormal N-linked glycosylation and ER stress [24]. HEK293 cells were treated for 30 min with 2-DG. Immunoblotting and immunocytochemistry were performed to monitor the autophagy flux (Figure 6A,B), and the accumulation of LC3B puncta (Figure 6C), respectively, which both were increased in MAGED2 depleted cells. Increased accumulation of LC3B puncta was observed in HeLa (Figure S3E) and U2OS (Figure S4E) cells upon knockdown of MAGED2.



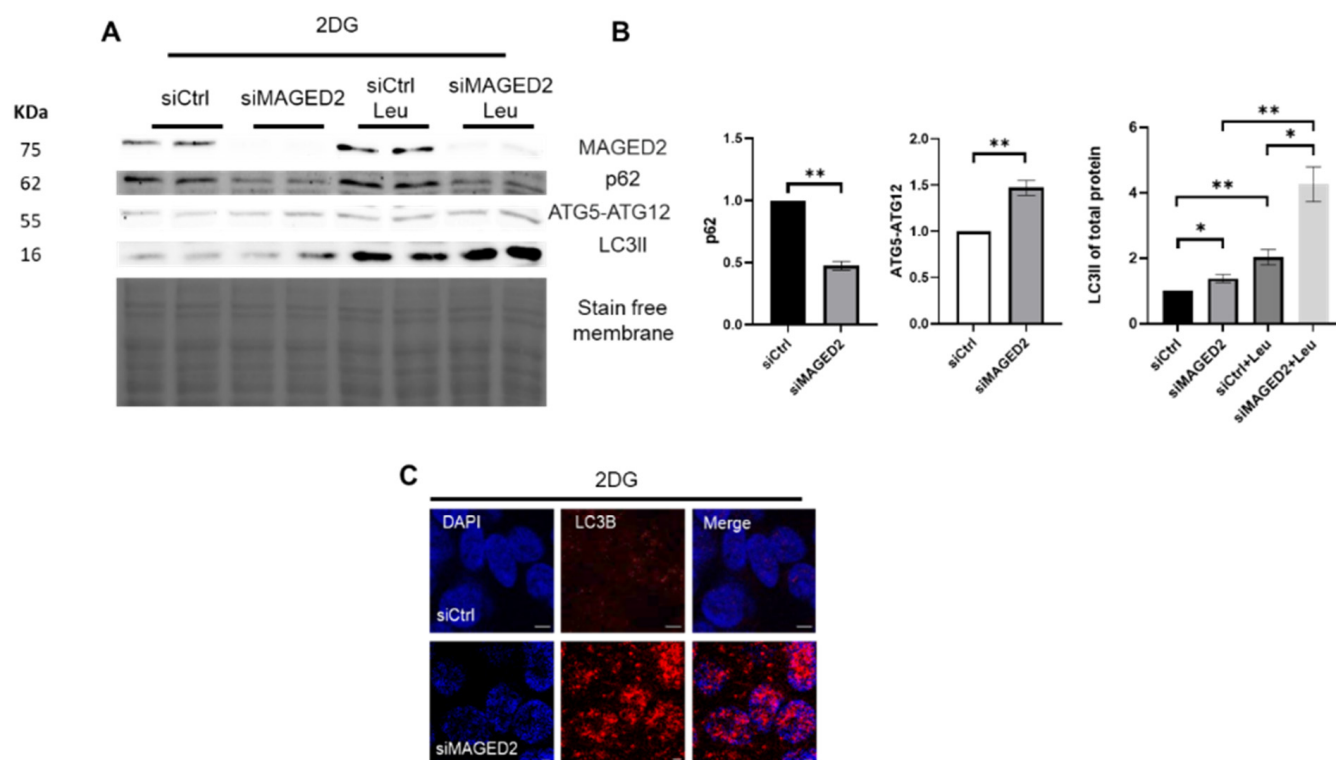


**Figure 6.** Nutritional stress promotes autophagy in MAGED2-depleted cells. Control or MAGED2 siRNAs were transfected into HEK293 cells. Cells were treated 24–48 h post transfection with 4 mM 2-Deoxy-D-glucose (2DG) for 30 min. SDS-PAGE was used to separate total cell lysates, which were next blotted for p62, ATGs and LC3B detection. Immunocytochemistry was conducted as mentioned before, and both HeLa and HEK293 cells were stained for the accumulation of LC3B puncta. **(A)** Representative Western blot images from HEK293 cells treated with 2DG shows decreased p62 levels, elevated expression of ATG5-ATG12 complex, higher LC3II abundance upon MAGED2 depletion and the highest ratio when co-incubating with Leupeptin. **(B)** Densitometric analysis of P62, ATGs and LC3II from the immunoblots in **(A)**. All blots are from the same experiment, and each represents an example of three independent experiments. Bar graphs show mean  $\pm$  SEM, \*  $p \leq 0.05$ , \*\*  $p \leq 0.01$ . **(C)** Representative immunofluorescence images showing LC3B staining in control and MAGED2-transfected HEK293 cells upon 2DG treatment. Scale bar 5  $\mu$ M.

## 2.6. Activation of cAMP/PKA Pathway Reversed the Stress-Induced Autophagic Machinery upon MAGE2 Depletion

We recently demonstrated that MAGED2 is essential under hypoxic conditions for correct localization of G $\alpha$ s at the plasma membrane, cAMP generation and PKA activation [6]. Therefore, we asked whether induction of autophagy in our experiments resulted from impaired functioning of G $\alpha$ s. Hence, we examined the effect of G $\alpha$ s-depletion in HEK293 cells exposed to normoxia or physical hypoxia. Induction of HIF-1 $\alpha$  protein confirmed hypoxia. Interestingly, knockdown of G $\alpha$ s induced autophagy under both conditions, although it was much more pronounced under hypoxic stress (lowest p62 level combined with increased LC3II and ATG5-ATG12 levels) (Figure 7A,B). It also led to increased abundance of LC3B-positive puncta as assessed by immunocytochemistry (Figure 7C). G $\alpha$ s depletion and the corresponding autophagic induction indicates cAMP/PKA implication.

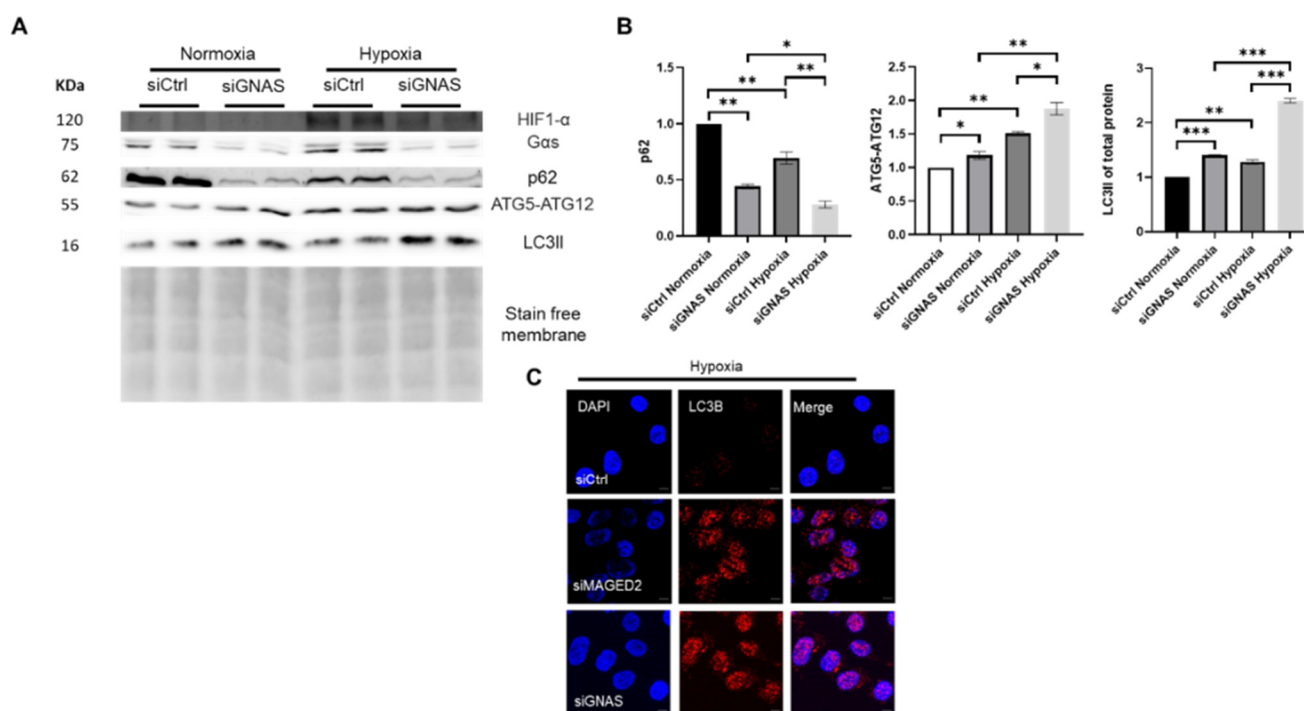


**Figure 7.** GNAS depletion induces autophagy under hypoxic conditions. Control or GNAS siRNAs were transfected into HEK293 cells. Upon confluency, 24–48 h post transfection, hypoxic stress was applied overnight for one set in a modular chamber while the other set was kept in normoxic conditions. Cells were then lysed and blotted for detection of p62, LC3B and autophagy-related genes. HIF-1α immunoblot confirmed hypoxia. (A) A representative Western blot from HEK293 cells demonstrates that GNAS depletion induced autophagy significantly under hypoxia where the low p62 levels and ATGs upregulation were accompanied by a higher conversion to the lipidated form LC3II under hypoxia. (B) Densitometric analysis of p62, ATG5-ATG12 complex and the LC3II from the immunoblot A. All samples shown on individual blots are from the same experiment, and each blot represents an example of three independent experiments. Bar graphs show mean ± SEM, \*  $p \leq 0.05$ , \*\*  $p \leq 0.01$ , \*\*\*  $p \leq 0.001$ . (C) Immunocytochemistry for HEK293 cells transfected with either control, MAGED2 or GNAS siRNAs and exposed to physical hypoxia for 14–16 h show the accumulation of LC3B puncta. Similar to MAGED2-depletion, knockdown of GNAS also led to an increased abundance of LC3B positive puncta. Scale bar is 5 μM.

To independently confirm an inhibitory role of cyclic AMP elevating agents on autophagy in MAGED2 hypoxic cells, HeLa and HEK293 cells were transfected with control or MAGED2 siRNA, treated with FSK and exposed to physical hypoxia. Interestingly, immunoblot analysis revealed a reduction in LC3II levels and a diminished autophagic response upon forskolin treatment (Figure 8A–D). FSK treatment was confirmed to activate PKA in HeLa and HEK293 cells by immunoblotting against phosphorylated PKA substrates (Figure S5). This finding was supported by immunocytochemistry, which showed that the accumulation of LC3B puncta was abrogated when MAGED2-depleted, hypoxic cells were pre-exposed to FSK (Figure 8E). A similar effect was observed in MAGED2-depleted cells treated with tunicamycin and FSK (Figure S6).

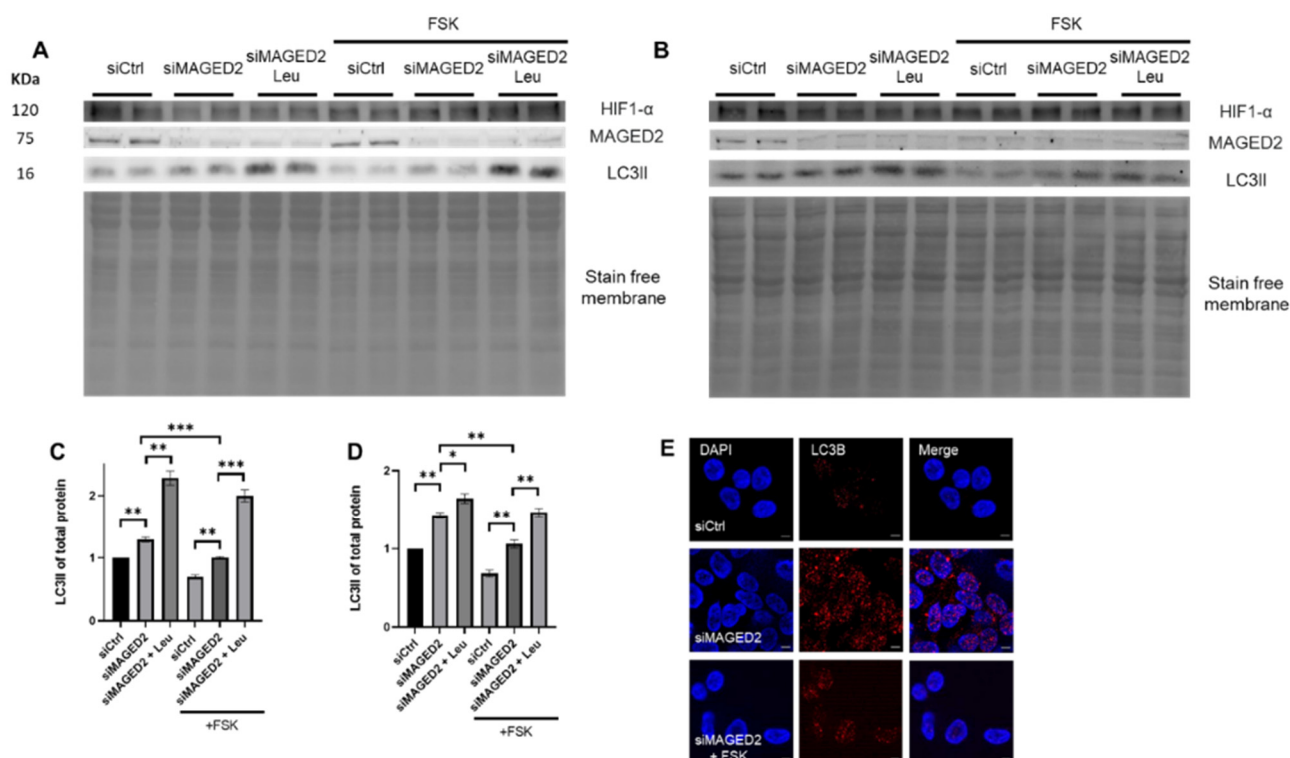


**Figure 8.** Forskolin reverses the induction of autophagy under stress conditions upon MAGED2 depletion. HeLa and HEK293 cells were both transfected with control and MAGED2 siRNA. After 24 to 48 h upon confluency, the media was changed to DMEM as control or DMEM containing 10  $\mu$ M FSK before subjecting all cells to physical hypoxia overnight. SDS-PAGE was used to separate total cell proteins, which were further immunoblotted for LC3B detection. Hypoxic condition was verified by blotting for HIF-1 $\alpha$ . Moreover, immunocytochemistry for HEK293 cells transfected with either control or MAGED2 siRNA and exposed upon confluency to overnight physical hypoxia with or without the addition of 10  $\mu$ M of FSK was performed and the accumulation of LC3B puncta was analyzed. (A,B) Representative Western blot images from (A) HeLa and (B) HEK293 cells treated with 10  $\mu$ M FSK show a reduction in LC3B expression and a diminished autophagy induction upon FSK treatment. The promoted autophagy seen when MAGED2 is knocked-down is rendered to control levels by FSK addition. (C,D) Densitometric analysis of LC3B immunoblots in (A,B), respectively. All blots are from the same experiment, and each represents an example of three independent experiments. Bar graphs show mean  $\pm$  SEM, \*  $p \leq 0.05$ , \*\*  $p \leq 0.01$ , \*\*\*  $p \leq 0.001$ . (E) Immunocytochemistry confirms that FSK addition to HEK293 cells prior to hypoxic stress reversed the observed autophagic induction, and the accumulation of puncta was rendered to control levels. Scale bar is 5  $\mu$ M.

### 3. Discussion

In this study, we demonstrated that MAGED2 blocks the induction of autophagy in three cell lines exposed to various stressors but not in unstressed cells. The *in vitro* data are independently supported by showing markedly enhanced abundance of LC3B puncta in the oxygen-deprived human fetal renal medulla of a patient carrying a mutation in MAGED2 but not in human fetal renal medulla from corresponding stages of renal development without a history of polyhydramnios. We also provide evidence that the inhibition of autophagy by MAGED2 requires activation of the cAMP/PKA pathway and does not rely on the functionality of p53 (Figure 9).

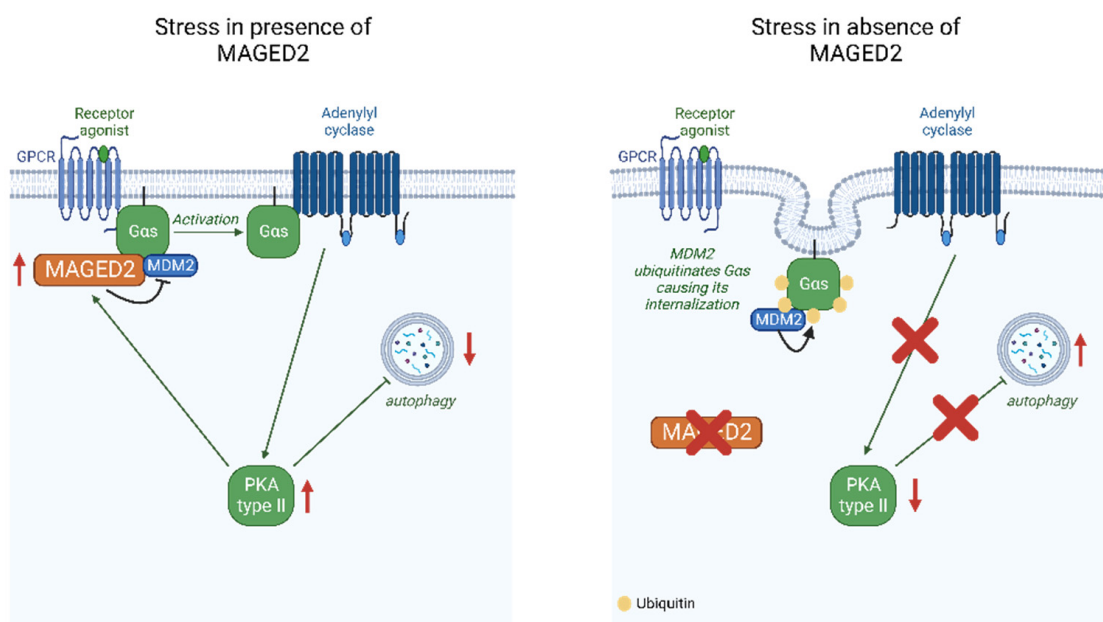


**Figure 9.** Proposed model for the role of MAGED2 under stress conditions (created with BioRender.com). Under stress, MAGED2 inhibits MDM2-dependent ubiquitination and endocytosis of G $\alpha$ s. This ensures activation of the adenylate cyclase and cAMP generation and activation of PKA under stress. Reduced PKA activity impairs regulation of autophagy mediated by the cAMP/PKA pathway.

Activation of the cAMP/PKA pathway is known to either activate or inhibit autophagy. In yeast, high glucose levels promote cAMP production, which inhibits autophagy by phosphorylation of ATG1 and ATG9, two key activators of macroautophagy [25]. In mammalian cells, cAMP can either inhibit [26–28] or promote [27,29] autophagy, depending on the cell type. Grisan and colleagues showed that the differential effects of cAMP on the regulation of autophagy depend on cell-type specific compartmentalization of PKA activity [30]. Of note, it was shown that only displacement of PKA type II (but not of PKA type I) reversed the effect of cAMP on autophagy, which concurs with our previous finding that MAGED2 regulates PKA type II [6]. In agreement with our data, knockdown of G $\alpha$ s has been shown to promote autophagy in HeLa cells [31].

Concurring with the general notion that MAGE protein family members are protective against various forms of stress [9], we have previously shown that MAGED2 is required for a functional G $\alpha$ s/cAMP/PKA pathway under hypoxic conditions [5,6]. Hence, our new finding that MAGED2 inhibits autophagy only under stressed conditions fits well with an important role of MAGED2, which is restricted to stress conditions. In this respect, our findings with MAGED2 differ from previous studies showing induction of autophagy upon deletion of MAGEA3/A6 in unstressed HeLa and U2OS cells [15], or unstressed MAGED1-depleted A549 and H1299 cells [32]. Given that activation of the cAMP/PKA pathway by forskolin abrogated autophagy in cells exposed to either physical hypoxia or the ER-stressor tunicamycin indicates that the latter stressor (like hypoxia) may also promote endocytosis of G $\alpha$ s. Hence, stress-induced internalization of G $\alpha$ s resulting from endocytosis induced by MDM2-dependent ubiquitination in the absence of MAGED2 [6] could be the switch activated by all stressors used in this study, which would explain why autophagy occurs only in MAGED2-depleted cells under stress in contrast to previous studies in MAGEA3/A6- or MAGED1-depleted cells. Analogously to the oncogenic potential of MAGEA3/A6 expression in tumors resulting in enhanced proliferation by limiting mTOR-dependent autophagy, a similar role of MAGED2 is conceivable, which is abundantly expressed in many types of cancers [33–36].

Previously, autophagy has been deemed dispensable for kidney development [37,38] in contrast to adult kidneys, where autophagy in diverse cells including glomerular mesangial



and endothelial cells, podocytes and proximal tubule epithelial cells has been shown to be essential for maintaining kidney integrity and normal physiology [39]. Our study now points to a potential role of autophagy in developing nephrons as shown by abundant LC3B positivity in collecting ducts. At the moment, direct evidence that salt-transporters such as NCC and NKCC2, which we have already shown to require MAGED2 and are aberrantly expressed in transient Bartter's syndrome [3], might be regulated by MAGED2 via autophagy, is missing. Of note, NCC has been shown to be degraded in lysosomes [40], which opens the possibility of regulation by autophagy. MAGED2 is abundantly expressed in the distal tubule in adult humans and rats starting from the cortical thick ascending limb of the loop of Henle down to the inner medullary collecting duct [3,41], where a number of cAMP-regulated salt-transporters are expressed [7]. Previously, induction of MAGED2 in the distal tubule in folic-acid induced acute kidney injury has been reported [42], in keeping with a role of MAGED2 in the protection against stress by preserving renal salt reabsorption in AKI. Of interest, rapamycin, which promotes autophagy by inhibiting mTOR [43], has been shown to alleviate hypertension in Dahl salt-sensitive rats [44], and deletion of raptor, which functions downstream of mTOR and inhibits autophagy, causes a Bartter's syndrome/furosemide-like renal phenotype including massive polyuria and hypercalciuria [45].

One limitation of this study arises from the limited access to human fetal kidney tissues. In addition to the marked LC3B staining, quantitative (qPCR) or semiquantitative (Western blot) assays from fetal tissues would have been advantageous. The second limitation concerns the potential effects of MAGED2 on the protection of renal salt transporters, particularly NKCC2 and NCC, from hypoxia-mediated autophagy. This needs to be determined in detail in forthcoming studies.

In sum, our study reveals that MAGED2 inhibits autophagy via the cAMP/PKA pathway in cells exposed to a diverse set of stressors in vitro and ex vivo as shown by massive autophagy in collecting ducts of a MAGED2-deficient human fetal kidney. Our data may indicate a probable reoccurrence of renal salt wasting, upon exposure of MAGED2-deficient individuals to certain stressors.

#### 4. Material and Methods

##### 4.1. Cell Culture

DMEM Glutmax containing 10% fetal bovine serum superior (Sigma-Aldrich, Schnell-dorf, Germany), penicillin (100 units/mL) and streptomycin (100 units/mL) was used to grow Human Embryonic Kidney (HEK293), Human Bone Osteosarcoma Epithelial Cells (U2OS Line) and HeLa cells (Table 1) at 37 °C in a humidified atmosphere of 5% CO<sub>2</sub>. Control and experimental cells were always derived and studied from the same flask and passage on the same day.

**Table 1.** Reagents and tools.

Reagent or Resource	Source	Identifier
<b>Antibodies</b>		
Anti-MAGED2 rabbit raised against this peptide (QVQENQDTRPKVKAK)	Eurogentec (Cologne, Germany)	
Anti-LC3B	Thermo Fisher Scientific (Dreieich, Germany)	PA1-46286
Cytokeratin	Agilent	M0821
ATG5 Antibody	Santa Cruz Biotechnology	sc-133158
P62 Antibody	Santa Cruz Biotechnology	sc-28359
Goat anti-rabbit IgG (H + L), Alexa Fluor Plus 555	Thermo Fisher Scientific (Dreieich, Germany)	A32732
Goat anti-rabbit IgG (H + L), Alexa Fluor Plus 555	Thermo Fisher Scientific (Dreieich, Germany)	A32732

Table 1. Cont.

Reagent or Resource	Source	Identifier
StarBright Blue 520 Goat Anti-Rabbit IgG	Bio-rad (Feldkirchen, Germany)	12005869
StarBright Blue 700 Goat Anti-Mouse IgG	Bio-rad (Feldkirchen, Germany)	12004158
<b>Chemical stressors</b>		
Cobalt(II) chloride hexahydrate	Sigma Aldrich (Schnelldorf, Germany)	C8661
Tunicamycin	Cayman Chemical (Ann Arbor, MI, USA)	11445
Camptothecin	Cayman Chemical (Ann Arbor, MI, USA)	11694
2-deoxy-D-glucose	TCI (Eschborn, Germany)	D0051
Brefeldin A	Sigma Aldrich (Schnelldorf, Germany)	B6542
<b>Transfection</b>		
DharmaFECT4	Dharmacon (Cambridge, UK)	T-2004-03
<b>Critical Commercial Assays</b>		
SingleShot Cell Lysis Kit	Bio-rad (Feldkirchen, Germany)	1725080
iScript Advanced cDNA Synthesis Kit for RT-qPCR	Bio-rad (Feldkirchen, Germany)	1725038
SsoAdvanced Universal SYBR Green Supermix	Bio-rad (Feldkirchen, Germany)	1725271
<b>Experimental Models: Cell Lines</b>		
HEK293	ATCC	CRL1573
HeLa	Gift from Dr. Vijay Renigunta	
U2OS	Gift from Prof. Thorsten Stiewe, ZIT, Philipps-University, Marburg	
<b>Oligonucleotides</b>		
ON-TARGETplus Non-targeting Control Pool	Dharmacon (Cambridge, UK)	D-001810-10-05
UGGUUUACAUGUCGACUAA		
UGGUUUACAUGUUGUGUGA		
UGGUUUACAUGUUUUCUGA		
UGGUUUACAUGUUUCCUA		
ON-TARGETplus Human MAGED2 siRNA—SMARTpool	Dharmacon (Cambridge, UK)	L-017284-01-0005
GGACGAAGCUGAUUUCGGA		
GCUAAAGACCAGACGAAGA		
AGGCGAUGGAAGCGGAUUU		
GAAAAGGACAGUAGCUCGA		
ON-TARGETplus Human GNAS siRNA—SMARTpool	Dharmacon (Cambridge, UK)	L-010825-00-0005
GCAAGUGGAUCCAGUGCUU		
GCAUGCACCUUCGUCAGUA		
AUGAGGAUCCUGCAUGUUA		
CAACCAAAGUGCAGGACAU		
GAPD, Human GAPDH, Real-Time PCR Primer Set	Biomol (Hamburg, Germany)	VHPS-3541
TTTTGGCTAAAGACCAGACG		

Table 1. Cont.

Reagent or Resource	Source	Identifier
AATAGCCTGCTCGTTCAATG		
ATG5	Sigma-Aldric (Schnelldorf, Germany)	
AAAGATGTGCTTCGAGATGTGT		
CACTTTGTCTAGTTACCAACGTCA		
ATG12	Sigma-Aldrich (Schnelldorf, Germany)	
CTGCTGGCGACACCAAGAAA		
CGTGTTCTGCTCTACTGCCC		
Software and Algorithms		
ImageJ	Schneider et al., 2012 [46]	<a href="https://imagej.nih.gov/ij/">https://imagej.nih.gov/ij/</a> , accessed on 22 July 2022
GraphPad Prism 9	GraphPad	
EndNote X9	Clarivate Analytics	
BioRender		<a href="https://www.biorender.com/">https://www.biorender.com/</a> , accessed on 22 August 2023

#### 4.2. siRNA (Small Interfering RNA) Knockdown

The ON-TARGETplus SMARTpools of the siRNAs for control, MAGED2 and GNAS were purchased from Dharmacon (D-001810-10-05 and L-010825-00-0005). By reverse transfection according to the manufacturer's instructions, cells were transfected with either control or MAGED2 siRNAs using DhramaFECT4.

#### 4.3. Establishment of Cellular Stress

At 24–48 h post transfection, the medium of the confluent cells was changed to a media containing one of the chemical stressors; endoplasmic reticulum (ER) stressors, Tunicamycin (Tun, 600 nM) or Brefeldin A (BFA, 10 µM); a genotoxic stressor, Camptothecin (CPT, 10 µM); a nutritional stressor, 2-deoxy-D-glucose (2DG, 4 mM); or a hypoxia mimetic, Cobalt Chloride (CoCl<sub>2</sub>, 300 µM) which induces HIF1-α expression “Chemical Hypoxia”. Overnight incubation of cells in a standard humidifier at 37 °C was needed for Tun, CPT and CoCl<sub>2</sub>, while incubation with BFA and 2DG lasted only for 2 h and 30 min, respectively, to evade toxic effects. Physical hypoxia was performed overnight in a modular hypoxia incubator chamber (Billups-Rothenberg, Inc., San Diego, CA, USA, Cat. MIC-101), as described previously [5].

#### 4.4. Immunocytochemistry

Cells were cultured in poly-L-lysine coated chamber slides. Fixation of cells was done at 4 °C by using 4% paraformaldehyde in PBS for 20 min followed by permeabilization in 0.1% Triton X-100 for 5 min at 4 °C. Cells were incubated afterwards with DAKO (antibody diluent with background-reducing components) for 30 min to prevent nonspecific antibody binding. Rabbit LC3B antibody (1:2000) was used as a primary antibody for 1 h at room temperature, and the Alexa Fluor Plus 555-coupled goat anti-Rabbit IgG antibody (1:500) was used as a secondary antibody. Visualization was done after mounting with VECTASHIELD Antifade Mounting Medium containing DAPI (Vector Laboratories, Newark, CA, USA) by employing a ZEISS Apotome 40× magnifying lens (Carl Zeiss, Oberkochen, Germany).

#### 4.5. Immunohistochemistry

Fetal human kidneys were obtained from medical abortions (20 and 23 weeks of gestational ages, respectively) and from a case of transient Bartter's syndrome (22 weeks of gestational age) as described previously [3]. Kidneys were embedded with paraffin and cut into 5 µm thick sections. The sections, after being deparaffinized with xylene and graded alcohol, were rehydrated in a succession of 100%, 90%, 80%, 70% and 50%. Staining with rabbit LC3B (1:500) and mouse cytokeratin (1:100) antibodies in 1% bovine serum albumin (BSA) was performed at 4 °C overnight. Both Alexa Fluor Plus 555 and Alexa Fluor Plus 488 coupled secondary antibodies (1:500) were added the following day after three PBS washes and kept for 1 h at room temperature. Autofluorescence was removed by TrueVIEW Autofluorescence Quenching Kit (Vector Laboratories, Newark, CA, USA). Mounting with VECTASHIELD Antifade Mounting Medium containing DAPI (Vector Laboratories, Newark, CA, USA) preceded visualizing the sections using ZEISS Apotome (Carl Zeiss, Oberkochen, Germany).

#### 4.6. Western Blotting

Lysis buffer (50 mM Tris pH 7.4, 5 mM EDTA, 150 mM NaCl, 1% Triton X-100 and protease inhibitors) was used to lyse the confluent cells after three ice-cold PBS washes. The lysates were centrifuged for 15 min at 13,000 × *g*, and the protein concentrations of the supernatants were measured by a Pierce™ BCA Protein Assay Kit (Thermo Scientific™, Dreieich, Germany). We used 12% TGX gels Stain Free gels (Bio-rad, Feldkirchen, Germany; Cat. 1610181) to separate the proteins before blotting them to nitrocellulose membranes 0.2 µm through a Trans-Blot Turbo Transfer System (Bio-rad, Feldkirchen, Germany). Identifying the proteins was carried out by fluorescence antibodies StarBright Blue 520 and 700 (Bio-rad, Feldkirchen, Germany) using the ChemiDoc MP imaging machine (Bio-Rad, Feldkirchen, Germany). ImageJ software provided by the National Institutes of Health, Bethesda, MD, USA, was used to assess the gray density of Western blots. The signal for the protein of interest is normalized to the total amount of protein loaded into the lane using a stain-free membrane [47].

#### 4.7. Quantitative Real-Time Reverse Transcription Polymerase Chain Reaction (qRT-PCR)

The quantities of ATG5 and ATG12 mRNA were measured using quantitative real-time RT-PCR (qRT-PCR), with the GAPDH gene serving as an internal control. Cell total RNA was extracted using the Bio-rad SingleShot Cell Lysis Kit and transcribed to complementary DNA (cDNA) using the Bio-rad iScript™ Advanced cDNA Synthesis Kit. PCR was performed employing a QuantStudio™ 3 Real-Time PCR System (Applied Biosystems, Waltham, MA, USA) with SsoAdvanced Universal SYBR Green Supermix (Bio-rad). Cycle threshold values were normalized to GAPDH amplification.

#### 4.8. Statistical Analyses

Results are displayed using mean ± SEM. Unpaired Student's *t*-tests were used to analyze mean differences. Statistical analyses were carried out with the aid of the program GraphPad Prism X9. *p* values of 0.05 or less were deemed statistically significant (\*), *p* values of 0.01 or less were deemed highly significant (\*\*), and *p* values of 0.001 or less were deemed extremely significant (\*\*\*)

**Supplementary Materials:** The supporting information can be downloaded at: <https://www.mdpi.com/article/10.3390/ijms241713433/s1>.

**Author Contributions:** Conceptualization, E.S. and M.K.; Formal analysis, S.N., E.S. and M.K.; Funding acquisition, E.S. and M.K.; Investigation, S.N., A.R., J.K.D., E.S. and M.K.; Methodology, S.N., E.S. and M.K.; Project administration, M.K.; Resources, S.W. and M.K.; Supervision, E.S. and M.K.; Visualization, S.N., A.R. and E.S.; Writing—original draft, S.N., E.S. and M.K.; Writing—review & editing, A.R., H.H. and S.W. All authors have read and agreed to the published version of the manuscript.

**Funding:** This work was supported by a grant from the German Research Foundation (DFG) Ko1855/4-1(MK), Behring Röntgen Foundation, grant 67-0061 (MK) and University Medical Center Giessen and Marburg UKGM 15/2021 (ES). Open Access funding provided by the Open Access Publication Fund of Philipps-Universität Marburg with support of the DFG.

**Institutional Review Board Statement:** Studying MAGED2 in human tissue was approved (Ethikkommission, Philipps-Universität Marburg, AZ: 113/22, 26 August 2022).

**Informed Consent Statement:** Written informed consent from the parents of the MAGED2-patient was obtained. The two human fetal control kidneys were de-identified samples to the research team at all points and therefore considered exempt for participation consent.

**Data Availability Statement:** All data are available in the main text or the Supplementary Materials.

**Acknowledgments:** We thank Michelle Auer and Nadine Schallop for technical support.

**Conflicts of Interest:** Authors declare that they have no competing interests.

## References

- Komhoff, M.; Laghmani, K. MAGED2: A novel form of antenatal Bartter's syndrome. *Curr. Opin. Nephrol. Hypertens.* **2018**, *27*, 323–328. [\[CrossRef\]](#) [\[PubMed\]](#)
- O'Hare, E.M.; Jelin, A.C.; Miller, J.L.; Ruano, R.; Atkinson, M.A.; Baschat, A.A.; Jelin, E.B. Amniotomies to Treat Early Onset Anhydramnios Caused by Renal Anomalies: Background and Rationale for the Renal Anhydramnios Fetal Therapy Trial. *Fetal Diagn. Ther.* **2019**, *45*, 365–372. [\[CrossRef\]](#) [\[PubMed\]](#)
- Laghmani, K.; Beck, B.B.; Yang, S.S.; Seayfan, E.; Wenzel, A.; Reusch, B.; Vitzthum, H.; Priem, D.; Demarets, S.; Bergmann, K.; et al. Polyhydramnios, Transient Antenatal Bartter's Syndrome, and MAGED2 Mutations. *N. Engl. J. Med.* **2016**, *374*, 1853–1863. [\[CrossRef\]](#)
- Legrand, A.; Treard, C.; Roncelin, I.; Dreux, S.; Bertholet-Thomas, A.; Broux, F.; Bruno, D.; Decramer, S.; Deschenes, G.; Djeddi, D.; et al. Prevalence of Novel MAGED2 Mutations in Antenatal Bartter Syndrome. *Clin. J. Am. Soc. Nephrol.* **2018**, *13*, 242–250. [\[CrossRef\]](#)
- Seayfan, E.; Nasrah, S.; Quell, L.; Radi, A.; Kleim, M.; Schermuly, R.T.; Weber, S.; Laghmani, K.; Kömhoff, M. Reciprocal Regulation of MAGED2 and HIF-1 $\alpha$ ; Augments Their Expression under Hypoxia: Role of cAMP and PKA Type II. *Cells* **2022**, *11*, 3424. [\[PubMed\]](#)
- Seayfan, E.; Nasrah, S.; Quell, L.; Kleim, M.; Weber, S.; Meyer, H.; Laghmani, K.; Kömhoff, M. MAGED2 Is Required under Hypoxia for cAMP Signaling by Inhibiting MDM2-Dependent Endocytosis of G-Alpha-S. *Cells* **2022**, *11*, 2546. [\[CrossRef\]](#)
- Fenton, R.A.; Knepper, M.A. Mouse models and the urinary concentrating mechanism in the new millennium. *Physiol. Rev.* **2007**, *87*, 1083–1112. [\[CrossRef\]](#)
- Ecelbarger, C.A.; Yu, S.; Lee, A.J.; Weinstein, L.S.; Knepper, M.A. Decreased renal Na-K-2Cl cotransporter abundance in mice with heterozygous disruption of the G(s)alpha gene. *Am. J. Physiol.* **1999**, *277*, F235–F244.
- Flörke Gee, R.R.; Chen, H.; Lee, A.K.; Daly, C.A.; Wilander, B.A.; Fon Tacer, K.; Potts, P.R. Emerging roles of the MAGE protein family in stress response pathways. *J. Biol. Chem.* **2020**, *295*, 16121–16155. [\[CrossRef\]](#)
- De Donato, M.; Peters, S.O.; Hussain, T.; Rodulfo, H.; Thomas, B.N.; Babar, M.E.; Imumorin, I.G. Molecular evolution of type II MAGE genes from ancestral MAGED2 gene and their phylogenetic resolution of basal mammalian clades. *Mamm. Genome* **2017**, *28*, 443–454. [\[CrossRef\]](#)
- Doyle, J.M.; Gao, J.; Wang, J.; Yang, M.; Potts, P.R. MAGE-RING protein complexes comprise a family of E3 ubiquitin ligases. *Mol. Cell* **2010**, *39*, 963–974. [\[CrossRef\]](#)
- Lee, A.K.; Potts, P.R. A Comprehensive Guide to the MAGE Family of Ubiquitin Ligases. *J. Mol. Biol.* **2017**, *429*, 1114–1142. [\[CrossRef\]](#) [\[PubMed\]](#)
- Zheng, N.; Shabek, N. Ubiquitin Ligases: Structure, Function, and Regulation. *Annu. Rev. Biochem.* **2017**, *86*, 129–157. [\[CrossRef\]](#)
- Fon Tacer, K.; Montoya, M.C.; Oatley, M.J.; Lord, T.; Oatley, J.M.; Klein, J.; Ravichandran, R.; Tillman, H.; Kim, M.; Connelly, J.P.; et al. MAGE cancer-testis antigens protect the mammalian germline under environmental stress. *Sci. Adv.* **2019**, *5*, eaav4832. [\[CrossRef\]](#) [\[PubMed\]](#)
- Pineda, C.T.; Ramanathan, S.; Fon Tacer, K.; Weon, J.L.; Potts, M.B.; Ou, Y.H.; White, M.A.; Potts, P.R. Degradation of AMPK by a cancer-specific ubiquitin ligase. *Cell* **2015**, *160*, 715–728. [\[CrossRef\]](#) [\[PubMed\]](#)
- Bernhardt, W.M.; Schmitt, R.; Rosenberger, C.; Munchenhagen, P.M.; Grone, H.J.; Frei, U.; Warnecke, C.; Bachmann, S.; Wiesener, M.S.; Willam, C.; et al. Expression of hypoxia-inducible transcription factors in developing human and rat kidneys. *Kidney Int.* **2006**, *69*, 114–122. [\[CrossRef\]](#) [\[PubMed\]](#)
- Kömhoff, M.; Hollinshead, M.; Tooze, J.; Kern, H.F. Brefeldin A induced dose-dependent changes to Golgi structure and function in the rat exocrine pancreas. *Eur. J. Cell Biol.* **1994**, *63*, 192–207. [\[PubMed\]](#)
- Pommier, Y. Topoisomerase I inhibitors: Camptothecins and beyond. *Nat. Rev. Cancer* **2006**, *6*, 789–802. [\[CrossRef\]](#)



19. Babbitt, J.L.; Eisenga, M.F.; Haase, V.H.; Kshirsagar, A.V.; Levin, A.; Locatelli, F.; Malyszko, J.; Swinkels, D.W.; Tarng, D.C.; Cheung, M.; et al. Controversies in optimal anemia management: Conclusions from a Kidney Disease: Improving Global Outcomes (KDIGO) Conference. *Kidney Int.* **2021**, *99*, 1280–1295. [\[CrossRef\]](#)
20. Jayasooriya, R.; Dilshara, M.G.; Karunarathne, W.; Molagoda, I.M.N.; Choi, Y.H.; Kim, G.Y. Camptothecin enhances c-Myc-mediated endoplasmic reticulum stress and leads to autophagy by activating Ca(2+)-mediated AMPK. *Food Chem. Toxicol.* **2018**, *121*, 648–656. [\[CrossRef\]](#)
21. Prasad Tharanga Jayasooriya, R.G.; Dilshara, M.G.; Neelaka Molagoda, I.M.; Park, C.; Park, S.R.; Lee, S.; Choi, Y.H.; Kim, G.Y. Camptothecin induces G(2)/M phase arrest through the ATM-Chk2-Cdc25C axis as a result of autophagy-induced cytoprotection: Implications of reactive oxygen species. *Oncotarget* **2018**, *9*, 21744–21757. [\[CrossRef\]](#) [\[PubMed\]](#)
22. Wick, A.N.; Drury, D.R.; Nakada, H.I.; Wolfe, J.B. Localization of the primary metabolic block produced by 2-deoxyglucose. *J. Biol. Chem.* **1957**, *224*, 963–969. [\[CrossRef\]](#)
23. Chen, W.; Guéron, M. The inhibition of bovine heart hexokinase by 2-deoxy-D-glucose-6-phosphate: Characterization by <sup>31</sup>P NMR and metabolic implications. *Biochimie* **1992**, *74*, 867–873. [\[CrossRef\]](#) [\[PubMed\]](#)
24. Kurtoglu, M.; Gao, N.; Shang, J.; Maher, J.C.; Lehrman, M.A.; Wangpaichitr, M.; Savaraj, N.; Lane, A.N.; Lampidis, T.J. Under normoxia, 2-deoxy-D-glucose elicits cell death in select tumor types not by inhibition of glycolysis but by interfering with N-linked glycosylation. *Mol. Cancer Ther.* **2007**, *6*, 3049–3058. [\[CrossRef\]](#) [\[PubMed\]](#)
25. Budovskaya, Y.V.; Stephan, J.S.; Reggiori, F.; Klionsky, D.J.; Herman, P.K. The Ras/cAMP-dependent protein kinase signaling pathway regulates an early step of the autophagy process in *Saccharomyces cerevisiae*. *J. Biol. Chem.* **2004**, *279*, 20663–20671. [\[CrossRef\]](#)
26. Palorini, R.; Votta, G.; Pirola, Y.; De Vitto, H.; De Palma, S.; Airolidi, C.; Vasso, M.; Ricciardiello, F.; Lombardi, P.P.; Cirulli, C.; et al. Protein Kinase A Activation Promotes Cancer Cell Resistance to Glucose Starvation and Anoikis. *PLoS Genet.* **2016**, *12*, e1005931. [\[CrossRef\]](#) [\[PubMed\]](#)
27. Jewell, J.L.; Fu, V.; Hong, A.W.; Yu, F.X.; Meng, D.; Melick, C.H.; Wang, H.; Lam, W.M.; Yuan, H.X.; Taylor, S.S.; et al. GPCR signaling inhibits mTORC1 via PKA phosphorylation of Raptor. *Elife* **2019**, *8*, e43038. [\[CrossRef\]](#)
28. Cherra, S.J., 3rd; Kulich, S.M.; Uechi, G.; Balasubramani, M.; Mountzouris, J.; Day, B.W.; Chu, C.T. Regulation of the autophagy protein LC3 by phosphorylation. *J. Cell Biol.* **2010**, *190*, 533–539. [\[CrossRef\]](#)
29. Xie, J.; Ponuwei, G.A.; Moore, C.E.; Willars, G.B.; Tee, A.R.; Herbert, T.P. cAMP inhibits mammalian target of rapamycin complex-1 and -2 (mTORC1 and 2) by promoting complex dissociation and inhibiting mTOR kinase activity. *Cell Signal* **2011**, *23*, 1927–1935. [\[CrossRef\]](#)
30. Grisan, F.; Iannucci, L.F.; Surdo, N.C.; Gerbino, A.; Zanin, S.; Di Benedetto, G.; Pozzan, T.; Lefkimmatis, K. PKA compartmentalization links cAMP signaling and autophagy. *Cell Death Differ.* **2021**, *28*, 2436–2449. [\[CrossRef\]](#)
31. Zhang, T.; Dong, K.; Liang, W.; Xu, D.; Xia, H.; Geng, J.; Najafav, A.; Liu, M.; Li, Y.; Han, X.; et al. G-protein-coupled receptors regulate autophagy by ZBTB16-mediated ubiquitination and proteasomal degradation of Atg14L. *Elife* **2015**, *4*, e06734. [\[CrossRef\]](#) [\[PubMed\]](#)
32. Zhou, Y.; Huang, N.; Wu, J.; Zhen, N.; Li, N.; Li, Y.; Li, Y.X. Silencing of NAGE induces autophagy via AMPK/Ulk1/Atg13 signaling pathway in NSCLC cells. *Tumour Biol.* **2017**, *39*, 1010428317709676. [\[CrossRef\]](#) [\[PubMed\]](#)
33. Kanda, M.; Nomoto, S.; Oya, H.; Takami, H.; Shimizu, D.; Hibino, S.; Hashimoto, R.; Kobayashi, D.; Tanaka, C.; Yamada, S.; et al. The Expression of Melanoma-Associated Antigen D2 Both in Surgically Resected and Serum Samples Serves as Clinically Relevant Biomarker of Gastric Cancer Progression. *Ann. Surg. Oncol.* **2015**, *23*, 214–221. [\[CrossRef\]](#)
34. Chung, F.Y.; Cheng, T.L.; Chang, H.J.; Chiu, H.H.; Huang, M.Y.; Chang, M.S.; Chen, C.C.; Yang, M.J.; Wang, J.Y.; Lin, S.R. Differential gene expression profile of MAGE family in taiwanese patients with colorectal cancer. *J. Surg. Oncol.* **2010**, *102*, 148–153. [\[CrossRef\]](#) [\[PubMed\]](#)
35. Tsai, J.R.; Chong, I.W.; Chen, Y.H.; Yang, M.J.; Sheu, C.C.; Chang, H.C.; Hwang, J.J.; Hung, J.Y.; Lin, S.R. Differential expression profile of MAGE family in non-small-cell lung cancer. *Lung Cancer* **2007**, *56*, 185–192. [\[CrossRef\]](#)
36. Kidd, M.; Modlin, I.M.; Mane, S.M.; Camp, R.L.; Eick, G.; Latich, I. The role of genetic markers--NAP1L1, MAGE-D2, and MTA1--in defining small-intestinal carcinoid neoplasia. *Ann. Surg. Oncol.* **2006**, *13*, 253–262. [\[CrossRef\]](#)
37. Hartleben, B.; Gödel, M.; Meyer-Schwesinger, C.; Liu, S.; Ulrich, T.; Köbler, S.; Wiech, T.; Grahmmer, F.; Arnold, S.J.; Lindenmeyer, M.T.; et al. Autophagy influences glomerular disease susceptibility and maintains podocyte homeostasis in aging mice. *J. Clin. Invest.* **2010**, *120*, 1084–1096. [\[CrossRef\]](#)
38. Liu, S.; Hartleben, B.; Kretz, O.; Wiech, T.; Igarashi, P.; Mizushima, N.; Walz, G.; Huber, T.B. Autophagy plays a critical role in kidney tubule maintenance, aging and ischemia-reperfusion injury. *Autophagy* **2012**, *8*, 826–837. [\[CrossRef\]](#)
39. Tang, C.; Livingston, M.J.; Liu, Z.; Dong, Z. Autophagy in kidney homeostasis and disease. *Nat. Rev. Nephrol.* **2020**, *16*, 489–508. [\[CrossRef\]](#)
40. Rosenbaek, L.L.; Rizzo, F.; Wu, Q.; Rojas-Vega, L.; Gamba, G.; MacAulay, N.; Staub, O.; Fenton, R.A. The thiazide sensitive sodium chloride co-transporter NCC is modulated by site-specific ubiquitylation. *Sci. Rep.* **2017**, *7*, 12981. [\[CrossRef\]](#)
41. Lee, J.W.; Chou, C.L.; Knepper, M.A. Deep Sequencing in Microdissected Renal Tubules Identifies Nephron Segment-Specific Transcriptomes. *J. Am. Soc. Nephrol.* **2015**, *26*, 2669–2677. [\[CrossRef\]](#) [\[PubMed\]](#)

42. Valiño-Rivas, L.; Cuarental, L.; Agustin, M.; Husi, H.; Cannata-Ortiz, P.; Sanz, A.B.; Mischak, H.; Ortiz, A.; Sanchez-Niño, M.D. MAGE genes in the kidney: Identification of MAGED2 as upregulated during kidney injury and in stressed tubular cells. *Nephrol. Dial. Transplant.* **2019**, *34*, 1498–1507. [[CrossRef](#)] [[PubMed](#)]
43. Dikic, I.; Elazar, Z. Mechanism and medical implications of mammalian autophagy. *Nat. Rev. Mol. Cell Biol.* **2018**, *19*, 349–364. [[CrossRef](#)] [[PubMed](#)]
44. Kumar, V.; Wollner, C.; Kurth, T.; Bukowy, J.D.; Cowley, A.W., Jr. Inhibition of Mammalian Target of Rapamycin Complex 1 Attenuates Salt-Induced Hypertension and Kidney Injury in Dahl Salt-Sensitive Rats. *Hypertension* **2017**, *70*, 813–821. [[CrossRef](#)]
45. Grahammer, F.; Haenisch, N.; Steinhardt, F.; Sandner, L.; Roerden, M.; Arnold, F.; Cordts, T.; Wanner, N.; Reichardt, W.; Kerjaschki, D.; et al. mTORC1 maintains renal tubular homeostasis and is essential in response to ischemic stress. *Proc. Natl. Acad. Sci. USA* **2014**, *111*, E2817–E2826. [[CrossRef](#)]
46. Schneider, C.A.; Rasband, W.S.; Eliceiri, K.W. NIH Image to ImageJ: 25 years of image analysis. *Nat. Methods* **2012**, *9*, 671–675. [[CrossRef](#)]
47. Taylor, S.C.; Posch, A. The design of a quantitative western blot experiment. *BioMed Res. Int.* **2014**, *2014*, 361590. [[CrossRef](#)]

**Disclaimer/Publisher’s Note:** The statements, opinions and data contained in all publications are solely those of the individual author(s) and contributor(s) and not of MDPI and/or the editor(s). MDPI and/or the editor(s) disclaim responsibility for any injury to people or property resulting from any ideas, methods, instructions or products referred to in the content.

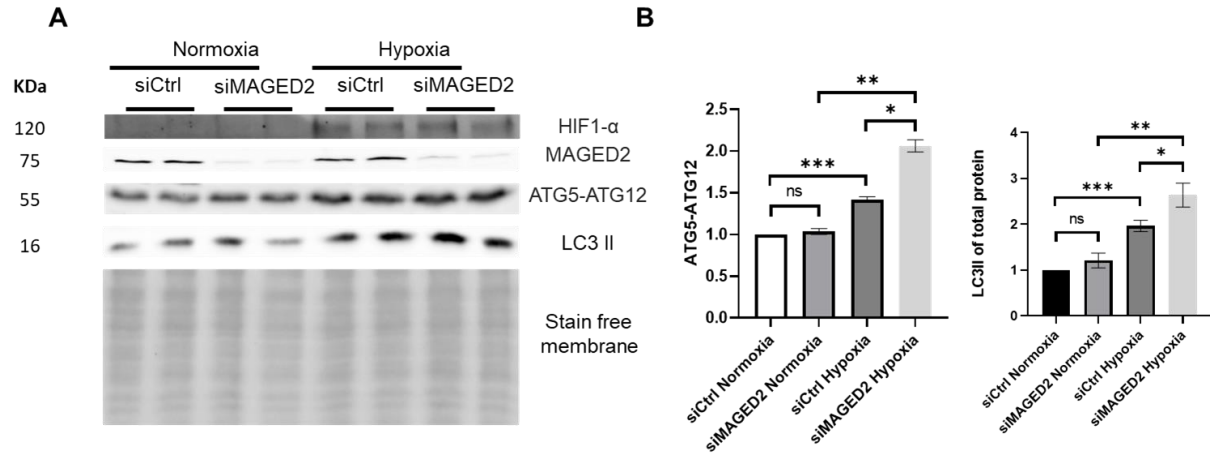


**Figure S1. Compared to normoxia, autophagy is induced in HEK293 cells under hypoxic stress and MAGED2 silencing markedly enhances the autophagic induction under hypoxia.**

Control or MAGED2 siRNAs were transfected into HEK293 cells. 24-48 hours post transfection, hypoxic stress was applied overnight for one set in a modular chamber (1% O<sub>2</sub>, 5% CO<sub>2</sub>, and 94% N<sub>2</sub>) while the other set was kept in a humidified atmosphere (normoxia). Cells were then lysed and blotted for LC3B and autophagy related genes detection. Of note, HIF-1 $\alpha$  immunoblotting confirmed the hypoxic condition (A) Representative western blot images from HEK293 cells reveal that hypoxia markedly induced autophagy in comparison to normoxia, as evident by upregulation of ATG5-ATG12 conjugate levels alongside the higher conversion to the lipidated form LC3II. MAGED2 depletion was dispensable under normoxic conditions in contrast to hypoxia where significantly augmented ATG5-ATG12 complex levels and increased LC3II abundance were observed. (B) Densitometric analysis of ATG5-ATG12 conjugate and LC3II from the immunoblot A. All samples shown on individual blots are from the same experiment and each blot represents an example of three independent experiments. Bar graphs show mean  $\pm$  SEM, \*  $p \leq 0.05$ , \*\*  $p \leq 0.01$ , \*\*\*  $p \leq 0.001$ .



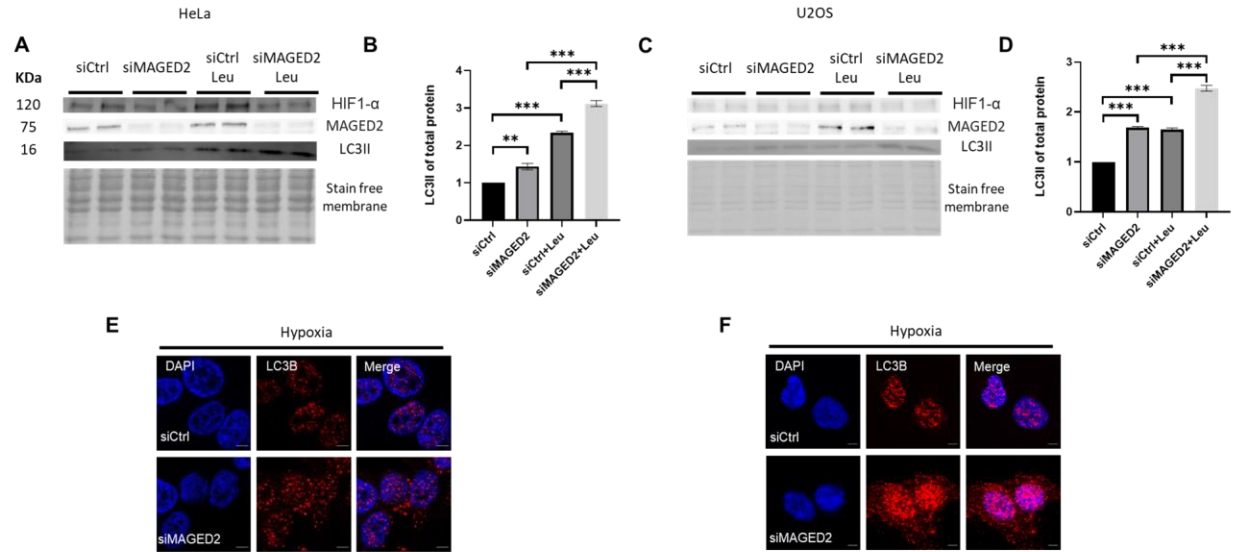


**Figure S2. MAGED2 depletion induces autophagy under hypoxia in HeLa and p53-positive U2OS cells.**

U2OS and HeLa cells were transfected with control and MAGED2 siRNA. 24-48 h post transfection, cells were exposed to physical hypoxia overnight. HIF-1 $\alpha$  immunoblots confirmed hypoxia. A, C: Representative immunoblots disclose higher LC3II prevalence upon MAGED2 depletion in HeLa (A) and U2OS (C) cells. Treatment with leupeptin blocked the autophagic flux and resulted in the highest LC3II accumulation when MAGED2 is knocked-down. B, D: Densitometric analysis of LC3II in the immunoblots A, C respectively. All blots are from the same experiment and each represents an example of three independent experiments. Bar graphs show mean  $\pm$  SEM, \*  $p \leq 0.05$ , \*\*  $p \leq 0.01$ , \*\*\*  $p \leq 0.001$ . Immunocytochemistry in HeLa (E) and U2OS (F) cells, transfected with control or MAGED2 siRNAs and exposed to physical hypoxia, reveal marked accumulation of LC3B puncta upon MAGED2 depletion. The scale bar is 5  $\mu$ m.

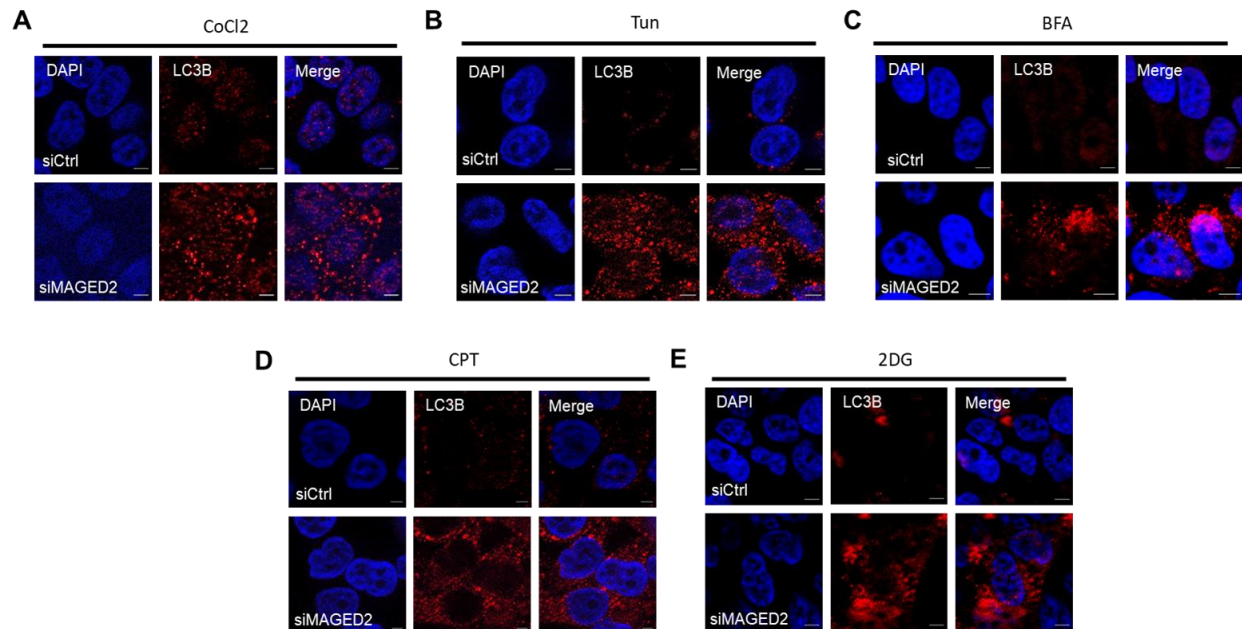


**Figure S3. MAGED2 depletion in HeLa cells induces autophagy significantly in response to numerous stress conditions.**

Control and MAGED2 siRNAs were transfected in HeLa cells. Upon confluency, 24-48 hours after transfection, cells were exposed to a variety of stress conditions; 300  $\mu$ M CoCl<sub>2</sub> overnight, 600 nM Tunicamycin overnight, 10  $\mu$ M Camptothecin overnight, 10  $\mu$ M Brefeldin A for 2 hours and 4 mM 2-Deoxy-D-glucose for 30 minutes to avoid toxic effects. Immunocytochemistry was conducted to stain against LC3B in control and MAGED2 transfected HeLa cells which were treated with CoCl<sub>2</sub> (A), tunicamycin (B), BFA (C), CPT (D) or 2DG (E). The scale bar is 5 $\mu$ M.

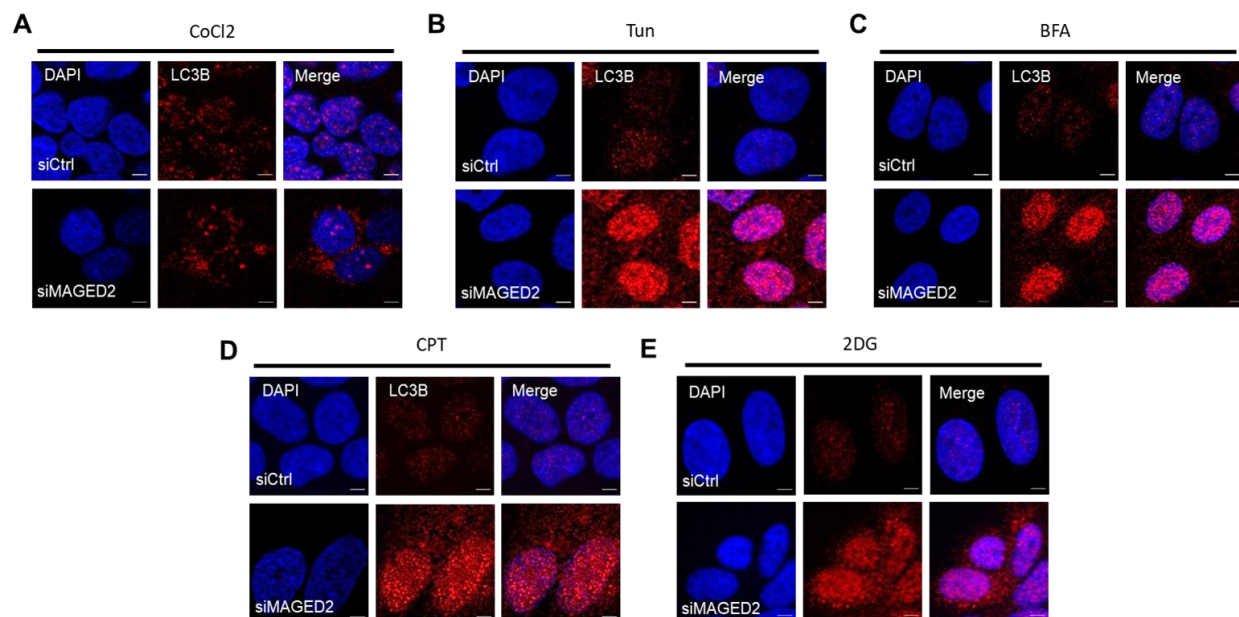


**Figure S4. Stress-induced autophagy is significantly promoted in U2OS cells upon MAGED2 depletion.**

U2OS cells were transfected with Control and MAGED2 siRNAs. 24-48 h post-transfection, cells were subjected to diverse stress conditions; 300  $\mu$ M CoCl<sub>2</sub> overnight, 600 nM Tunicamycin overnight, 10  $\mu$ M Camptothecin overnight, 10  $\mu$ M Brefeldin A for 2 hours and 4 mM 2-Deoxy-D-glucose for 30 minutes to avoid toxic effects. Immunocytochemistry was performed to stain against LC3B in control and MAGED2 transfected U2OS cells which were treated with CoCl<sub>2</sub> (A), tunicamycin (B), BFA (C), CPT (D) or 2DG (E). The scale bar is 5 $\mu$ M.

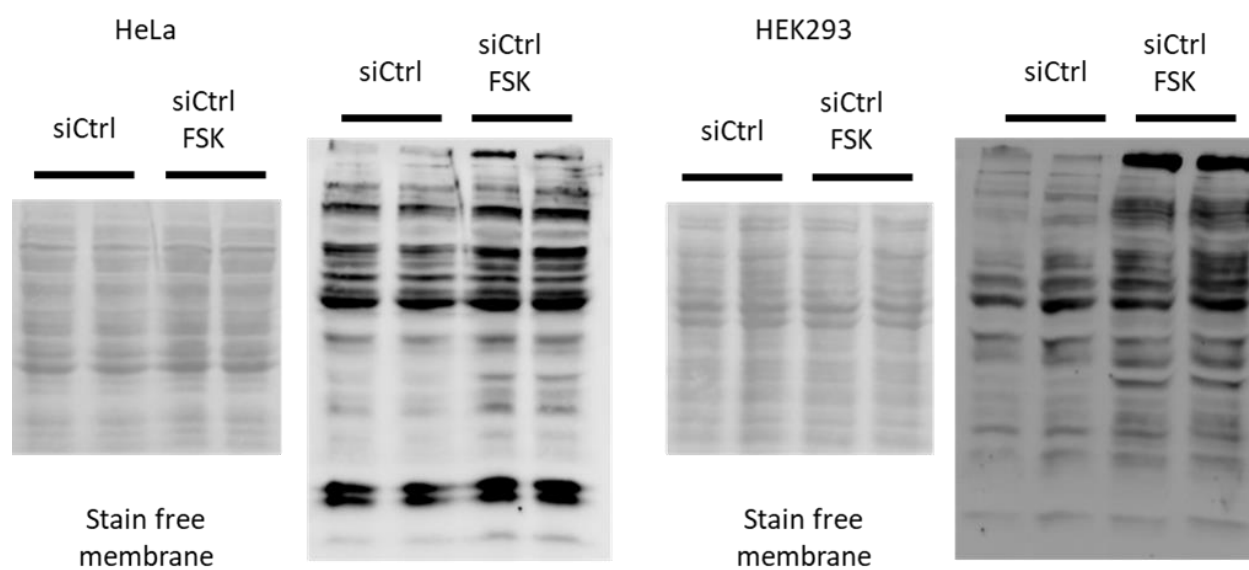


**Figure S5. Forskolin treatment increases the phosphorylation of PKA substrates.**

HeLa and HEK293 cells were transfected with control siRNA following our standard protocol and upon confluency 24-48 h post transfection, the medium of the cells was altered to either DMEM or DMEM containing 10  $\mu$ M FSK. The cells were incubated overnight and the lysates were collected afterwards and blotted for phosphorylated PKA substrates.

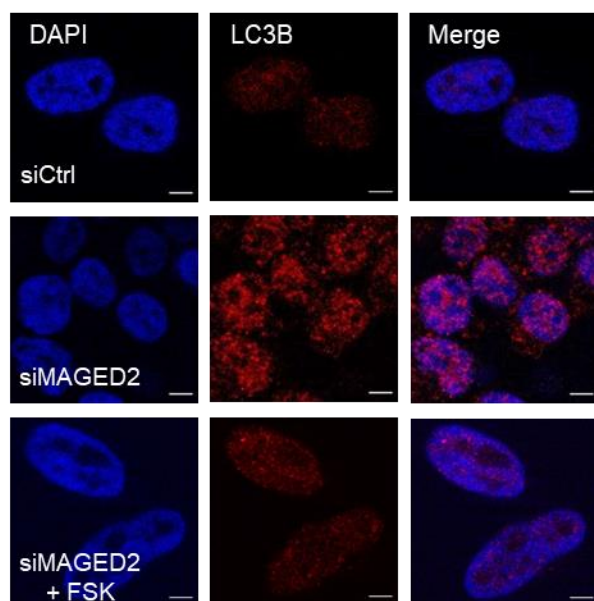


**Figure S6. In MAGED2 depleted HeLa cells, forskolin treatment limits autophagy induction under ER stress.**

HeLa cells were transfected with either control or MAGED2 siRNA. 24-48 h post transfection, the medium of the cells was changed to DMEM containing 600 nM tunicamycin or DMEM containing 10  $\mu$ M forskolin together with 600 nM tunicamycin. The cells were stained for the accumulation of LC3B puncta and surprisingly the accumulation upon MAGED2 depletion was abrogated and rendered to control level when forskolin was added to the media.